GEOHISTORY ANALYSIS

[redacted]

APPLICATION OF

MICROPALEONTOLOGY IN EXPLORATION GEOLOGY

INTRODUCTION

'Geohistory analysis' is the use of quantitative stratigraphic techniques to unravel and portray geologic history. Quantification of routine stratigraphic well information is possible as a result of recent advances in microbiostratigraphy that allow exploration paleontologists to determine geologic ages in terms of millions of years, and to express depositional environments in terms of water depths. Geohistory diagrams and numerical stratigraphic techniques, such as the calculation of rates of sediment accumulation and rates of subsidence or uplift (with and without corrections for consolidation), are useful in widely different aspects of petroleum exploration. Knowledge of rates and timing of vertical movements is of local importance in distinguishing between different kinds of movements and determining timing, rates and magnitudes of inversion. On a larger scale these data should constitute a parameter in any structural classification. In general, such knowledge is a key to understanding the mechanics, rates and magnitudes of basin evolution and plate tectonics (with and without corrections for isostatic crustal response).

Geohistory analysis, that is,the use of numerical stratigraphic techniques to unravel and portray geologic history, has important practical potential in the interpretation of geologic events and in the determination of geologic controls of oil and gas that are rate or age dependent. The quantitative approach allows the combination of a formations' burial and uplift history with heatflow models to calculate timing and duration of its passage through the oil window. The use of numbers rather than a multitude of names affords more disciplined geologic analysis and reasoning, facilitates computer applications, and, perhaps foremost, increases communication between members of an exploration team with different backgrounds such as micropaleontologist and engineers.

This manual presents the principles and basic applications of geohistory analysis and gives some schematized exploration examples.

Unreferenced figures and tables are from Van Hinte 1978, Van Hinte 1982 and unpublished lecture notes.

Jan E. van Hinte
Amsterdam May 1988
Oct-1989

CONTENTS

INTRODUCTION

ACKNOWLEDGEMENTS

A.1 BASIC PRINCIPLES AND TECHNIQUES OF GEOHISTORY ANALYSIS

A.1.1 HISTORY OF THE GEOHISTORY DIAGRAM

In his book 'Géologie du Bassin de Paris', Lemoine (1911) summarized the geologic history of the Paris Basin in a 'schema des mouvements d'ascension et de descente de la surface' (op.cit. Fig.136: diagram of rising and descending movements of the surface) combined with a 'schema de la descente generale du fond' (op.cit. Fig. 137: diagram of basement subsidence). See Figure A-1. Burollet (1956, Figs. 85-87) applied Lemoine's graphic approach to summarize stratigraphic conclusions for different sections in central Tunisia, entitling his diagrams 'variations de la profondeur des mers en Tunisie centrale en relation avec les mouvements de trefonds' (variations of the depth of the seas in central Tunisia in relation with the movements of the basement) See Figure A-2.

Diagrams such as these are an excellent method of portraying stratigraphic data and conclusions and provide a direct means of reading the timing and magnitude of geologic events. Quantification of paleontologic conclusions on age and environments now permits considerable refinement and the routine use of linear scales in such potrayals. Geohistory diagrams thus were developed and have been used in our work since 1970 (Ruffman and Van Hinte, 1971).

Philipp (1961) and later German petroleum geologists, following a personal suggestion by A. Roll, constructed burial history curves (Zeit-teufenkurve, Absenkingskurve) in connection with studies on maturation, migration and porosity prediction. They commonly used a linear time scale, and these plots were very similar to geohistory diagrams except that paleo-water depth was not taken into account and interest was focussed on geochemical and physical rather than geologic processes.

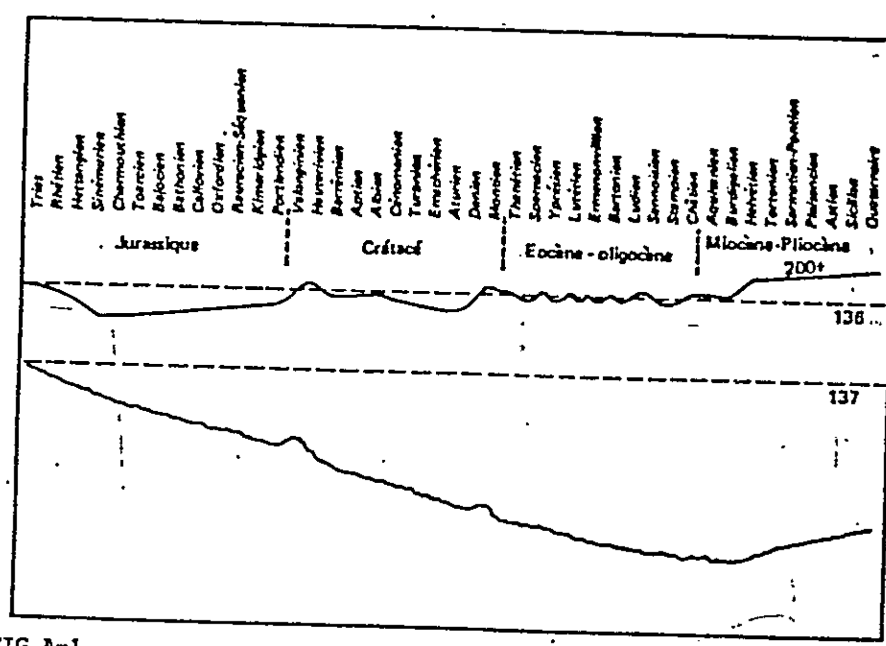

FIG A-1 Qualitative geohistory diagram for Paris basin as constructed by Lemoine (1911, Figs. 136, 137). Numbers 136 and 137 are added to Lemoine's figure, indicating two baselines he used: 136 shows water depth or elevation; 137 shows subsidence and uplift.

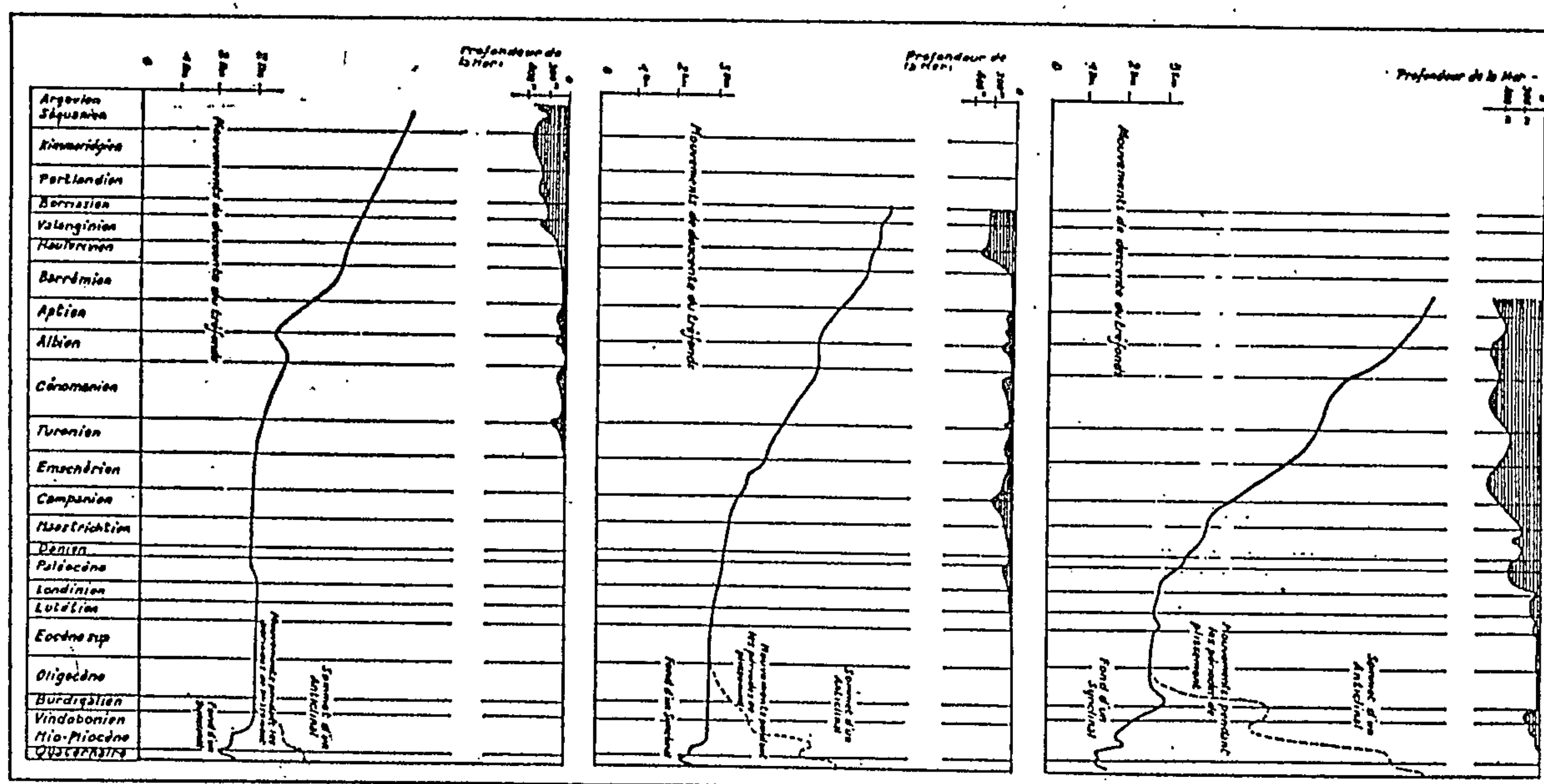

Profondeur de la Mer
Argovien
Séquanien
Kimméridgien
Portlandien
Berriasien
Valanginien
Hauterivien
Barrémien
Aptien
Albien
Cénomanien
Turonien
Emschérien
Campanien
Maestrichtien
Danien
Paléocène
Londinien
Lutétien
Eocène sup
Oligocène
Burdigalien
Vindobonien
Mio-Pliocène
Quaternaire

FIGURE A-2

A.1.2 NUMERIC STRATIGRAPHY

A.1.2.1 ADVANCES IN CHRONOSTRATIGRAPHIC RESOLUTION

Notably increased capability has been developed for a multiplicity of microfossil groups to determine the age of Mesozoic and Cenozoic sedimentary sections (Haq et al., 1988; enclosure 1) and to estimate the water depth at which beds were deposited. The use of numbers for paleontologic conclusions (e.g., age in years, and water depth in meters) lead to a new, numerical stratigraphy. Placing the geologic record of an area in a linear geochronologic framework brings the sequence of events into proper proportion and allows for calculating rates and magnitudes as well as for numeric modeling and graphic portrayal of geologic processes.

Also, 'standard' biostratigraphy zonations now are tied with greater precision to a linear, numeric time scale (Table A. 1a). Consequently, paleontologists can assign geologic ages accurately to most fossiliferous sections and can express these ages in megayears (1 megayear = 1 Ma).

The typical micropaleontologic biochronologic unit comprises about 1 Ma for the Cenozoic and about 2 Ma for the Mesozoic. Additional biohorizons and the integration of zonations of different fossil groups increase resolution. The correlation and zonal integration between different groups of age-significant microfossils is improving, as is their correlation with magnetic polarity reversals. Consequently, integrated schemes can approach a resolution of a few hundred ka (hundred-thousand years).

Within a biostratigraphically well-dated section, the extrapolation of sediment accumulation rates calculated between known magnetic_reversals permits age assignments in terms of 10 ka. And so does the recognition of cyclic variations in lithology, isotope ratios, or physical/chemical rock properties expressed on logs (Milankovitch cycles). Our limit of geologic time identification lies at the duration of events that are globally recognizable in the sedimentary record. A magnetic reversal takes appr. 1000 years, a significant global sealevel change may only take 50 years (change from glacial to non-glacial mode and v.v., or refill of salt basin) while the effects of an asteroid impact may be globally recorded over an even shorter span of time.

origin of LINEAR time scale

EXTRAPOLATION BETWEEN RADIOMETRIC AGES

assuming

EQUAL TIME PER STAGE
EQUAL TIME PER ZONE
CONSTANT ACCUMULATION RATE

marine aeromagnetics >>>>>> seafloor anomalies >>>>>> completion of and tie with magnetic reversal scale
CONSTANT SPREADING RATE
(Heirtzler scale)

DSDP >>>>>> biostratigraphic ages of magn. anomalies + improved zonations
CONSTANT SPREADING RATE
(Berggren, vHinte scales)

kryogene magnetometer >>>>>> direct tie biostratigraphy with magnetostratigraphy
CONSTANT ACCUMULATION RATES
>>>>>> high resolution, small scale proportionality to be tested/calibrated with astro-cyclicity

NEEDED: more radiometric ages.

Table A.1a

A.1.2.2 Advances in Paleobathymetric Resolution

Paleo-waterdepth determination is a highly complex art. The quantity and quality of knowledge on benthic microfossils from a greater variety of environments are increasing steadily - also, we now can obtain additional ecologic insight from diversity trends, distribution patterns, etc. of benthic microfossils. Recent oceanographic research has provided more reliable data on the depth distribution of plankton in the water column and has uncovered useful details on time-depth-related phenomena such as calcium carbonate dissolution. Further, when dealing with frontier material, paleontologists have to attempt to incorporate available knowledge on paleogeography and paleooceanography of the area. Although a certain amount of circular reasoning or even guessing is hard to avoid, a reasonable estimate of paleo-waterdepth usually can be made. Fortunately, in areas of intensive exploration where the explorationist needs more details, consideration of local geologic factors and paleontologic experience can make for sharper estimates.

Irreversibility of the evolution of the organic world is the basis for paleontologic dating of sediments. Organisms, however, not only occurred during a particular time but also lived in certain environments having their own habitat. Paleontologic well reports, therefore, should include conclusions on both age and environment of deposition of penetrated sections. In the present discussion, one aspect of the environment, paleobathymetry, is most important. Although the distribution of some species of assemblages seems to be related to depth per se (hydrostatic pressure), availability of direct depth indicators is limited so that paleobathymetric conclusions commonly are obtained indirectly.

Depending on the material at hand, a paleontologist may try one or more of the several available ways to determine the marine depositional-environment, qualitatively, by comparison with the modern occurrence of certain species or assemblages and by recognition of ecophenotypic trends (benthos and plankton), or, quantitatively, by determining relative frequencies (e.g., plankton/benthos, arenaceous/calcareous forams, percentages of radiolarians or ostracods), species number, species dominance, species diversity, coiling ratio, sex ratio, ontogenetic age, and, for deep-water deposits, solution facies. Thus, he obtains an idea about one or a combination of environmental factors which may be chemical (salinity, pH, availability of oxygen, nutrients, carbon dioxide), physical (temperature, substratum energy level, light penetration, turbidity, circulation, barriers), or biological (intracommunity, intercommunity, plants). Many of these factors can be depth indicators, and the better we know the paleo-oceanographic conditions, the better we can determine to what degree 'cool', 'dark', or 'euxinic' means 'deep'.

Paleo-waterdepth estimates can be quite accurate in areas where the recent faunal distribution, fossil record, and regional geologic history are well known (e.g., the Gulf Coast). Elsewhere, waterdepth estimates may have to be somewhat less precise, the older the sediments the more speculative the paleodepth determinations become. The accuracy with which paleo-waterdepth determinations can be made in frontier areas is indicated in Fig. A-4. The resolution may seem too general to be of practical use, but it should be realized that, although individual determinations may be inconclusive, a succession of determinations (e.g., based on side-wall cores in a well) shows a trend through which a line can be drawn establishing with some confidence relative changes in water depth between parts of the section (eg., see Fig. A-5).

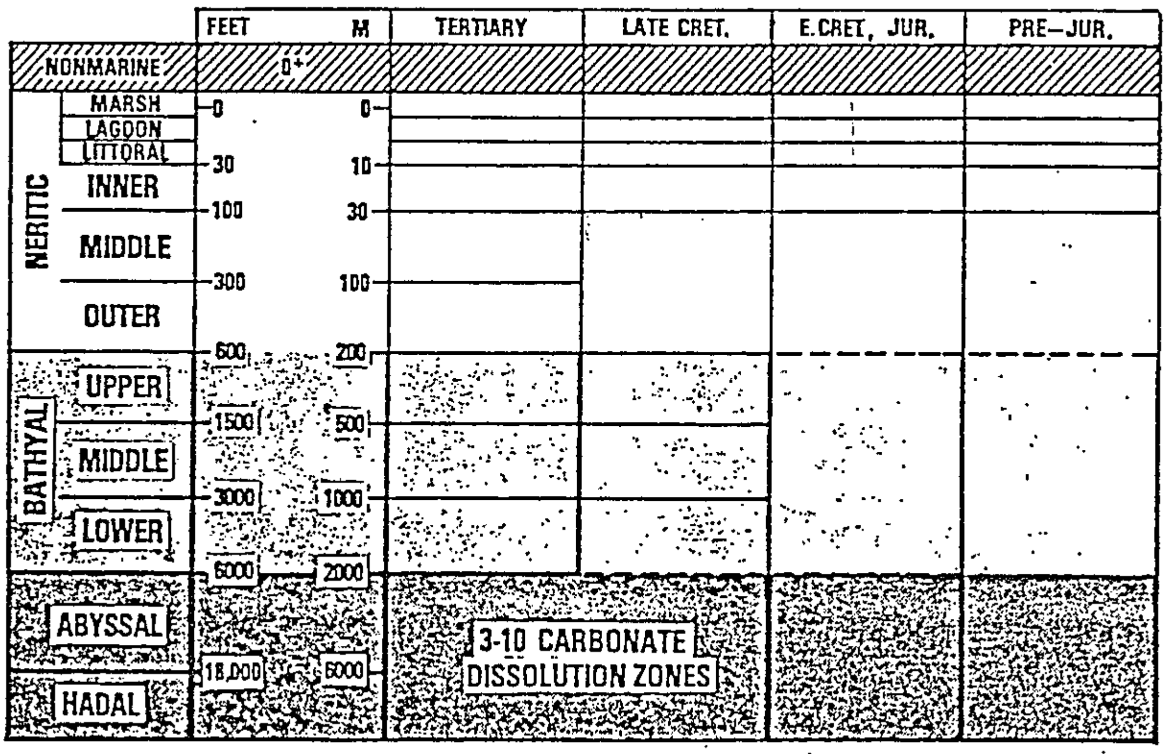

FIG. A-4 - Approximate micropaleontologic paleobathymetric resolution using forams, ostracods, and microfacies. Pre-Tertiary sections deposited under particular conditions (e.g., carbonate shelf) may be interpreted with greater precision than shown.

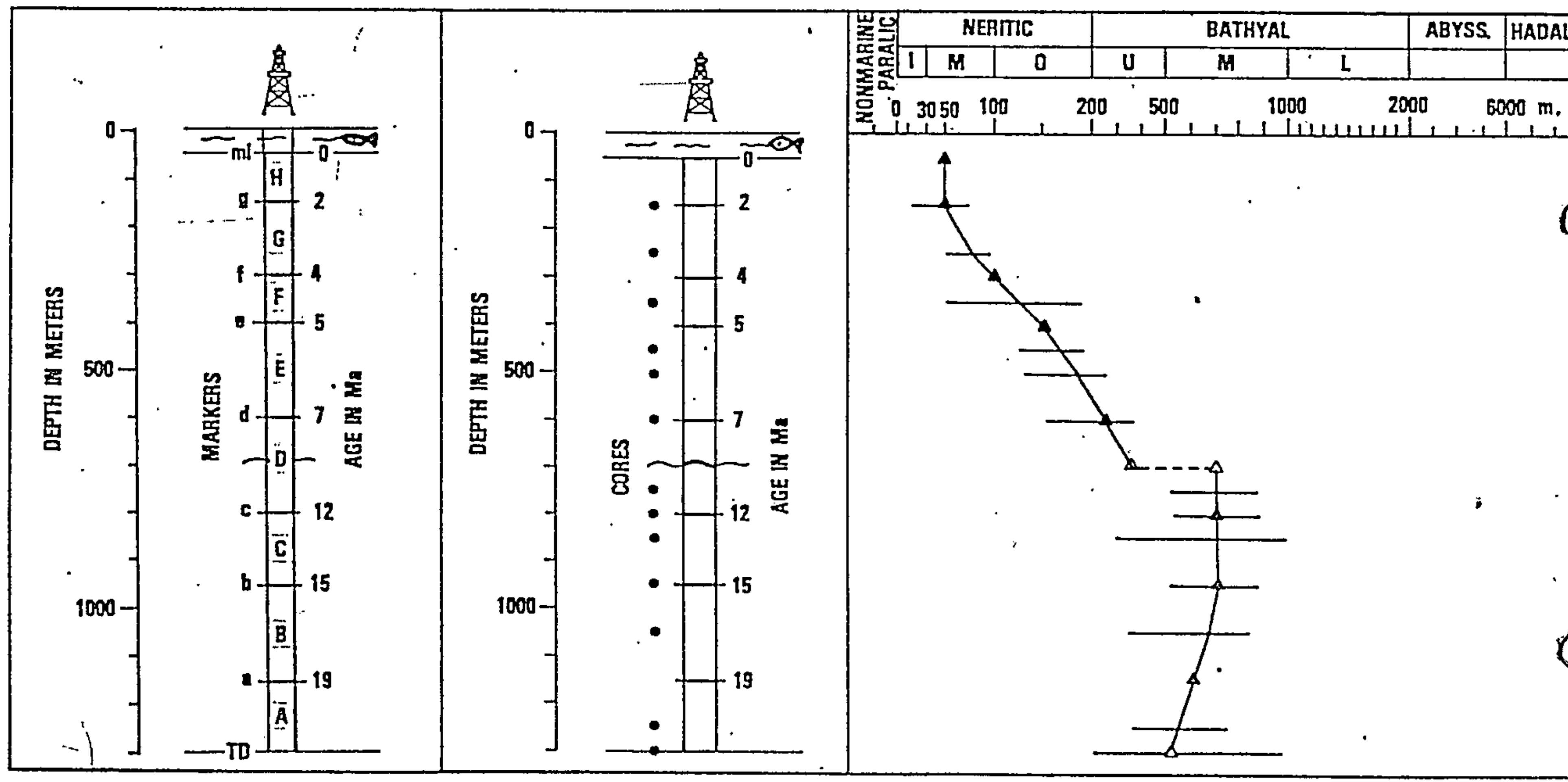

Fig A-5 : Left hand figure shows a hypothetical well section. Markers may be index fossil tops, log picks etc. Units between markers are referred to by capital letters. Centre figure shows core samples. Palybathymetric determinations for cores are shown at right as bars. Triangles show paleontologists best fit guess of paleobathymetry (NB. this may not always be centre of bar, eg., for cuttings study).

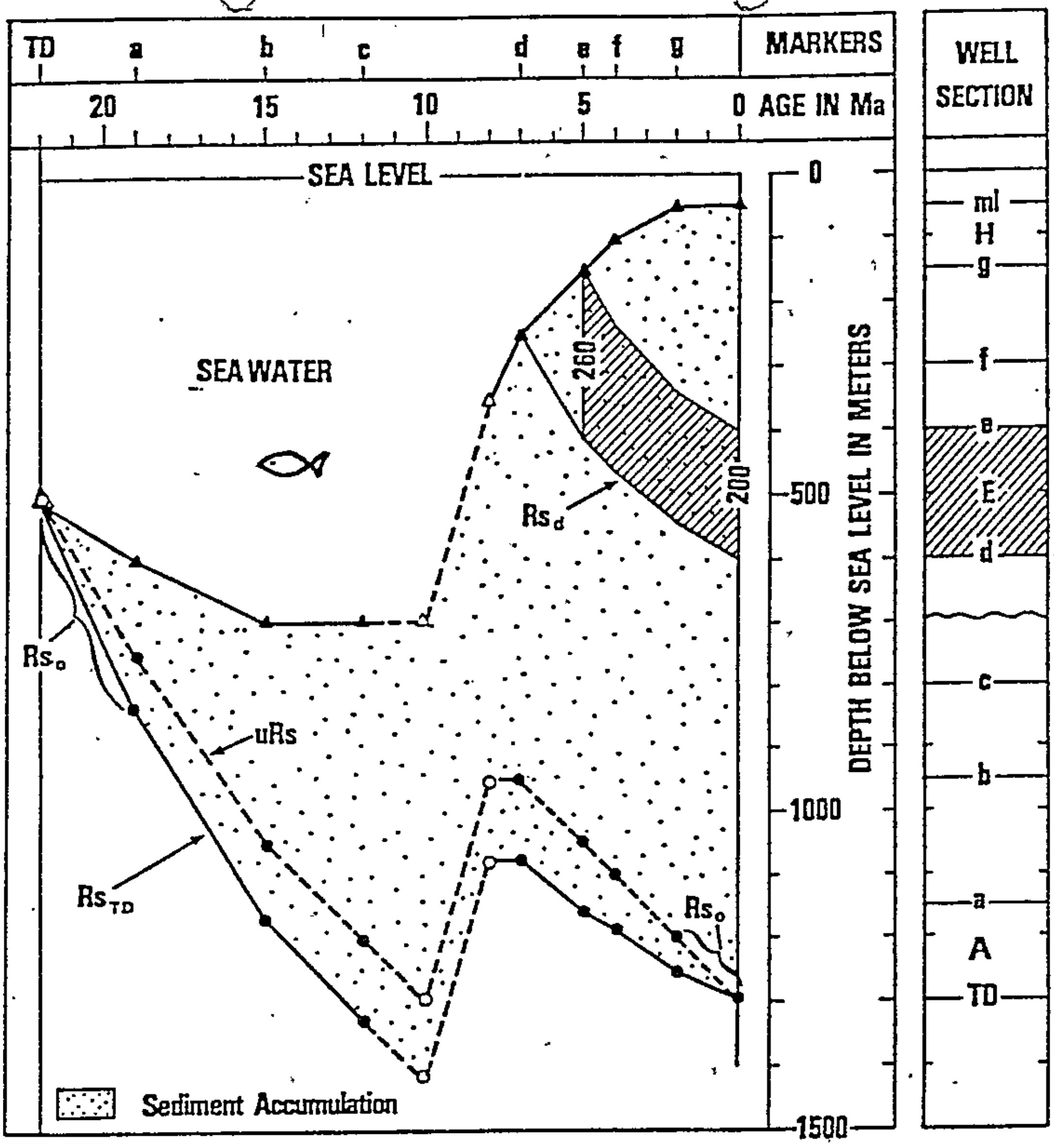

FIG. A-6—Geohistory diagram for hypothetical well of Figure A-5.
Upper curve shows water-depth history for location; lower curves show subsidence and uplift at that location. Shaded path shows subsidence and reduction in thickness of unit E. For further explanation, see text.

A.1.3 THE GEOHISTORY DIAGRAM

A.1.3.1 Construction of an uncorrected Geohistory Diagram

Numerical geologic time, coupled with direct geologic measurements (e.g., interval thickness) and interpreted data (e.g., paleo-waterdepth), permits the expression of significant stratigraphic conclusions in quantitative terms. For example, we can now determine rates of fill, subsidence, or uplift, and can estimate the time span of unconformities, the amount of removed section, or the rate of fluid expulsion. This will be discussed in detail in a later section.

The same significant stratigraphic conclusions can be presented graphically and portray the timing and magnitude of geologic events and processes, and permit (by extrapolation) estimates on unknown parts of the section.

The data shown in Figure A-5 can be used to construct a time/depth plot with a linear time scale as the horizontal axis and a depth scale as the vertical (Fig. A-6). First, the paleobathymetry at the time of the datum levels is determined from the paleodepth curve (solid triangles, Fig. A-5), these water depths then are plotted against the linear scales (solid triangles, Fig. A-6). Next, the ages at total depth (TD) and at the unconformity are determined by extrapolation of sedimentary-accumulation rates, and their paleobathymetry is plotted (open triangles). Finally, the cumulative thickness for each level is plotted on the graph as solid and open circles.

A.1.3.2 Applications of the uncorrected Geohistory Diagram

The inclusion of a geohistory diagram in a paleontologic well report has the following obvious advantages.

1. The construction itself forces the biostratigrapher to be aware of the geologic implications of his conclusions. He sees, for example, where more data are needed, what the consequences are of reporting an unconformity, and which of his interpretations do, and which do not, make geologic sense. For example, when a displaced shallow-water fauna is not recognized as such, it will plot too high on the diagram, and consequently the subsidence curve will show an uplift 'kick'.

2. Comparisons between wells and areas are possible at a glance.

3. The diagram forms a convenient linear time-depth frame for the geologist to plot other parameters, such as heat-flow data, porosity changes, and mineralizations.

4. Generalized diagrams are most informative models of basin evolution, tectonic style, continental-margin history, etc.

5. Extrapolation of the curves fills gaps in cases of fragmentary information.

A.1.3.3 Examples of Geohistory Analysis (uncorrected)

A.1.3.3a Interpretation of Presumed Unconformity

Paleontologic analysis of two Gulf Coast wells shows a marked break in paleobathymetry (Fig. A-7), which raises the question of whether this represents an unconformity and, if so , how much section is missing. No markers were found at the presumed unconformity (Fig. A-7a). Extrapolation of the uncorrected rate of sediment accumulation (uR) above the break (calculated from 1.7 and 2.0 Ma) and below the break

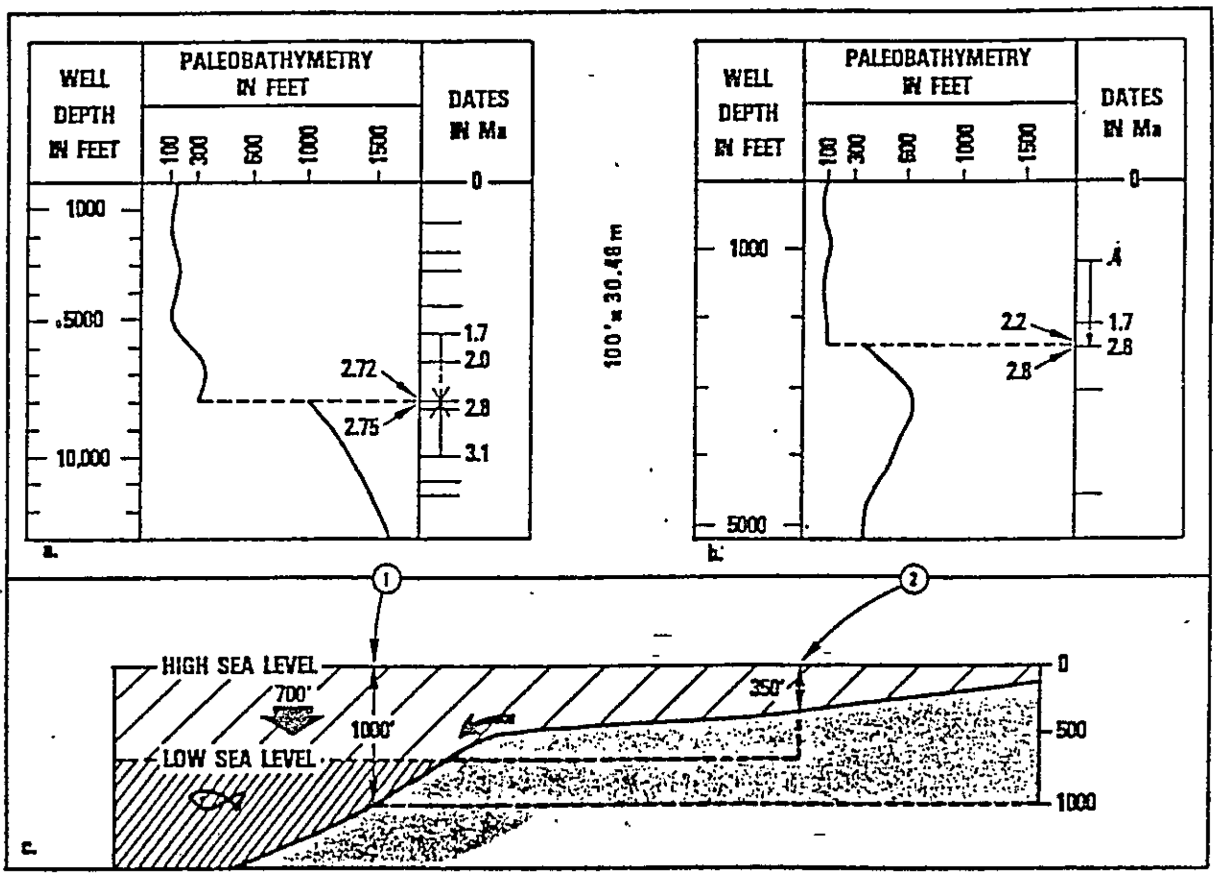

FIG A-7 Paleobathymetry curves and numerical age of markers for parts of two offshore Gulf wells a, well 1; b, well 2. Ages at break in water depth (2.72 and 2.75 Ma in well 1; 2.2 and 2.8 Ma in well 2) are derived from extrapolation of sediment accumulation rates. c, Schematic reconstruction of bathymetric profile at time of sea-level lowering to illustrate different effects of drop.

(calculated from 3.1 and 2.8 Ma) suggests 2.72 Ma and 2.75 Ma as the ages at the break. The difference of 30,000 years is negligible, and we conclude that the paleobathymetry break in well 1 represents a eustatic change in sealevel of 700 ft (213 m). In well 2, however, the water-depth break is only 250 ft (76 m, Fig. A-7b). The ages at the break are 2.2 and 2.8 Ma. The difference of 600,000 years is a considerable hiatus in this young section. A schematic reconstruction for the time of sea-level drop is shown in Figure A-7c. Sediments were being deposited in 1,000 ft (350 m) of water at well 1, so the 700-ft (200 m) drop in sea level did not necessarily disrupt sedimentation. At well 2, however, lowering of the sea level by only 350 ft (107 m) would have exposed the shelf and caused an unconformity. We may asked how much section was eroded at well 2. The sea-level drop occurred at 2.75 Ma or somewhat later if the calculation of 30,000 missing years for well 1 is correct, so at well 2 at least 50,000 pre-event years are not represented. With sediment accumulating (uR) below the break at a rate of 25 cm/1,000 years, substitution in Equation A-2 of the next section reveals that the equivalent of a present thickness of 12.5 m (about 40 ft) was deposited and subsequently eroded.

A.1.3.3b Depiction of Structural Style and Timing

The directness with which structural style and timing can be portrayed is illustrated in Figure A-8. An Exxon Company U.S.A. paleontologic study of three wells drilled offshore from Louisiana in an area underlain by mobile shale (Fig. A-8a) provides age and environmental interpretations from which geohistory diagrams were constructed (Fig. A-8b-d), the major sea-level drop at 2.8 Ma was taken into account.

It is readily apparent that sites 1 and 2 continuously subsided at a rapid rate during the past 4 Ma. Site 3, however, remained high while the surrounding area subsided, later this site even showed some uplift as a response to rapid loading. During the past 0.5 Ma, site 3 subsided at a rate more than 1.5 times greater than the regional rate at the other two sites. The cause of this seemingly excessive rate may be interpreted as either fluid release from the shales or shale withdrawal. Regardless of which interpretation is accepted by the regional geologist, the paleontologist has provided him with a clear picture from which to start.

Smaller differences in the slope of subsidence curves (Fig. A-8) are hard to evaluate visually, therefore, when different wells are compared, bar diagrams are useful (Fig. A-9). Local sharp changes in rates shown by these graphs probably are due to movements and changes in density anomalies within the sediment column. For example, the initial high rates at site 1 clearly are due to growth-fault activity (Fig. A-8a) and the high rate between 1 Ma and 2 Ma at site 2 could be caused by withdrawal and be coincident with the uplift of site 3.

Apart from changes in rates that occur at the different locations at different times, all three sites simultaneously show an acceleration in the average sediment accumulation and subsidence rates for the latest 0.5 Ma. This acceleration also was observed in other wells in the Gulf of Mexico and probably is a regional phenomenon related to massive deposition of glacial detritus from the continent. Although the rates are high at all three sites, they are low at sites 1 and 2 compared with site 3 (Fig. A-9). One could imagine that (1) rapid regional loading and subsidence possibly caused development of growth faults that functioned as fluid escape routes, enabling the shale dome to

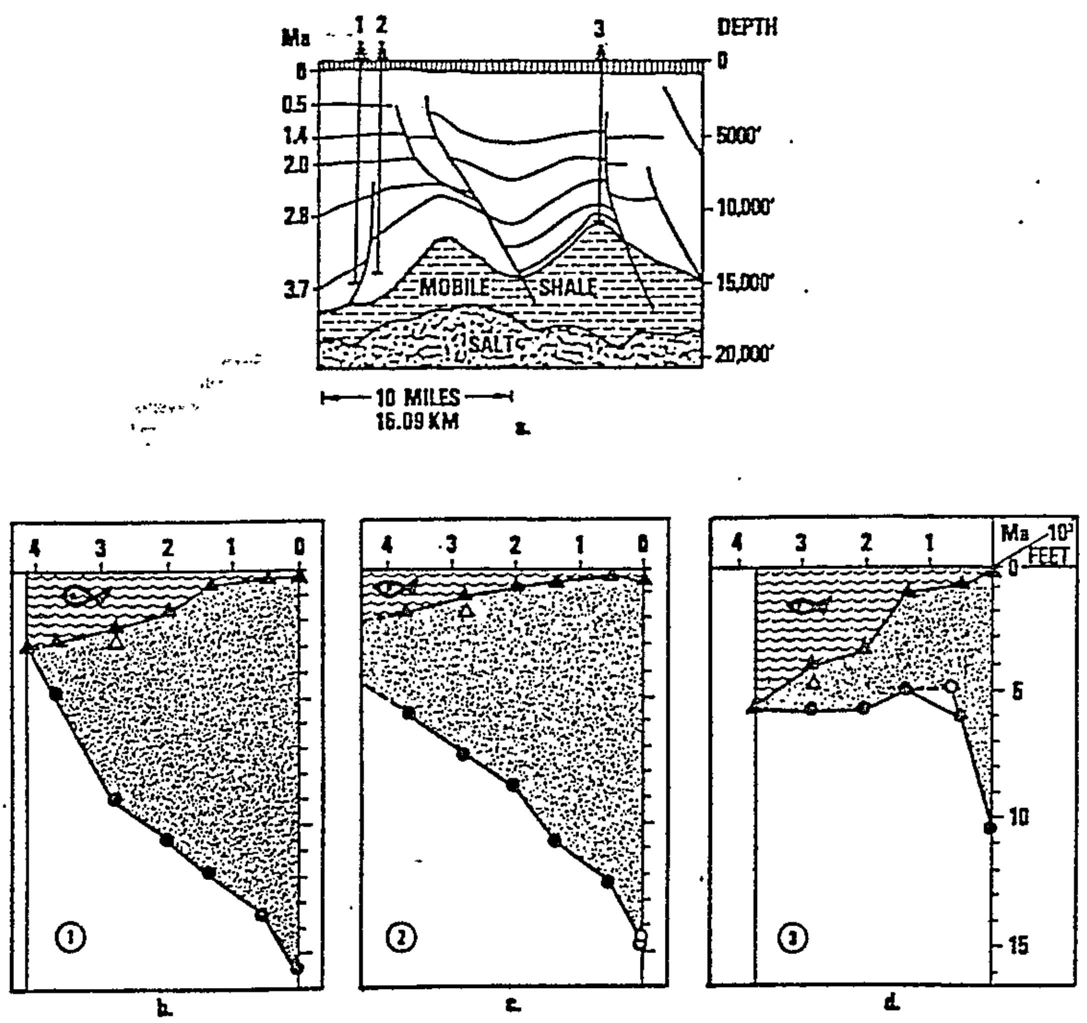

FIG. A-8 -a. Cross section in Mississippi delta area of offshore Louisiana based on seismic data and three wells. Ma numbers are megayears before present (1,000 ft = 304.8 m).
b-d. Geohistory diagrams for wells show that dome is suspended in sediment column where its top remains at about same level while surrounding area subsides.

collapse, or (2) redistribution of load (prograding depocenter) initiated the growth of younger domes that are withdrawing shale from the older ones. In either case, accelerated regional subsidence under the gigantic sediment load seems especially favorable here for petroleum accumulation, it brought sediments into warmer levels and triggered the collapse of overpressure, thus accelerating hydrocarbon maturation and initiating large-scale fluid migration.

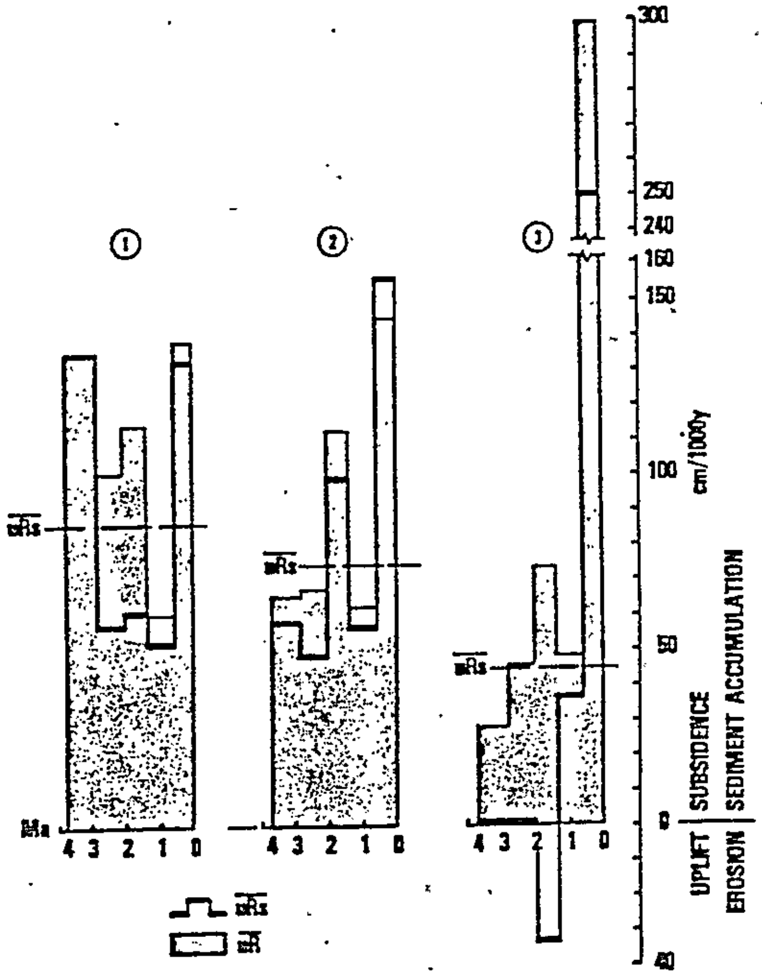

FIG A-9 -Bar diagrams showing rates of vertical movement and sediment accumulation for wells 1 to 3 of Fig A-8. Horizontal axis is linear time scale, and vertical axis shows rates of sediment accumulation and subsidence in cm/1,000 years. Width of each bar is determined by spacing of time markers. Mean rates of subsidence (uRs) for latest 4 Ma suggest that site 3 will continue to subside at higher than regional rate to catch up with "normal" area. That is, shales still are overpressured unless difference has been made up by sediment added from withdrawal toward site 3.

A.2 APPLICATIONS IN EXPLORATION GEOLOGY

A.2.1 SEDIMENT ACCUMULATION RATES

A.2.1.1 Determination of Accumulation Rates uR, Rf, and 'R'

Assignment of numerical ages to paleotops or other marker horizons enables the calculation of the average rate ('R') at which the sedimentary rock accumulated during the time interval bounded by the markers. The concept of accumulation is summarized in Table A-1.

R	=	average rate of sediment accumulation
	≠	rate of deposition
DEPOSITION	-	particle emplacement on sea floor
ACCUMULATION	-	sum of particle emplacement and removal over a longer period of time
ACCRETION	:	DEPOSITION > REMOVAL
EROSION	:	DEPOSITION < REMOVAL
SEDIMENTATION	-	overall process of transport, emplacement, removal, preservation.

TABLE A-1 : Terminology of sedimentation processes.

If the time span (A) of the interval is expressed in megayears and the thickness (T) in meters, then

$$'R' = \frac{T}{10A} \text{ cm/1,000 yrs.} \qquad \text{Eqn (A-1)}$$

In the example of Figure A-5, 100 m of sediment accumulated during the most recent 2 megayears (unit H, Table A-5) at an average accumulation rate of 100/(10 * 2) = 5 cm/1,000 years, or 'R' = 5. In the same example, 200 m of sediment between markers a and b was deposited during 4 Ma (unit B), also at an average of 5 cm/1,000 years.

Rates of deposition for unit B and H are not the same, however, because unit B is deeply buried and consequently is more consolidated than unit H. Thus, equation (A-1) should be modified to express the uncorrected rate (uR) as

$$uR = \frac{T_p}{10A} \text{ cm/1000 yrs} \qquad \text{Eqn (A-2)}$$

where T_p is present thickness. In other words, units should be restored to their original thickness (T_o) to obtain comparable rates of fill (Rf):

$$Rf = \frac{T_o}{10A} \text{ cm/1000 yrs} \qquad \text{Eqn (A-3)}$$

Rates so calculated, however, still do not fully represent the sedimentation process because thick units (as a whole) have lower initial porosity than thin units, inasmuch as their own load results in increased compaction downward. Consequently, neither uR nor Rf can be used to compare rates of sediment accumulation for units having different initial thicknesses and depth of burial. A 'pure' rate of sediment-mass accumulation can be calculated from the net thickness (T_n, porosity = 0) of a unit:

$$R_{\phi=0} = \frac{T_N}{10A} \text{ cm/1000 yrs} \qquad \text{Eqn (A-4a)}$$

If present porosity is p, this expression can be written as:

$$R_{\phi=0} = \frac{T_p(1-p)}{10A} \text{ cm/1000 yrs} \qquad \text{Eqn (A-4b)}$$

Of course, accumulation rates also are comparable if they all are converted to the same shale porosity - for instance, if porosity = a,

$$R_{\phi=a} = \frac{T_N}{10A(1-a)} \text{ cm/1000 yrs} \qquad \text{Eqn (A-4c)}$$

or, if present porosity = p,

$$R_{\phi=a} = \frac{T_p(1-p)}{10A(1-a)} \text{ cm/1000 yrs} \qquad \text{Eqn (A-4d)}$$

Equations 4a and 4b are the special case when a=0.

Table A-2 summarises these rate equations. Figure A-10 shows the effect of compaction on a shale bed while Figure A-11 shows the relationship between initial thickness and net thickness. Figure A-12 shows compaction in terms of porosity change, while Table A-3 gives some equation forms of these changes. Table A-4 gives averaged porosity changes in a compacting section. Figure A-13 is a nomogram of thickness versus burial depth.

Assume that the example of Fig. A-5 is a normally pressured clay-shale section. Then, an estimate for the porosity of the units (from Table A-4) gives the net thickness (T_n), which in turn (using Fig. A-11) gives an estimate of the initial thickness (T_o, Table A-4). For example, the porosity of the 100 m thick unit F is estimated as 0.373 (Fig. A-11) and T_n

= (1 − 0.373) * 100 m = 63 m (or 207 ft). The dashed line on Figure A-11 shows the initial thickness to be 375 ft (115 m). Values derived from the nomogram of Figure A-13 (based on data from a different basin) are considerably higher (see Table A-6) which suggests that, if available, local empirical data should be used as a basis for correction.

Table A-5 lists the three kinds of average accumulation rates calculated separately using equations A-2, A-3 and A-4a respectively. The differences in rates obtained by the three methods of calculation emphasize the need to apply rate equations consistently with due regard for assumptions inherent in each.

The volume reduction (consolidation, compaction) is difficult to generalize for sandstone and limestone because sorting, solution, crushing, and cementation play varying roles and their timing and intensity are unknown.

These reductions are not considered in the present general discussion. However, they should not be ignored in detailed studies (Chilingarian and Wolf, 1975 : Shinn et al, 1977).

TABLE A-2 RATES OF SEDIMENT ACCUMULATION

UNCORRECTED	$uR = \frac{T_p}{10A}$ cm/1000 yrs
RESTORED (rate of fill)	$Rf = \frac{T_o}{10A}$ cm/1000 yrs
'PURE'	$R_{\phi=0} = \frac{T_N}{10A}$ cm/1000 yrs
or	$R_{\phi=a} = \frac{T_p(1-p)}{10A(1-a)}$ cm/1000 yrs

where

T_p = present thickness
T_o = original thickness
T_n = net thickness

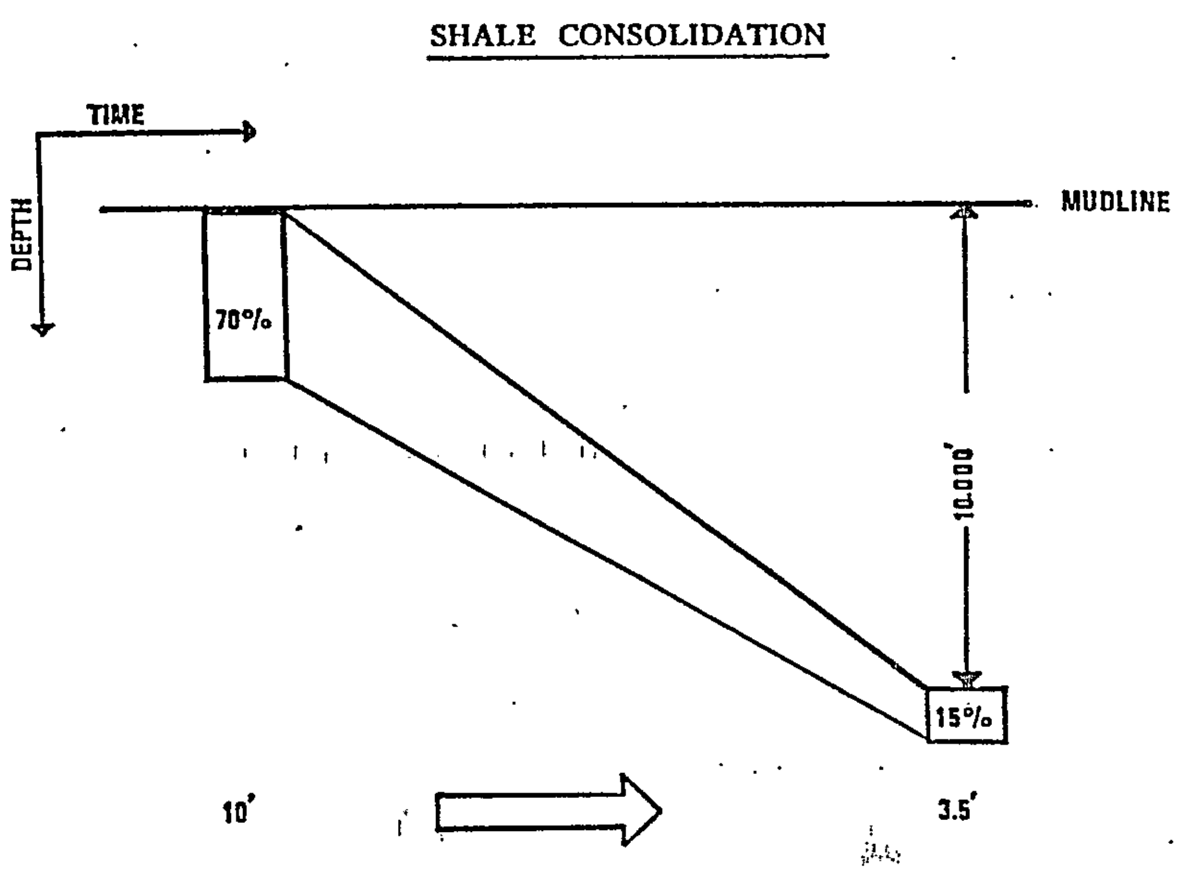

FIGURE A-10

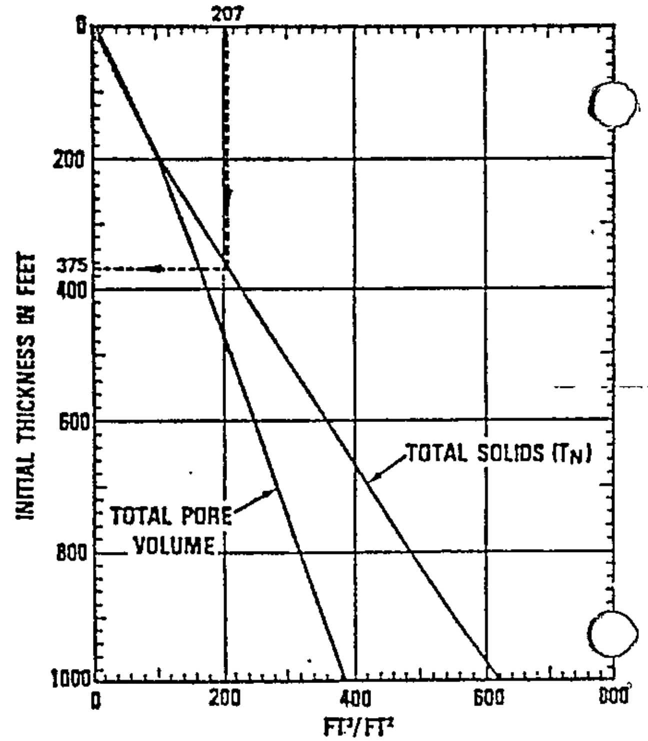

FIG A-11 –Relation between total pore volume, net thickness (T_N), and initial thickness (T_o) of shales (from Gretener and Labute, 1969, Fig. 2). 100 ft = 30.48 m.

FIGURE A-12

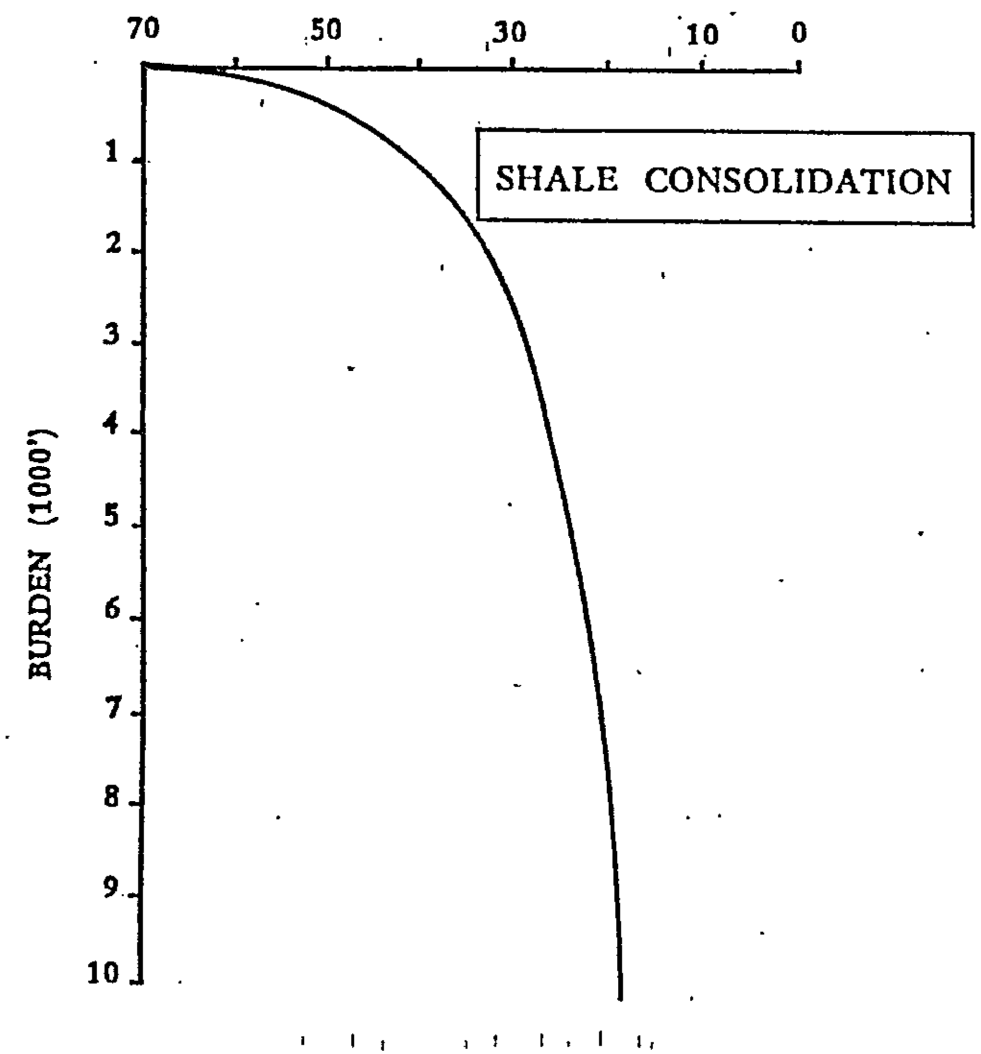

TABLE A-3

CORRECTIONS FOR COMPACTION

ϕ = porosity   z = depth in kilometres

A. Hardenbol et al (1981).

$$\phi(z)_{shale} = \frac{0.7}{1 + z}$$

$$\phi(z)_{sand} = 0.38 \exp(-0.05 * z)$$

Carbonate : Micrite - 65% shale + 35% sand.
Grain - 30% shale + 70% sand.
Reef - 100 % sand.

B. Falvey and Middleton (1981), Falvey and Deighton (1982)

$$\frac{1}{\phi_z} = \frac{1}{\phi_o} + kz$$

	ϕ_o	k (km^{-1})
Shale :	0.7	2.43
Sand :	0.4	1.20
Silt :	0.53	2.18

φ	DEPTH METER	AVERAGE UNIT φ PER 50 M	PER 100 M	PER 200 M
.490	0	.4730	.4598	.4384
		.4465		
.436		.4265	.4170	
		.4070		
.400	200	.3920	.3855	.3735
		.3790		
.373		.3670	.3615	
		.3560		
.351	400	.3463	.3415	.3323
		.3368		
.332		.3275	.3230	
		.3185		
.314	600	.3098	.3055	.2973
		.3013		
.297		.2930	.2890	
		.2850		
.281	800	.2773	.2735	.2663
		.2698		
.266		.2625	.2590	
		.2555		
.252	1000	.2488	.2455	.2393
		.2423		
.239		.2360	.2330	
		.2300		
[illegible]	1200	.2243	.2215	.2163
		.2188		
.216		.2135	.2110	
		.2085		
.206	1400	.2035	.2010	.1963
		.1985		
.196		.1938	.1915	
		.1893		
.187	1600	.1848	.1825	.1783
		.1803		
.178		.1760	.1740	
		.1720		
.170	1800	.1680	.1660	.1623
		.1640		
.162		.1603	.1585	
		.1568		
.155	2000			

φ	DEPTH METER	AVERAGE UNIT φ PER 50 M	PER 100 M	PER 200 M
.155	2000	.1533	.1515	.1483
		.1498		
.148		.1465	.1450	
		.1435		
.142	2200	.1405	.1390	.1360
		.1375		
.136		.1345	.1330	
		.1315		
.130	2400	.1287	.1275	.1250
		.1263		
.125		.1238	.1225	
		.1213		
.120	2600	.1188	.1175	.1150
		.1163		
.115		.1138	.1125	
		.1113		
.110	2800	.1088	.1075	.1050
		.1063		
.105		.1038	.1025	
		.1013		
.100	3000	.0990	.0980	.0960
		.0970		
.096		.0950	.0940	
		.0930		
.092	3200	.0910	.0900	.0880
		.0890		
.088		.0870	.0860	
		.0850		
.084	3400	.0835	.0830	.0820
		.0825		
.082		.0815	.0810	
		.0805		
.080	3600	.0795	.0790	.0780
		.0785		
.078		.0775	.0770	
		.0765		
.076	3800	.0755	.0750	.0740
		.0745		
.074		.0735	.0730	
		.0725		
.072	4000			

TABLE A-4.—Shale porosity at increasing burial depth (according to Roll, 1974, Table I). Left column indicates porosity at 100-m intervals. Other porosity columns record average porosity for units 50, 100, and 200 m thick.

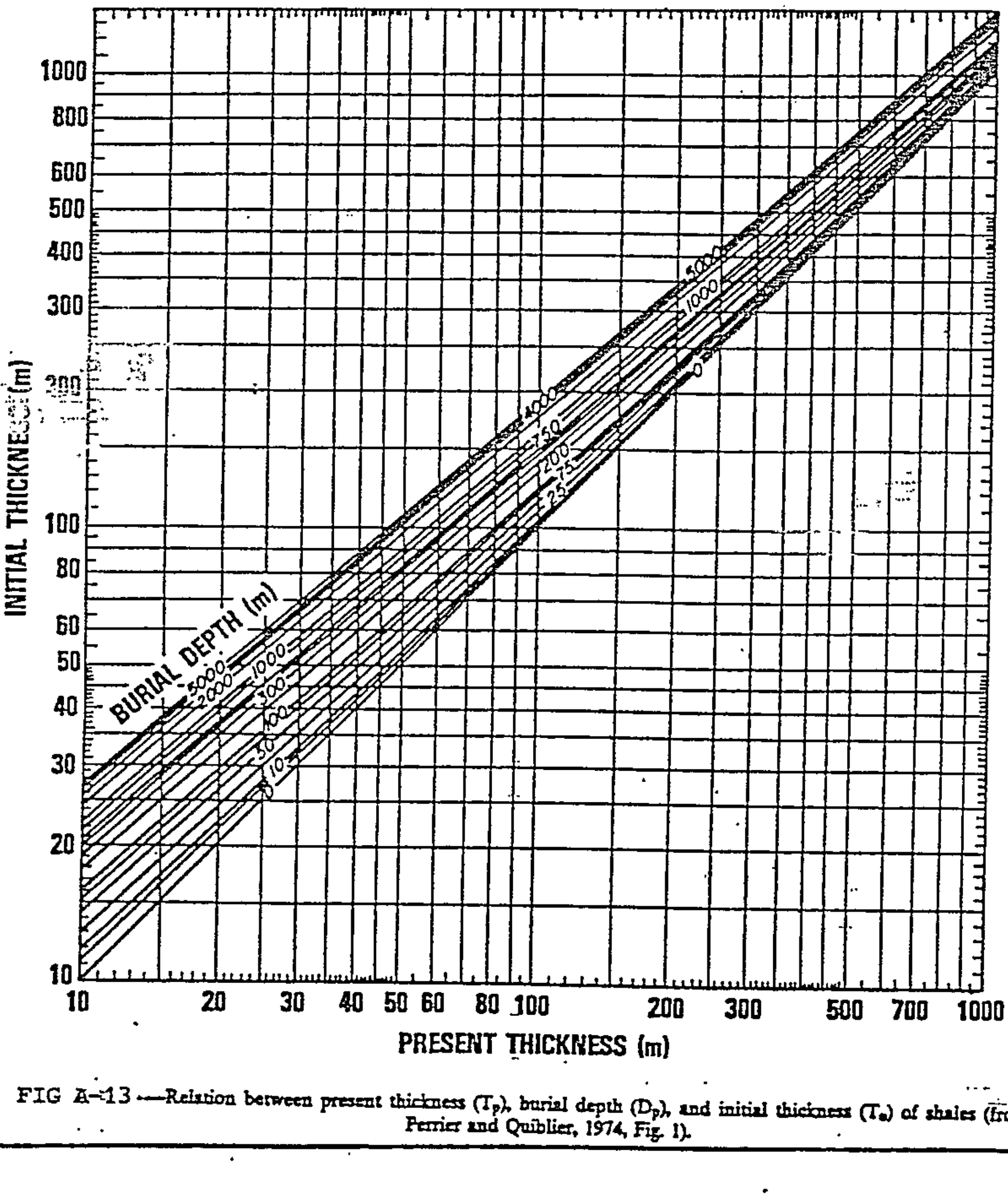

FIG A-13 — Relation between present thickness (T_p), burial depth (D_p), and initial thickness (T_o) of shales (from Perrier and Quiblier, 1974, Fig. 1).

MARKER	UNIT	THICKNESS IN M			ACCUMULATION RATES CM/1000y			ϕ	age
		T_p	T_o	T_N	R_u	R_f	R		
ml	H	100	100	54	5.00	5.00	2.70	.459	0
g	G	150	155	89	7.50	7.75	4.45	.409	2
f	F	100	115	63	10.00	11.50	6.30	.373	4
e	E	200	220	132	10.00	11.00	6.69	.342	5
d	D	200	230	139	4.00	4.60	2.78	.306	7
c	C	150	180	108	5.00	6.00	3.60	.277	12
b	B	200	255	150	5.00	6.38	3.75	.252	15
a	A	150	185	116				.230	19
TD									

TABLE A-5 Thickness and sediment-accumulation rates for well units shown in Fig A-5. T_p is present thickness; T_o is initial thickness; T_N is net thickness.

	H	G	F	E	D	C	B	A	
H	100								
G	150	180							
F	100	110	140						
E	200	205	225	260					
D	100 / 200 / 100	102 / 206 / 102	105 / 210 / 105	114 / 230 / 116	150 / 280 / 130 150				
C	150	152	155	160	170 (185)	220			
B	200	202	205	210	215 (220)	235	290		
A	150	151	152	165	165 (170)	175	185	235	
ΣT_{R_i}	1250	1205	1067	1015	830 (730)	630	475	235	0

PRESENT THICKNESS
INITIAL THICKNESS
RESTORED THICKNESS

TABLE A-6—Present thickness, initial thickness, and restored thickness for units in hypothetical offshore well (Fig. A-5 Letters across top of diagram indicate time at end of unit deposition; letters at left indicate unit. For example, at marker-g time (top of unit G), unit D was 205 m thick and the total section was 1,205 m thick. Numbers were obtained from nomogram of Fig. A-13.

A.2.1.2 Applications of Accumulation Rate Analyses

A.2.1.2a Single Site

Dating a section while it is being drilled and therefore knowing the sedimentation rates, has distinct advantages for well-site geologist. Application of this knowledge depends, of course, on the particular geologic or technologic questions involved. A few of the more common well-site application are discussed here.

1. Drill Time Prediction of Age or Thickness of Deeper Levels. It is possible to make a prediction of age or thickness ahead of the bit. By using equation 2, we can calculate estimates of the sedimentation rate and answer such questions as, 'At what depth will we reach the top of the Miocene?' or 'What is the age of the age of the reflector at 500 m?' For example, assume that drilling is at 450 m as shown in Figure A-5, and the question is: 'Will the reflector at 500 m be the expected top of unit D?' We are 50 m below marker e, and our latest uR is 10 cm /1,000 years - the top of D, by definition, is 2 Ma older than e. Hence, substituting in equation 2 gives 10 = Tp/(10 * 2), so Tp = 200 m, which indicates that we must drill 200-50 = 150 m before the top of D is reached. This depth, of course, is 1000 m deeper than the reflector. Then, what age is the reflector? Its depth below marker e is 100 m = Tp, substituting in equation 2 gives 10 = 100/10A, so A = 1 Ma. Because e is 5 Ma old, the reflector marks beds that are 5 + 1, or 6 Ma old.

2. Estimation of Age at TD. The same kind of extrapolation permits an estimate of the age at total depth in the absence of marker fossils. In our example of Figure A-5, uR above the lowest marker is 5 cm/1,000 years. Substituting in equation 2 gives 5 = 150/10A from which A = 3 Ma, and the age at total depth can be estimated to be 19 + 3, or 22 Ma. In the same way, the age can be estimated for any particular level below total depth (such as a seismic reflector). The basic assumption in these extrapolations is that no change in sedimentation rate occurs below (or above, in case of upward extrapolation) the last marker. This is a weak assumption, but comparisons with nearby wells may determine its reliability. Of course, extrapolation across different lithologic or seismic facies and across unconformities should be avoided.

3. Estimation of Time Span of Missing Section. A third application is to estimate the time span of missing section ('hiatus' of Mitchum et al, 1974, Vail et al, 1974, 'lacuna' of Wheeler, 1958). The age

of beds directly above and below an unconformity rarely is known precisely from marker fossils. Rather than simply guessing at what the magnitude of the unconformity might be within certain reasonable limits, we now can calculate an estimated age at the unconformity by extrapolating uncorrected rates of sediment accumulation (uR) downward and upward, respectively, from the nearest markers. Because of an unconformity at 700 m in the section of Figure A-5, the average rate of sediment accumulation for unit D (as given on Table A-5) is quite meaningless. What to do about it? An unconformity can be considered as the record of a geologic event. Thus, the section directly below an unconformity most likely was part of the sedimentary regime that prevailed prior to the event, and the section directly above an unconformity was part of the sedimentary regime that established itself after the event took place. From upward extrapolation of the uncorrected accumulation late (uR = 5 cm/1,000 years for unit C), the age at the unconformity is 12 - 2 = 10 Ma derived from substituting in equation 2,5 = 100/10A, A = 2 Ma. From downward extrapolation of uR (= 10 cm/1,000 years for unit E), the age at the unconformity is 7 + 1 = 8 Ma [10 = 100/10A, A = 1 Ma]. Hence, 10 - 8 = 2 Ma is missing.

If more wells have been drilled in the area, we may, for example, know that elsewhere the age span 7 to 12 Ma is missing, and somewhere else 7.5 to 9 and at the third location 8 to 10.5 etc. By combining this information, we can obtain an idea of when the event that caused the unconformity took place. In our example (Fig. A-14), it occurred about 8.5 Ma ago. Irregularities in the time span of the gap, like those in Figure A-14, may suggest that we are dealing with a tectonic event. To the contrary, one would expect a lacuna to decrease regularly in an offshore direction, suggesting that the event is a downward movement of base level (Barrell, 1917, Eicher, 1968) owing to a eustatic drop in sea level or other cause. Graphic extrapolation of such a situation may give a sharper estimate of the timing of the event (Fig. A-15).

4. Estimation of Thickness of Missing Section. Once the age of an event is known, we can estimate the amount of removed section ('erosional hiatus' of Mitchum et al, 1974, 'erosional vacuity' of Wheeler, 1958) by extrapolation of the pre-unconformity accumulation rate. We saw previously that in the case shown in Figure A-5, sedimentation continued until 8.5 Ma ago, that is 3.5 Ma after 12 (marker c) Where uR = 5, 3.5 Ma of deposition will

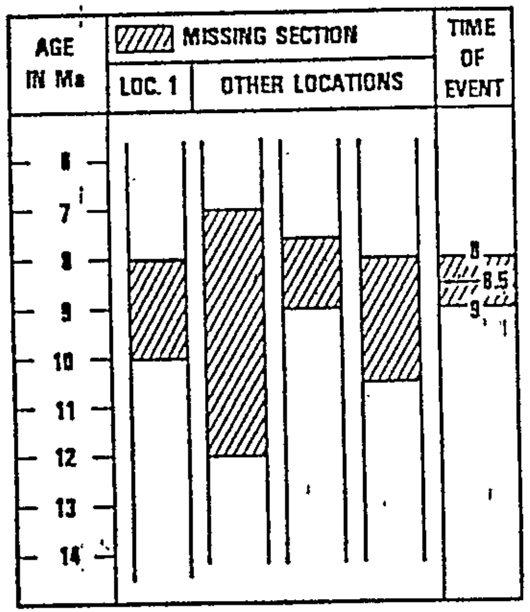

FIG. A-14 —Comparison of calculated estimates of missing section at various locations in one area. Such comparison permits reliable estimate of timing of event causing unconformity.

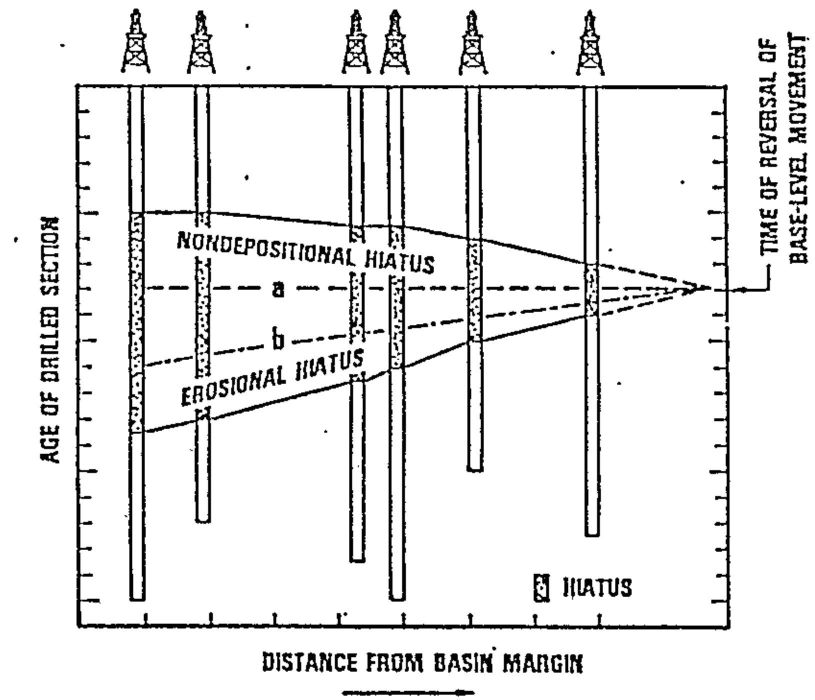

FIG A-15 —Derivation of time of reversal in downward base-level movement that caused unconformity of basinward-decreasing magnitude. Drawing line *a* as boundary between erosional and nondepositional hiatus assumes that base-level drop occurred within limits of time-stratigraphic resolution and appears as "instantaneous:" line *b* assumes that base level moved downward and upward at about same rate: first assumption generally is preferred (Frazier, 1974; Mitchum et al. 1974). Wheeler (1958) used terms "lacuna," "hiatus," and "erosional vacuity," respectively, for hiatus, nondepositional hiatus, and erosional hiatus. Broken lines at right of wells are extrapolation.

have resulted in 175 m of sediment accumulation, calculated 5 = Tp/(10 * 2.5), where Tp = 175 m. Of this 175 m, 100 m is now preserved – consequently 75 m has been eroded.

5. Identification of possible Eustatic Sea Level Changes. If an abrupt change in water depth occurs in a section, the procedure of point 3 can be followed downward and upward toward the break. Such a paleo-waterdepth break most likely records an eustatic change in sea level if no time gap is found – it could or could not represent such a change if an unconformity is present.

Examples 1 to 5 are applications at the well site where the initial thickness (T_O) or net thickness (T_N) cannot be determined because sandstone/shale ratios and shale porosities are unknown and uncorrected rate values (uR) must be used. This procedure is not a inaccurate as it may seem, because in each case the rates are extrapolated from one unit to its adjacent unit only – hence, compaction differences are mostly minor and errors tend to be small and irrelevant with respect to the accuracy of the method. The same holds for regional comparisons of uR's of similar formations at more or less equivalent burial depths, although in these cases the use of corrected values is more appropiate. Corrections for compaction are imperative, however, in other regional and in general applications.

A.2.1.2b Regional Interpretations

1. Rate-of-fill Contour Maps. Contour maps of rate-of-fill (Rf) values outline depocenters and other trends in the depositional environment for selected time intervals. Rate-of-fill maps have an advantage over isopach maps because a correction is made for distortion caused by regional variation in burial depth of mapped units. Rf values, however, are unit-thickness dependent, so that R(ϕ=a) has to be used to compare information on units of widely different initial thicknesses. Lithologic variation further complicates the picture. Thus, an area where initially a relatively thin but sandy section was deposited may appear as a 'thick' on an R-contour map if the unit is less sandy elsewhere.

2. R-contour maps independant of time and space. An R-contour map, therefore, may be similar to a sand-percentage map. The R map has the advantage that even though no sand is detected, trends show up that may lead to discovery of sand outside the mapped area. Further, an R map of, for example, a reservoir time-stratigraphic unit from offshore Louisiana can be compared directly with one

from Nigeria, regardless of differences between the two regions in age, thickness or sand percentage.

3. R-contour maps as source potential indicators The corrected average rate of sediment accumulation (R) is a meaningful sedimentary parameter for general studies. For example, in order to improve predictions on the presence of source rocks and their possible yield, one could investigate relations between hydrocarbon source potential (amount and type of organic matter) and accumulation rate of shales (Rogers and van Hinte, in press). Or, for example, regional R maps for large time slices can be compared with hydrocarbon occurrences. Depending on results of such studies, R may be recognized as a useful parameter in quantitative assessment techniques.

In any case, R is a highly informative number that should be considered in the description and classification of sediments. It ranges from >0.1 cm/1,000 years for red, deep-sea clay (Berger, 1974) to several meters /1,000 years for some deltaic deposits (cf. Fig. A-9). Anomalously low average numbers for a certain kind of sediment suggest the presence of unconformities - anomalously high numbers also can have important geologic implications that one might not recognize otherwise.

P[illegible]ROLEUM POTENTIAL
OF A TIME-STRATIGRAPHIC UNIT
DEPENDS ON:

R → SEDIMENT VOLUME
THERMAL MATURATION
ORGANIC CONTENT
- volume
- type of organic matter
- R → degree of degradation (of preserved OM)

R-TOC Relationship fine grained sediment

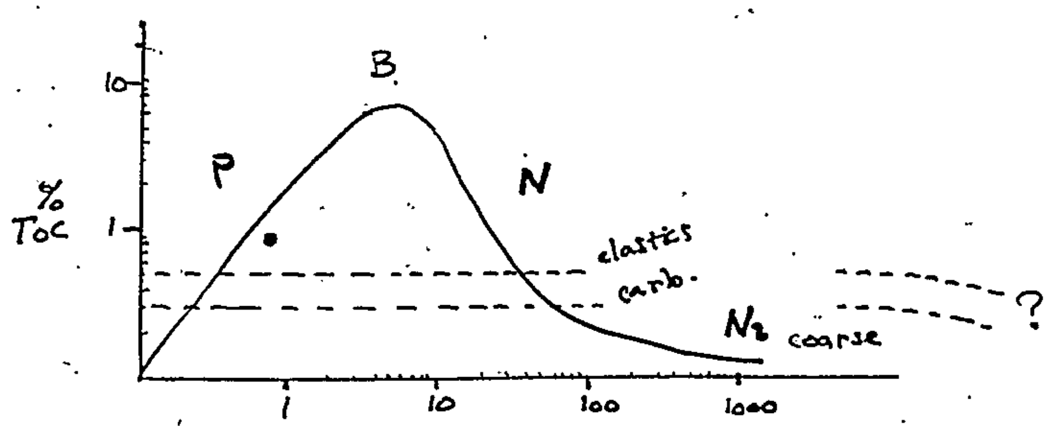

Positive: decreased biodegradation time
Negative: grain dilution; high quality
N_2 - lots of it → source potential?
B - breakpoint differs per lithology

JOHNSON I BACH '82

BE CAREFULL
WITH AVERAGE RATE OF SED. ACC.

R=2.5

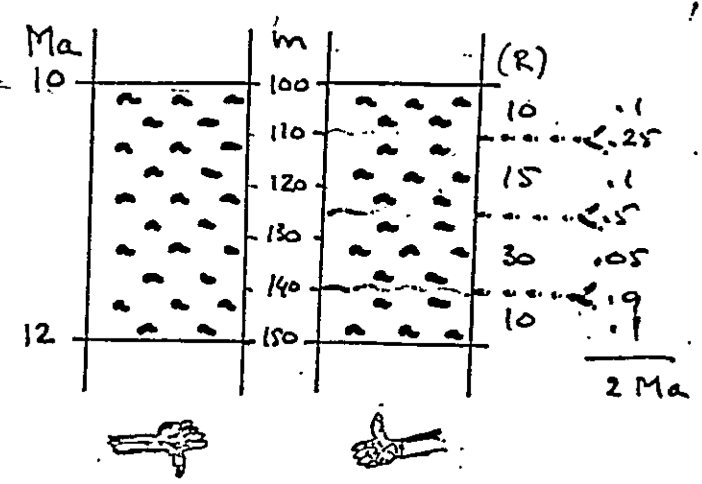

A.2.2 SUBSIDENCE RATES

A.2.2.1 Determination of Subsidence Rates

Assume that during the past 2 megayears the waterdepth did not change at the location of Figure A-5. This would mean that in order to accommodate the sediments of unit H, the site must have subside 100 m with respect to sea level. If, however, shoaling or deepening had occurred, the amount of subsidence would have been, respectively, less than or greater than the sediment thickness (see Bandy and Arnal, 1960). What holds for the amount of subsidence is also valid for the rate, which can be written as

$$'Rs' = 'R' - \frac{A(W + E)}{10A} \text{ cm/1,000 yrs.} \qquad \text{Eqn (A-5)}$$

in which W is the change in water depth, and E is the eustatic sea-level change during deposition of the unit. Deepening from 0 to -50 m would mean that W = -50, in the same sense a eustatic rise in sea level of 20 m would make E = -20.

In the preceding example 'Rs' is 5 cm/1,000 years. That is, during the time of deposition of the unit, its base went down (subsided) at an average velocity of 5 cm/1,000 years. To obtain a comparable subsidence rate for older units, the thickness prior to compaction, or initial thickness To is used.

$$Rs_o = \frac{T_o - A(W + E)}{10A} = Rf - \frac{A(W + E)}{10A} \text{ cm/1,000 yrs.} \qquad \text{Eqn (A-6)}$$

Use of present thickness (Tp) for units other than the highest one would give uncorrected rates that are lower than Rs_o:

$$uRs = \frac{T_p - A(W + E)}{10A} = uR - \frac{A(W + E)}{10A} \text{ cm/1,000 yrs.} \qquad \text{Eqn (A-7)}$$

Subsidence at or near the surface is not caused exclusively by subcrustal forces but includes the effects of loading: (1) compaction of the underlying section ('pseudosubsidence' of Roll, 1974), and (2) isostatic adjustment. The calculated Rs_o value, therefore, applies only to the base of a unit. Deeper levels at that time subsided at a slower rate, because lower section was being less compacted, and higher units, of course, did not exist. The calculated uRs value is the rate at which all levels subsided during that time and is 'correct' only if the entire section consists of noncompactible sediment. Fortunately, more and more empirical compaction data are becoming available for estimating the subsidence rate of any chosen level in a compacting section (Rs_n). Knowing the compaction also allows for distinguishing the 'tectonic' subsidence rate (R_T), which

	UNIT	AGE A	T_p	T_e	WATER DEPTH W	uRs $\frac{T_p-(W+E)}{10A}$	Rs_o $\frac{T_e-(W+E)}{10A}$	FOR TD D_R ΔD	FOR TD Rs $\frac{\Delta D-(W+E)}{10A}$	FOR e D_R ΔD	FOR e Rs $\frac{\Delta D-(W+E)}{10A}$	DURING ML ΔTR $(TR_{ml}-TR_i)$	DURING ML Rc_{ML}
1250		0			50			1250		350			
	H	2	100	100	0	5.0	5.0	45	2.25	60	3.0	(150)	(7.5)
1150		2			50			1205		290			
	G	2	150	180	50	5.0	9.0	118	3.4	150	5.0	30	1.5
1000		4			100			1087		140			
	F	1	100	140	50	5.0	14.0	72	2.2	140	9.0	10	1.0
900		5			150			1015		0			
	E	2	200	260	100	5.0	13.0	185	4.25			5	.25
700		7			250			830					
		(1)	(100)	(150)	100	0	5.0	100	0				
600	D	(8) (10) (2)	200	280	350/700 < 350	-5.0 -17.5	-1.4 -17.5	730	-5.0 -17.5			5	.10
		(2)	(100)	(155)	0	5.0	7.75	100	5.0				
500		12			700			630					
	C	3	150	220	0	5.0	7.33	155	5.16			2	.06
350		15			700			475					
	B	4	200	290	-100	7.5	9.75	240	8.5			2	.05
150		19			600			235					
	A	(3)	150	235	-100	8.33	11.16	235	11.16			1	.03
		(22)			500			0					

TABLE A-7—Different "average rates of subsidence" and average rate of compaction. Numbers needed to calculate rates for hypothetical well shown in Fig A-5. are given. T_p = present thickness; T_o = initial thickness; W = change in water depth; E = eustatic sea-level change; A = duration of unit; uRs = uncorrected subsidence rate; Rs_o = initial rate of subsidence; Rs_{rn} = rate of subsidence at base of section; D = burial depth (= Σ TR, in which TR is restored thickness); Rc = rate of compaction. Ages at unconformity in unit D are discussed in paragraph on applications of sediment accumulation rates.

may be entirely a result of isostasy or of isostasy together with other basement-involved and/or basement-uninvolved structuring.

For example, Table A-6 gives, step by step, the loading effect of the deposition of each new unit on the section below it. The estimates are made using the nomogram of Figure A-13 and assuming 100% shale. We now can read the restored thickness (TR) for any part of the section at any of the marker times. For example, 5 Ma ago, at time e, unit D was 230 m thick (TR_{De} = 230 m), and the entire section at that time was 155 + 210 + 160 + 230 + 260 = 1,015 m thick (TR_i = 1,015 m, i = a through e). That is, this is the depth of burial of TD at time e, or D_{TD}. The actual subsidence of a particular level (n) can be expressed as its increase in burial depth minus the water-depth change, so that

$$Rs_n = \frac{\Delta D_n - \Delta(W + E)_n}{10A} \text{ cm/1000 yrs} \qquad \text{Eqn (A-8)}$$

'Rate of subsidence' stands for 'average rate of subsidence with respect to sea level' if E is excluded from the form, and for 'average rate of subsidence with respect to the geoid' if E is included in the form.

Differences between the subsidence rates for a particular unit are significant and have to be taken into account, as shown in Table A-7, which lists the uRs (uncorrected rate of subsidence), Rs_o (initial rate of subsidence), Rs_n (rate of subsidence of level n), Rc (rate of compaction during an interval), and the data needed to calculate these values.

Rs_{TD} is the tectonic rate of subsidence (R_T) if the bottom of the well is in basement, but usually Rs_{TD} results largely from compaction of sediments underlying the penetrated well section. In that case, one has to make an assumption as to the lithology (shale percentage) and thickness of the underlying sediments in order to calculate an estimate for the tectonic subsidence rate.

$$R_T = Rs_B \qquad \text{Eqn (A-9)}$$

for B = top of basement or top of compacted section, or

$$R_T = Rs_n - pRs_n \qquad \text{Eqn (A-10)}$$

in which pRs is the rate of 'pseudosubsidence' or compaction of the section below n.

The rate of compaction (Rc) for any unit at any chosen time can be calculated from data like those in Table A-6. For example, during the 2 Ma of deposition of unit G, the thickness of unit B decreased from 205 to 202 m, that is, 3/(10 * 2)= 0.15cm/1,000 years (Rc = 0.15). During the same time, unit E shrank from 225 to 205 m, that is 20/(10 * 2)= 1 cm/1,000 years (Rc = 1).

$$Rc = \frac{TR_n - TR_{n-1}}{10A} \text{ cm/1000 yrs} \qquad \text{Eqn (A-11)}$$

hence

$$pRs = \frac{(TR_n - TR_{n-1})}{10A} \text{ cm/1000 yrs} \qquad \text{Eqn (A-12)}$$

In the absence of data on the section below TD, uRs and Rs_{TD} values can be used to estimate Rt. For the older part of the section, uRs is smaller than Rs_{TD}, the basal units being thinner than they were at earlier times. For the younger part of the section, uRs is larger than Rs_{TD} because the compaction of the section below TD becomes less important whereas the thicknesses of the younger units on which uRs is based increase. Below the point where uRs>Rs_{TD} reverses and uRs<R_{TD}, uRs is the best estimate for R, whereas for the section younger than the reversal point, Rs_{TD} is the best estimate. If drilling continues, that is, deeper section is being drilled, the reversal point will move down (get older) until it reaches a level where compaction is complete (or basement is reached). From there down, $Rs_{TD} = R_T$.

The average rate at which each unit of Table A-7 shrank during the last 2 Ma (i.e., during deposition of unit H) is shown in the table. Unit H also compacted during its deposition, and the numbers in parentheses are based on the assumptions that present average porosity of the unit is 50% and that porosity of the upper inches was 80%. For this 100% shale example, it is obvious that Rc decreases with depth. In nature, variation in shale per percentage can be the reason that the deeper units of a section compact at a higher rate than the shallower units.

In summary, five 'average rates of subsidence' are distinguished:

1. Rs_o during an interval is the rate at which the base of its rock record subsides -
2. Rs_n during an interval is the rate at which an older level n subsides -
3. uRs during an interval is the rate at which all levels of a section would side if no compaction took place -
4. R_T during an interval is the rate at which the top of the fully compacted section or of basement subside -
5. and pRs during an interval is the rate at which a level subsides because of compaction of the older section.

A sixth rate, Rc, is the rate of compaction of a unit as a result of loading by a later unit.

These rates are tabulated in Table A-8 and presented diagrammatically in Figure A-16.

A.2.2.2 Applications of Subsidence Rate Analyses

The use of subsidence and compaction rates as parameters has countless applications in exploration and general geology. The following are a few of the possible uses.

A.2.2.2a Single site

1. Prediction of overpressuring. Noting, while drilling, that subsidence rates are significantly lower than regional rates is a warning that drilling is over a dome of either salt or shale and may penetrate overpressured formations.

A.2.2.2b Regional Interpretations

1. Prediction of Facies Distribution. A map of Rs_o can be used to predict facies distribution. Areas with the highest surface subsidence are potentially lowest topographically and will be sand prone if a sand source is available. Rs_o contours may further outline areas affected by growth faults or diapirs. Rs_o contours do not necessarily conform to those of sediment accumulation rates (Rf).

2. Quantification of Structuring. Estimation of R_T values from well data allows conclusions on magnitude and timing of structuring to be drawn with unprecedented precision. A suite of maps portrays the dynamics of subsurface geometry.

3. Basement subsidence vs intra-column deformation. Maps of R_T values distinguish between regional, basement-involved subsidence and anomalies caused by movements within the sediment column (growth faults, shale or salt domes). A suite of R_T anomaly maps shows the dynamics of such structures.

4. Characterization of Structural Styles - Basin Classification. Subsidence rates are a useful parameter in the characterization and early recognition of structural styles and, on a larger scale, in basin classification and characterization of plate-tectonic setting.

5. Paleo-hydrodynamic analysis. Rs_n values give the proper history of vertical movement of a level. Thus, an Rs_n contour map of a reservoir sandstone can be made for a particular time interval. Superimposing this map on a paleosurface map ($D_{n-1} + W_{n-1}$) shows

the direction of buoyant flow during that time.

A contour map of compaction rates (Rc) for a particular unit during a selected (younger) time interval is like a piezometric contour map. The pattern of fluid movement will have been away from the high compaction rates and toward the low rates. If hydrocarbons were present in the formation, then the fluid movement pattern will have been the migration pattern. Also, if the compacting formation itself were immature, hydrocarbons that came from elsewhere will have had to travel those routes. A superimposed paleostructure map shows which structures could have been functioning as traps and which more likely were being drained at that time.

6. <u>Basement Geophysical Analysis</u>. R_T values are fundamental data in geophysical (geodynamic) studies on crustal thickness, isostasy, and, in succession, on properties and processes below the Moho.

7. <u>Quantification of Global Eustatic Changes</u>. Over the past 10 years much industry effort has been expended on determining a global sea level curve (see for example, Watts and Steckler, 1979, Hardenbol et al, 1981, and discussion in Falvey and Deighton, 1982). The methods used are one of two main types : via relative coastal onlap curves (eg., Vail et al, 1977, Haq et al, Science, in press) : or via consideration of isostatically compensated geohistory curves (eg., Watts and Steckler, 1979, Hardenbol et al, 1981). While the gross form of the second order sea level curve is generally agreed, the peak magnitude of the curve and the frequency (and even existence) of third order fluctuations is not, even among individual groups of workers (compare the differences between the Exxon versions of Vail et al, 1977 and Haq et al, in press). Obviously this study is still in an early stage of rapid development.

Some considerations of the origin of eustatic sea level differences is given in Section A.3, while the relevance of such studies to basin modelling is detailed in Section B.4.

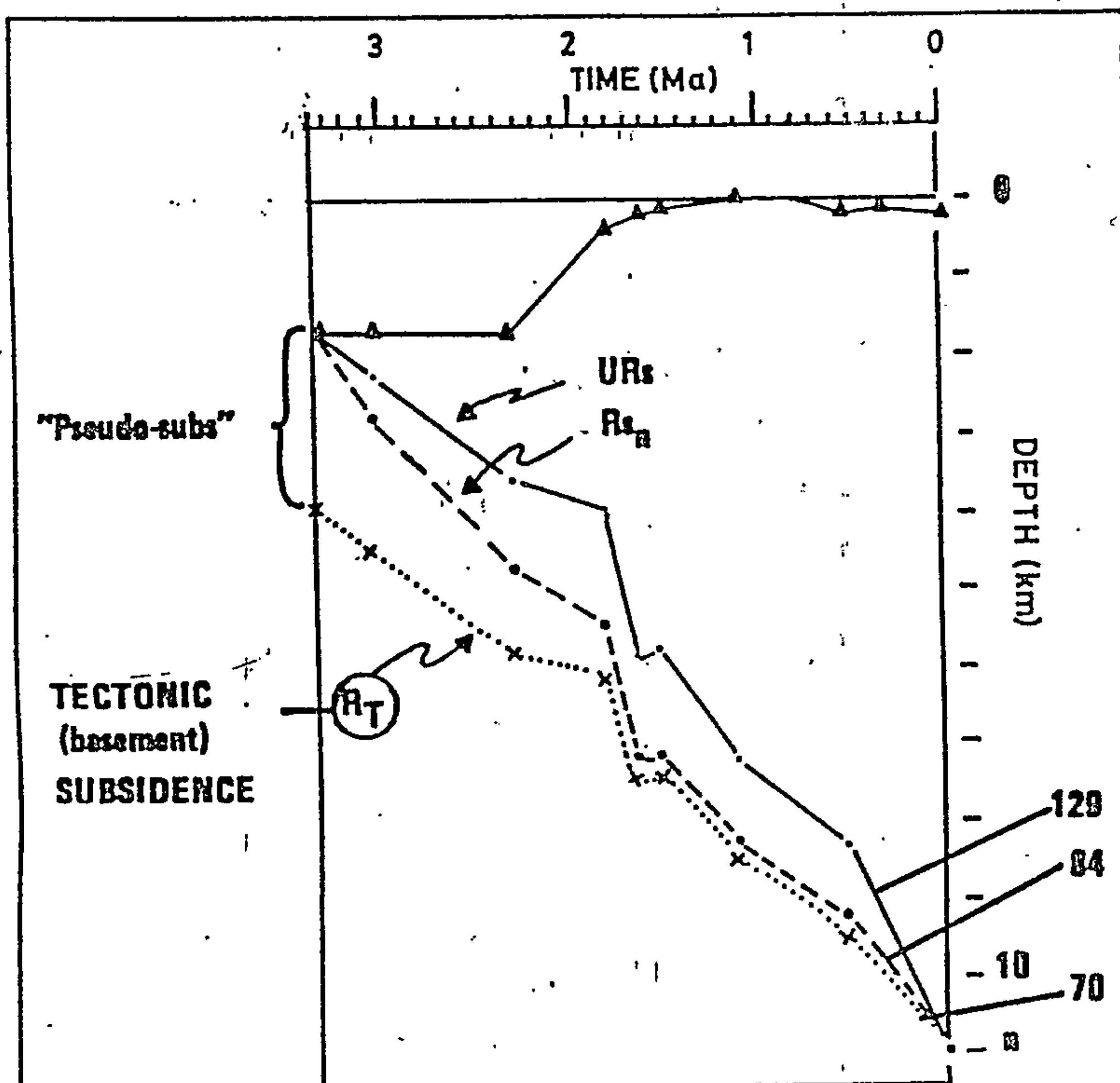

FIGURE A-16

TABLE A-8

AVERAGE RATES OF SUBSIDENCE

$$uRs = \frac{T_p - \Delta(W + E)}{10A} = uR - \frac{\Delta(W + E)}{10A}$$

$$Rs_o = \frac{T_o - \Delta(W + E)}{10A} = Rf - \frac{\Delta(W + E)}{10A}$$

$$Rs_n^A = \frac{\Delta D_n^A - \Delta(W + E)^A}{10A}$$ subsidence during A

$$R_T = Rs_n - pRs_n$$

$$Rc = \frac{TR_n - TR_{n-1}}{10A}$$

where D = depth of burial of level n

p = pseudosubsidence or compaction below n.

TR = restored thickness

T_p = present thickness

T_o = initial thickness

Rc = rate of compaction

A.2.3 EXAMPLES

A.2.3.1 Implications of Correcting for Compaction

The examples in section A.1.3 dealt with calculations made on beds at comparable burial depths and, therefore, uncorrected values of sediment accumulation rate (uR) could be used without significant errors being introduced. In the second example, the use of uR and uRs (uncorrected subsidence rate) served the illustrative purpose and allowed for general conclusions but would have been unacceptable for quantitative estimates and predictions. The following example illustrates some aspects of geohistory analysis of wells for which lithology and pressure data are available so that corrections for compaction can be made.

Geohistory diagrams of seven wells drilled in one area offshore Louisiana (Fig. A-17) are based on marker points that are both fossil tops and electric-log picks. The uRs line (uncorrected subsidence using present thickness) diverges from the Rs_{TD} line ('true' subsidence rate for TD using restored thickness) in the older part of the section and converges in the younger part, hence uRs and Rs_{TD}, respectively, in turn are the better estimates for the tectonic subsidence rate R_T. A still better estimate for the tectonic subsidence can be obtained in the following way. From regional geologic and geophysical observations, a thick sedimentary section is known to be present below TD. Under normal conditions, compaction of an interval now 10,000 ft (3,048 m) below TD would have been practically complete at TD time - thus subsidence of that interval after TD time is a measure of tectonic subsidence. To obtain the lower R_T curves (Fig. A-17), we assumed a normally pressured 10,000 ft unit below TD with 80% shale. When the tectonic subsidence curves were 'smoothed', three anomalies became apparent in all wells (vertically shaded areas in Fig. A-17). Differences in shape and size of these areas between the wells probably are due to inaccuracies in the paleontologic conclusions, but their presence is real and in our opinion reflects eustatic changes in sea level. The first change is in order of 700 ft (213 m) - later ones are considerably smaller. (The first change appears too large in Figure A-17 because the 'interpreted tectonic subsidence' line has been drawn on large increments, and because the 2.2 Ma control point is not well defined and possibly older than 2.2 Ma). The resolution of our example does not permit determination of the beginning and end of low or high stands of sea level. Research focused toward that goal, however, may reveal such detail. Another general conclusion that could be drawn from this example is that the rate of net-sediment accumulation (averaged for the seven wells) during the past 3.7 Ma was 58 cm/1,000 years, whereas the tectonic subsidence rate for the same period was 51cm/1,000 years.

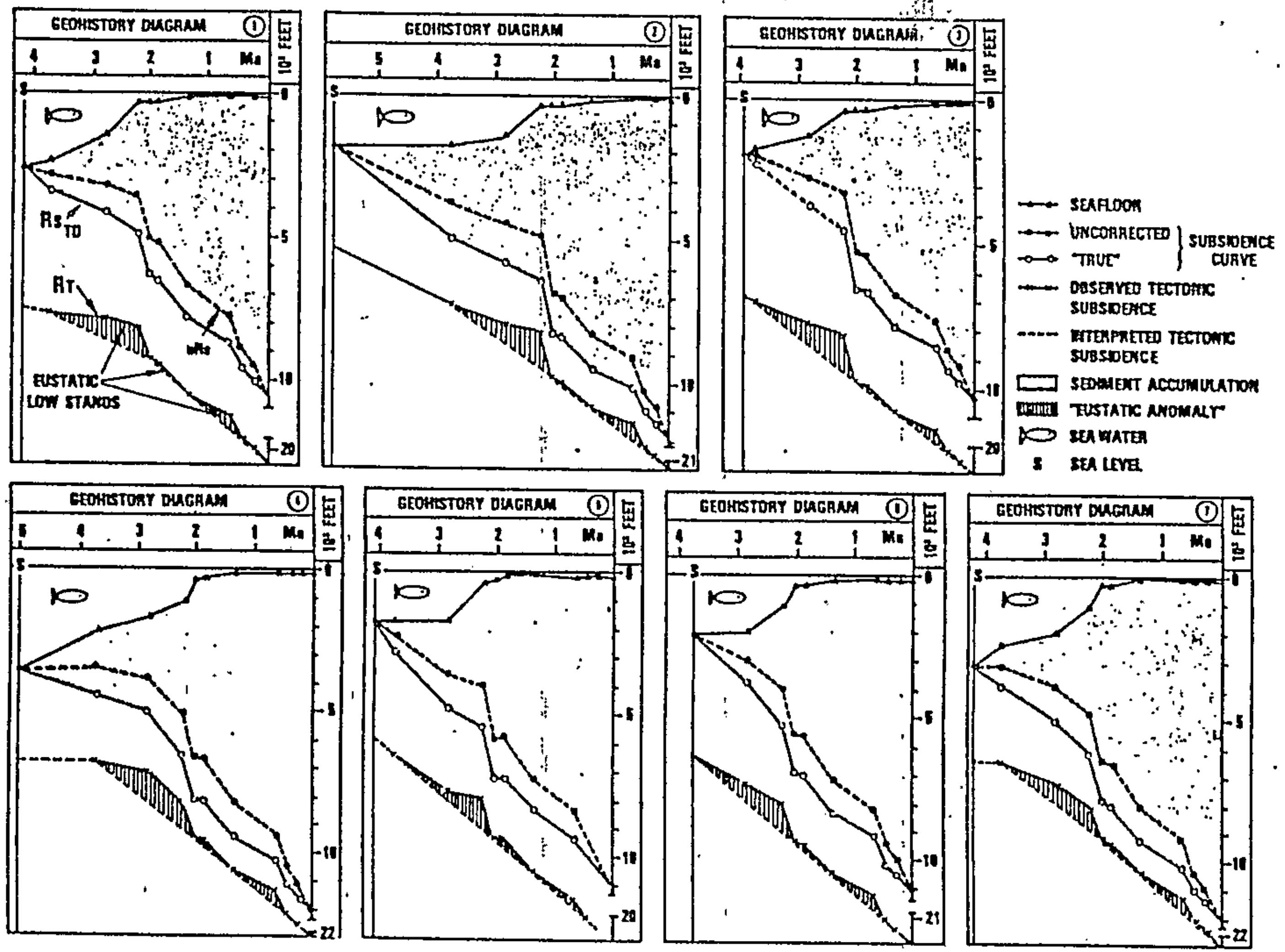

FIG A-17—Geohistory diagrams showing past 6 to 4 Ma of subsidence and shoaling at seven well sites offshore Louisiana. Lower part of vertical scales is interrupted. 10^3 ft = 304.8 m.

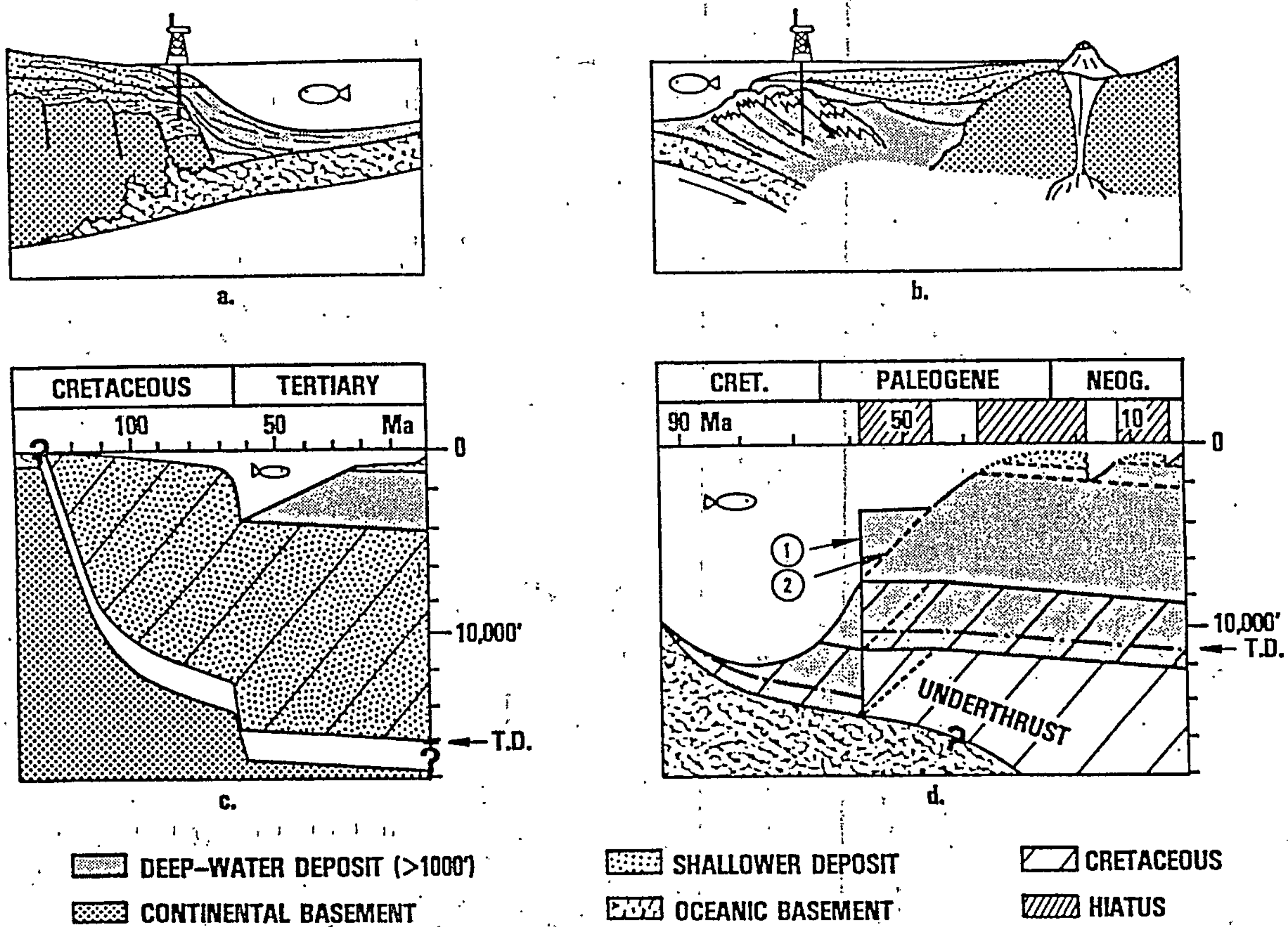
a.
b.
CRETACEOUS
TERTIARY
100
50
Ma
0
10,000'
T.D.
c.
CRET.
PALEOGENE
NEOG.
90 Ma
50
10
0
1
2
10,000'
T.D.
UNDERTHRUST
d.
DEEP-WATER DEPOSIT (>1000')
CONTINENTAL BASEMENT
SHALLOWER DEPOSIT
OCEANIC BASEMENT
CRETACEOUS
HIATUS

FIGURE A-18

A.2.3.2 Geohistory of a Continental Margin

The schematic cross sections of Figure A-18a and b show tectonostratigraphic models of continental margins: a passive (or block-faulted, or divergent, or Atlantic-type) margin in Figure A-18a (Vogt, 1970, Bott, 1971), and an active (or compressional, or convergent, or Pacific) margin with a trench, an underthrust ridge, and a fore-arc basin in Figure A-18b (Seely et al, 1974). The well symbols give the approximate drill locations of actual exploration wells. Schematic geohistory diagrams for these wells (Fig. A-18c, d) reveal at a glance the marked differences in their geologic histories.

The passive margin subsided at a rate of about 20 cm/1,000 years during the Early Cretaceous when shallow-water sedimentation more or less kept up with subsidence. During the late Early Cretaceous and the Late Cretaceous, subsidence slowed but, nevertheless, the sea deepened because sedimentation slowed even more. A sudden (within the time equivalent of one planktonic foraminiferal biozone) rapid subsidence occurred at the end of the Cretaceous-beginning of the Tertiary, followed thereafter by only slight subsidence - the area simply filled with sediment. Different paleontologists may interpret the paleobathymetry somewhat differently, which may change slightly the rates and magnitudes of the movements - however, the general trend is apparent: early rapid subsidence that decreases, then accelerates briefly before stopping. A similar pattern has been observed in several wells drilled near the edge of the continent, whereas more landward wells show the same trend but without the sudden brief acceleration in subsidence. The subsidence curve of these wells closely resembles that of oceanic crust (Fig. A-19) except that initial rates higher (the more so with more sediment accumulating) and, if the sedimentation rate continues to be high, substantial subsidence ceases later than would be expected from the oceanic subsidence curve. Confirming the suggestion by Vogt and Ostenso (1967), it seems that passive-margin fault blocks move downward only (not up) after spreading has commenced and that the rate of their subsidence depends merely on distance from the spreading center (cooling) and isostatic response to loading (Sleep, 1971, Keen and Keen, 1973). Where geohistory diagrams reveal diversions from this general pattern, the activity of other forces (e.g. wrenching) may be concluded, or, generally on a smaller scale, such diversions may be apparent and the result of eustatic sea-level changes.

The geohistory diagram is entirely different for a well drilled on an active margin (Fig. A-18d). Here, deep-water sediments accumulated on a normally subsiding oceanic seafloor until about 58 m.y. ago when they were uplifted abruptly as a result of under thrusting that accompanied subduction (Seely et al, 1974). The rate of uplift cannot be interpreted from the well data because of a hiatus of 58 to 43 Ma. Three possibilities exist (Fig. A-18d): (1) uplift occurred 'instantaneously' 58 Ma ago and was followed by a period of nondeposition because of increased current velocities over the new seafloor high - (2) uplift was spasmodic or gradual during the entire period of the hiatus (with a minimum average rate about 10 cm/1,000 years), and increased current velocities over the rising seafloor prevented sediment accumulation, or if sediments were deposited, they were eroded subsequently - or (3) uplift occurred rapidly but later than 58 Ma, and pre-event sediments have been eroded. Whatever actually occurred, thew paleontologic conclusions point out that uplift (underthrusting) apparently took place within a specific time span upon which the location had become part of the continent and thereafter subsided slowly under an increasing sediment load. The two younger hiatuses in this particular well (stippled parts in Fig. A-18d) may be the result of erosion caused by eustatic sea-level drops or by changes in current regime. A second active-margin exploration well for which a paleontologic report was available showed the same basic pattern.

The two examples (Fig. A-18) illustrate that geohistory diagrams are useful for depicting sedimentary history and structural timing. Because the diagrams characterize tectonic settings, they will be particularly useful in basins having more complex histories than the two straightforward margins discussed here. Recent developments in global tectonics have emphasized large-scale horizontal movements and related the geologic history of large areas to their plate positions. It now seems opportune to resolve the more subtle vertical movements that are of immediate importance to the explorationist. A classification of vertical movements according to their rates will have predictive value in undrilled areas of known tectonic setting - conversely, geohistory diagrams (see Fig. A-18) can serve as models from which one can recognize the former plate positions of, for example, known Paleozoic sections.

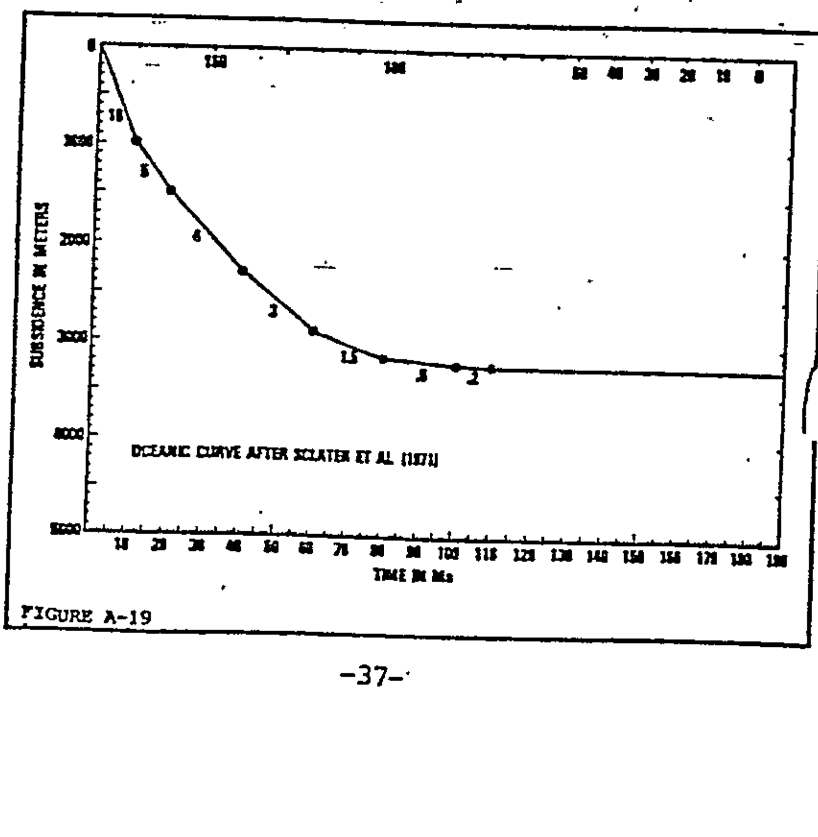

FIGURE A-19

A.3 CONSTRUCTION OF SYNTHETIC SEISMIC SECTIONS

A.3.1 INTRODUCTION - SYNOPSIS OF COURSE SO FAR.

Linear time scales are used by exploration paleontologists to establish a numeric chronostratigraphy for marine well sections. Thus they can calculate estimates for the missing intervals at unconformities. This section deals with a new kind of cross section can be constructed using isochrons rather than conventional stage names.

Using modern time scales paleontologists can assign numeric ('absolute') geological ages to marine sedimentary successions like those of continental margins. Adding further quantitative stratigraphic elements - such as present position with respect to sea level, paleobathymetry, and unit thickness - determines the position of the geologic record of a rock-unit in space and time. It is now possible to replace much of the traditional qualitative deliberations on the geologic history of a site or an area with unambiguous geohistory analysis (Van Hinte, 1978). Viewing the geologic record in a linear time perspective facilitates evaluation of geologic events and processes because it brings them to proportion. This provides a new and rewarding approach to geology and facilitates the use of a computer. Figure A-20 shows the four elements that were used in the construction of Cenozoic and Mesozoic time-scales, and now are complemented by empirical curves such as for sea-level change and $^{87}Sr/^{86}Sr$ ratios which further improve time-resolution.

This section discusses a theoretical example of one application of geohistory analysis techniques originally presented at a 1979 meeting of the Petroleum Circle of the Dutch Geology and Mining Society, and at a 1980 Conference on Ancient Sea Levels at Lamont-Doherty Geological Observatory (New York).

A.3.2 TIME-STRATIGRAPHY OF A WELL SECTION

A conventional paleontologic report usually contains the kind of data summarized in Figure A-21 and Table A-9 for hypothetical well A. This information permits the geologist to make cross sections like the one of Figure A-22, showing well A and two other wells B and C. Today, we can present this information in numbers, for the numeric ages at stage boundaries and of fossil markers are known. This is illustrated for well A in Figure A-23 under the column Ma (= Mega-annus or megennium or 1 million years).

Recognizing and defining unconformities in well sections is an important contribution to the exploration effort because unconformities form the boundaries of depositional sequences that can be recognized in seismic

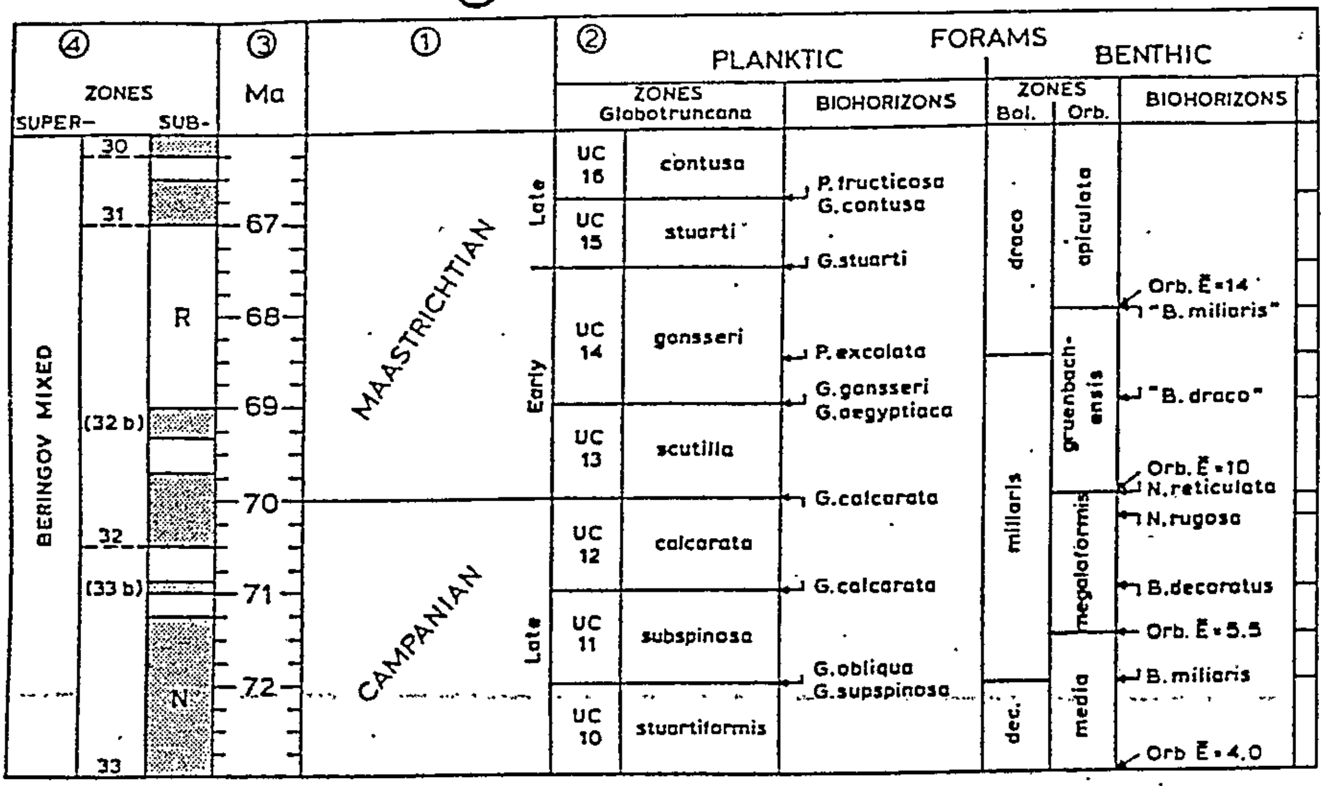

Fig A-20 . Portion of Cretaceous time scale showing the four elements used during the past decade in the construction of Mesozoic and Cenozoic time scales: 1. units of "relative time scale"; 2. selected foraminiferal biostratigraphy; 3. linear numeric scale derived from first and second order radiometrically dated calibration points; 4. earth magnetic polarity reversal scale. Note that average planktic zone spans .88 Ma, that average unit of combined planktic and benthic subdivision spans .64 Ma, that only three benthic genera (Bol.-*Bolivinoides*, Orb.,-*Orbitoides*, and N.-*Neoflabellina)* are included and that the steady increase in number of epi-auxiliary chambers (E) in *Orbitoides* makes a continuous scale possible (after Van Hinte, 1976; later work suggests changes should be made that are beyond the scope of the present paper).

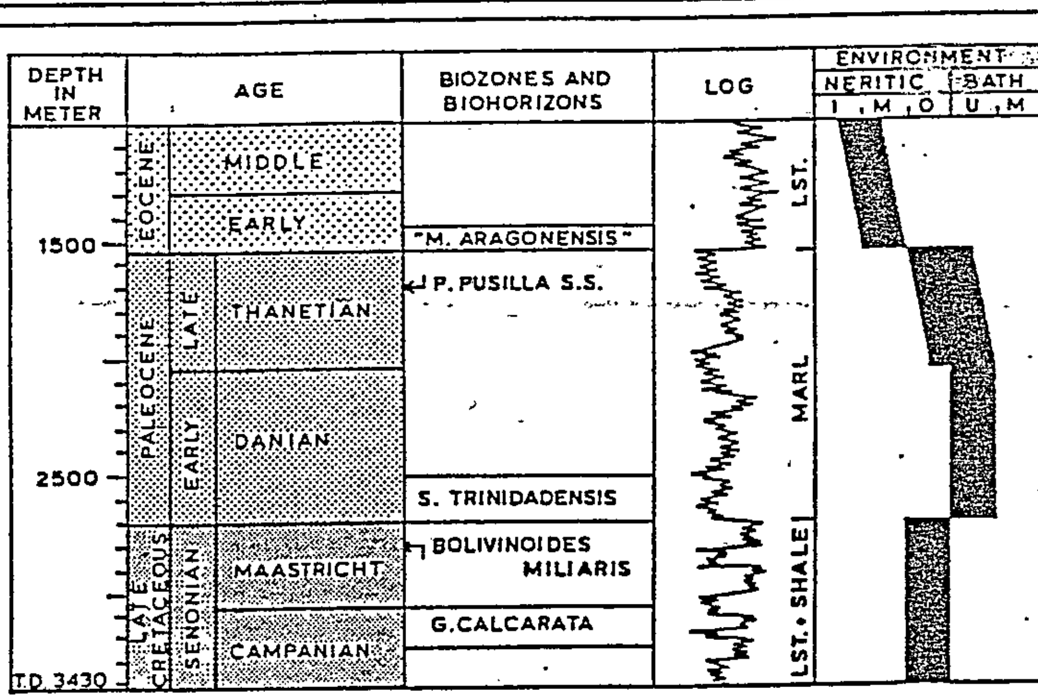

FIG A-21 Portion of stratigraphic log of hypothetical Well A summarizing information usually available for exploration wells: age, biostratigraphy, log patterns, gross lithology, and an environmental interpretation (TABLE A-9)

TABLE A-9 Paleontologic report on hypothetical well A		
DEPTH	TOP	ENVIRONMENT
top of section 1300 m	Middle Eocene Limestone Lower Eocene Limestone	Inner - Middle Neritic
1550 m	Upper Paleocene (Thanetian) Marl	Outer Neritic - Upper Bathyal
2050 m	Lower Paleocene (Danian Marl	Upper Bathyal
2700 m 2700 m 3050 m	Upper Cretaceous Limestone and shale Maastrichtian Campanian	Outer Neritic

Notes : The paleo-log further gives the top of a shallow water equivalent of the M. aragonensis zone at 1450 m, a marker for the top of the M. angulata zone at 1700 m and for the S. trinidadensis zone at 2500 m, the top of Bolivinoides militaris at 2800 m and the base of G. calarata at 3250 m. No other markers were recorded till TD at 3430 m. E-log pattern changes occur at 1550 and 2700 m.

TABLE A-10 Whole number numeric age depths and the ages at unconformities for wells B and C

WELL B		WELL C	
Age (Ma)	Depth (m)	Age (Ma)	Depth (m)
49	1300	49	1300
50	1500	50	1525
51	1650	51	1700
51.9	1800	52	1900
56	1800	53	2100
57	2000	54	2200
58	2200	55	2240
59	2300	56	2280
60	2400	57	2320
61	2460	58	2360
62	2500	59.0	2400
62.4	2520	69.7	2400
69.5	2520	70	2500
70	2650	71	2800
71	2850	72	3200
72	3100	73	3500
73	3300	TD 73.7	3700
74	3450		
TD 74.5	3500		

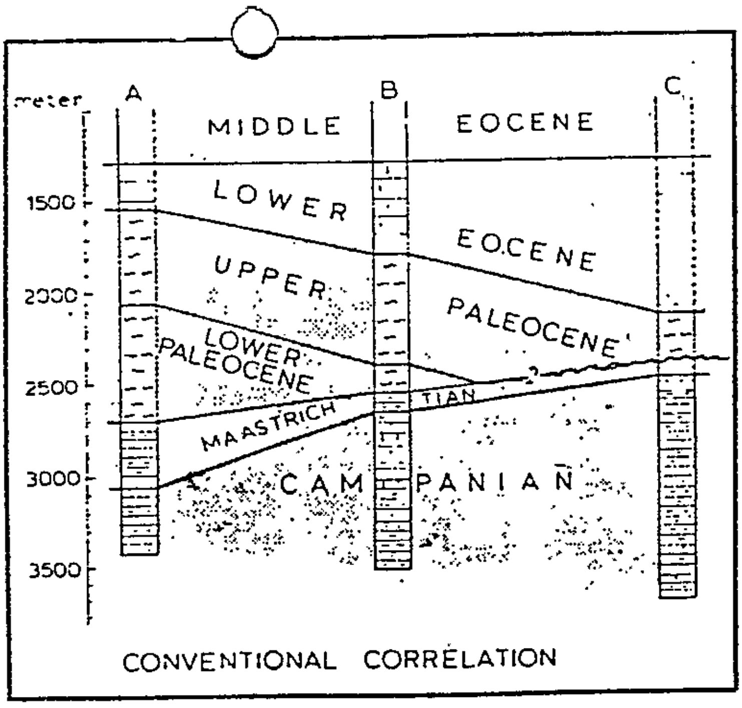

Fig A-22— Regional Cross section through Well A of Fig A-21 and two other hypothetical Wells B and C showing "complete" section at A and B and an unconformity on a paleo-high at C.

TABLE A-11 - Well Record of Paleo-waterdepth change.

	LITHOSTRATIGRAPHY	BIOSTRATIGRAPHY
Shelf, Upper Slope	LITHOLOGIC CHANGES: grain size, terrigenous material. LITHOFACIES CHANGES: shore-line, channels. PEAT-SOIL SEQUENCES HARDGROUND RESIDUALS PEBBLES DENSITY CHANGE (Log) DISSOLUTION	REWORKING time: HIATUS IN STANDARD SPECIATION habitat: PALEO-WATERDEPTH CHANGE CHANGE IN ORGANIC MATTER
	REEF GROWTH R - CHANGES	REEF GROWTH R - CHANGES
Lower Slope, Ocean Floor	Change in abundance or nature of TURBIDITES TERRIGENOUS MATERIAL	REWORKING DISSOLUTION FACIES

sections. These boundaries are the primary levels for calibration between conventional stratigraphy and seismo-stratigraphy, the sequences being the basic mapping units for the exploration seismic interpreter. We should be alert to detect them in our well bio- and litho-stratigraphy.

One way to go about it is to calculate average rates of sediment accumulation. In our example (see Figure A-23) this draws our attention to two parts of the section where rates are anomalously low and remain low even if we take a wider average assuming the boundaries were misplaced. This suggests either that there is section missing or that these units differ from adjacent units in facies. Figure A-21 shows no changes within the units, but between them changes in lithology, log pattern, and water depth confirm our suspicion of an unconformity.

After recognizing the unconformity we adjust numbers by calculating the ages at the unconformities (x and y in Figure A-24). This is done by downward extrapolation of the accumulation rate of the nearest unit above the unconformity (R_1, given by markers A and B) and by upward extrapolation of the rate of the nearest unit below the unconformity (R_2, given by markers C and D).

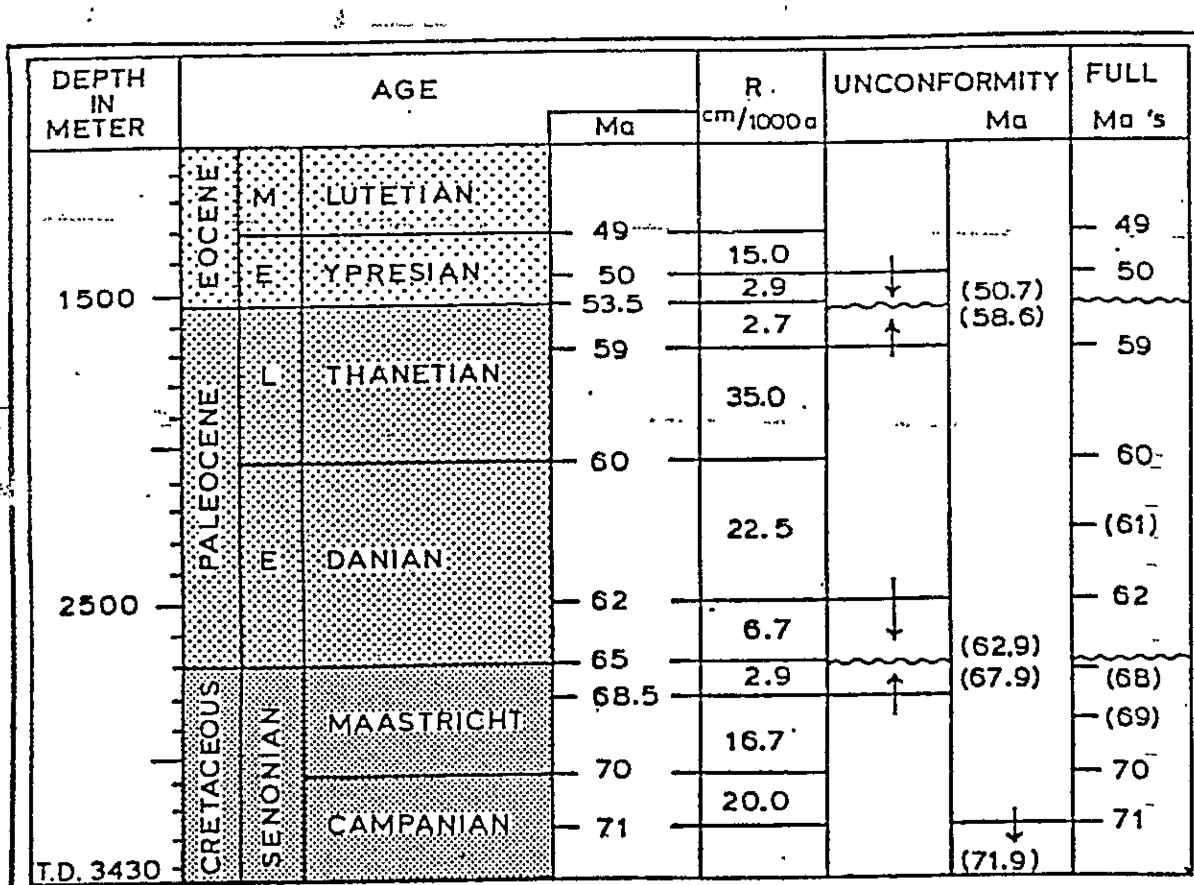

Fig A-23 - Portion of stratigraphic log of Well A. Same information as Fig A-21(TBL A-9) translated in numeric time (Ma after Hardenbol and Berggren, 1978; Van Hinte, 1976b) and used to calculate the average rate of sediment accumulation (R) of units between markers. Ages at unconformities and TD, and the depth of full number ages calculated using R = T/10A cm/ka (cf Fig A-24) Calculated numbers in brackets. R = 22.5, using 61 Ma lies at 2275 m; 68 Ma and 69 Ma lie at 2717 and 2883 m respectively, using R = 16.7.

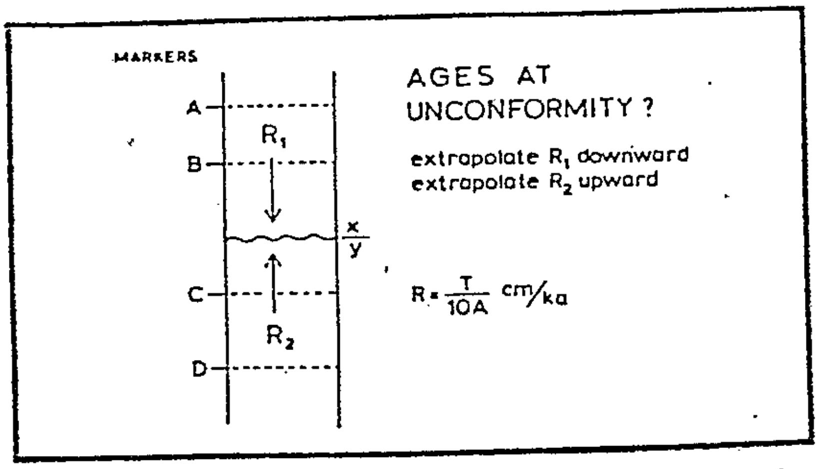

Fig. A–24 - Extrapolation of average rate of sediment accumulation (R1 for interval B-A, and R2 for interval D-C) to estimate ages above (x) and below (y) unconformity. Event that caused unconformity ended D-C depositional environment and new B-A depositional environment followed; calculation of R for unit C-B makes no sense. A, B, C, and D are numeric ages from markers; T = thickness of unit between markers; 10A = 10 × duration of unit in million years; ka = kilo-annus = 1000 years.

To complete the quantification the age at T.D. is calculated in the same manner, and we determine the depth of full number ages assuming constant R for each unit and using the same equation as in Figure A-24.

Unconformities are caused by changes in base-level, which are often changes in sea level, most of which are of a global nature and referred to as eustacy. Past sea level changes have been recorded by man in history and archaeology. The rest of nature records these changes in geomorphology and in the sedimentary strata, as seen in seismostratigraphy, lithostratigraphy, and biostratigraphy. Table A-11 lists some criteria for the lithologic and paleontologic recognition of sea level changes - change in rate of sediment accumulation (R, defined above) is only one of them.

A.3.3 TIME-STRATIGRAPHY OF A CROSS-SECTION

A.3.3.1 Construction

Having made calculations for wells A, B and C (Table A-10) we make the 1 Ma isochron cross section shown in Figure A-25. At a glance, the section shows areas with high rates of sediment accumulation where isochrons are widely spaced, and areas of low rates of sediment accumulation with closely spaced isochrons. The cross section also gives an impression of the structural history and the importance of area unconformities. Such a plot can be expanded to include lithology, paleo-waterdepth, or other geologic information.

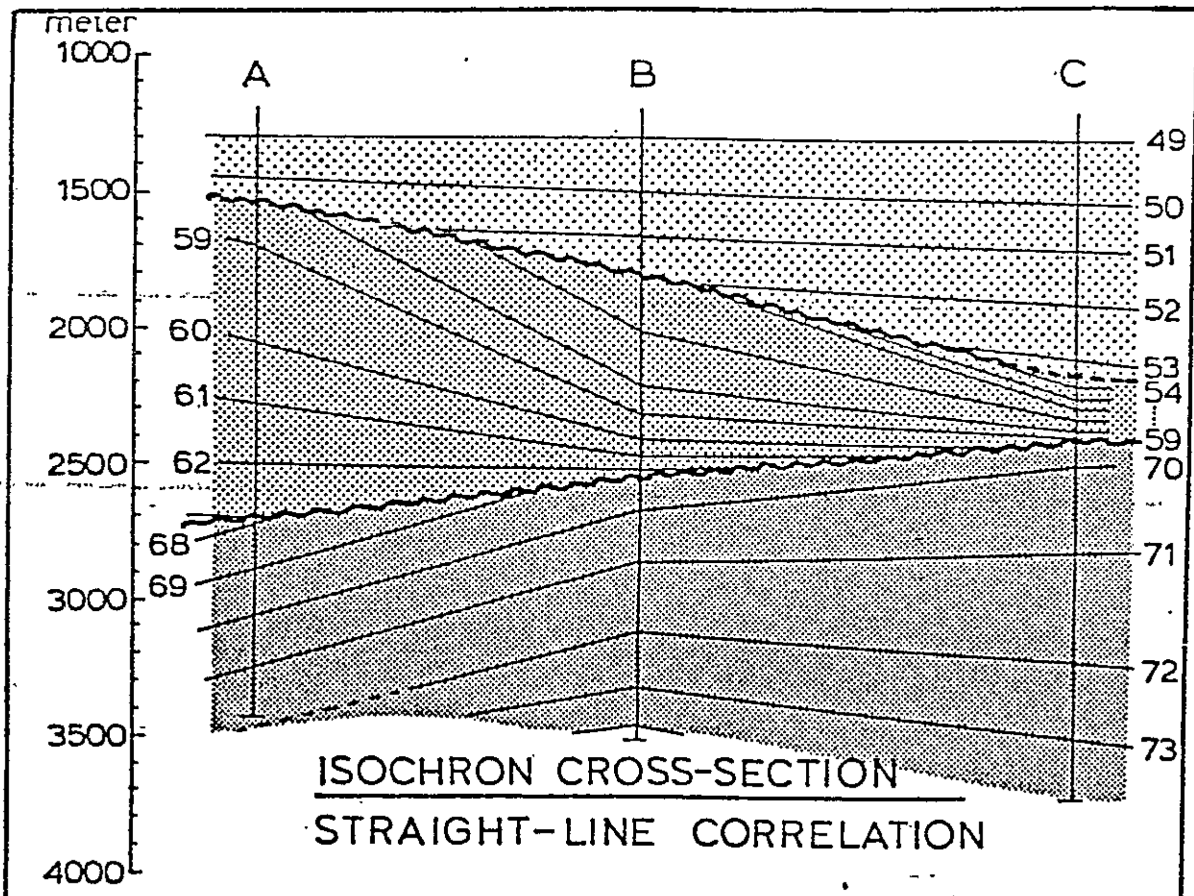

Fig A-25— Straight line isochron cross section through wells A, B and C (data in Fig A-23, TBL A-10'). Interval 1 Ma (one million years). Note correlation of unconformities and difference between high and low rates of sediment accumulation. 52 Ma and 53 Ma lines between wells B and C drawn parallel with 51 Ma line, which implies geologic assumption (compare with FIGURE A-22

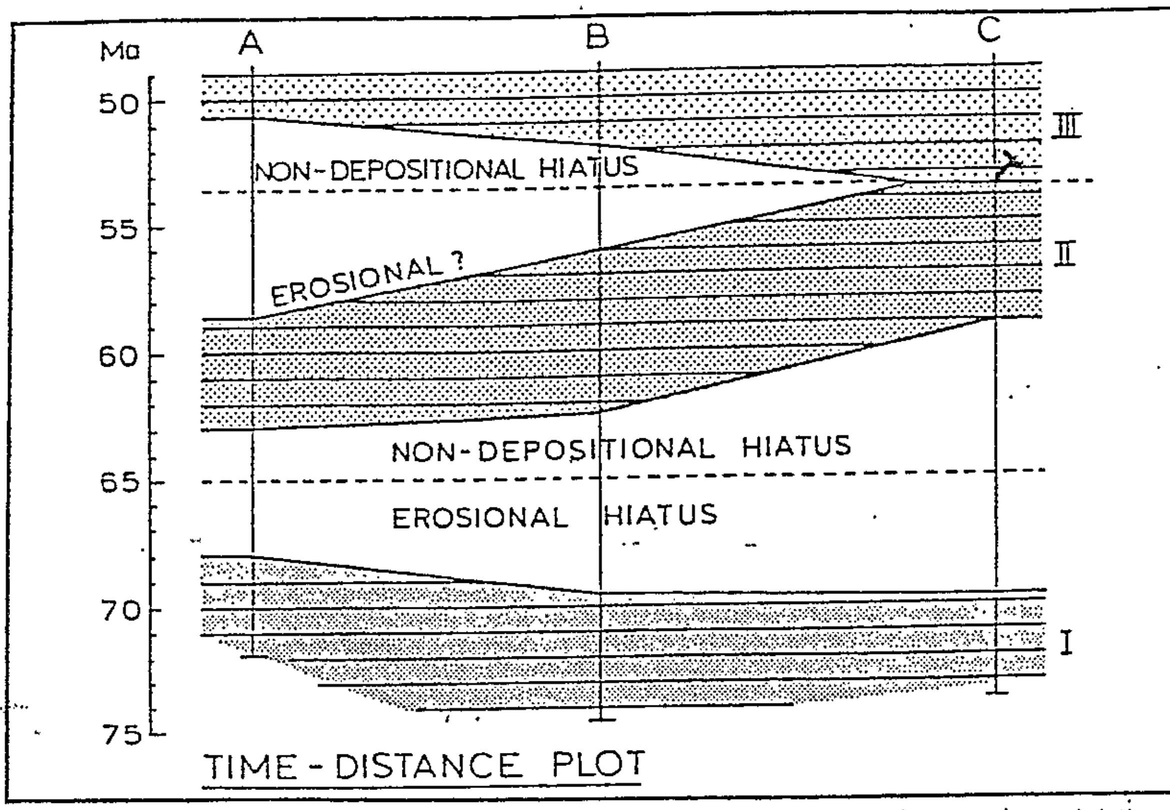

Fig A-26 - Time-distance plot for wells A, B, and C of Fig A-25 Note choice of 53.5 Ma and 65 Ma as ages for events that caused unconformities (compare with Figure 16 and 17 in Van Hinte, 1978). Interval I, II, and III are natural time-stratigraphic units. Nail at 53.5 Ma in C marks the only level where a boundary stratotype would not disrupt natural time-stratigraphic classification. Broken line at 65 Ma drawn at Cretaceous Tertiary boundary event.

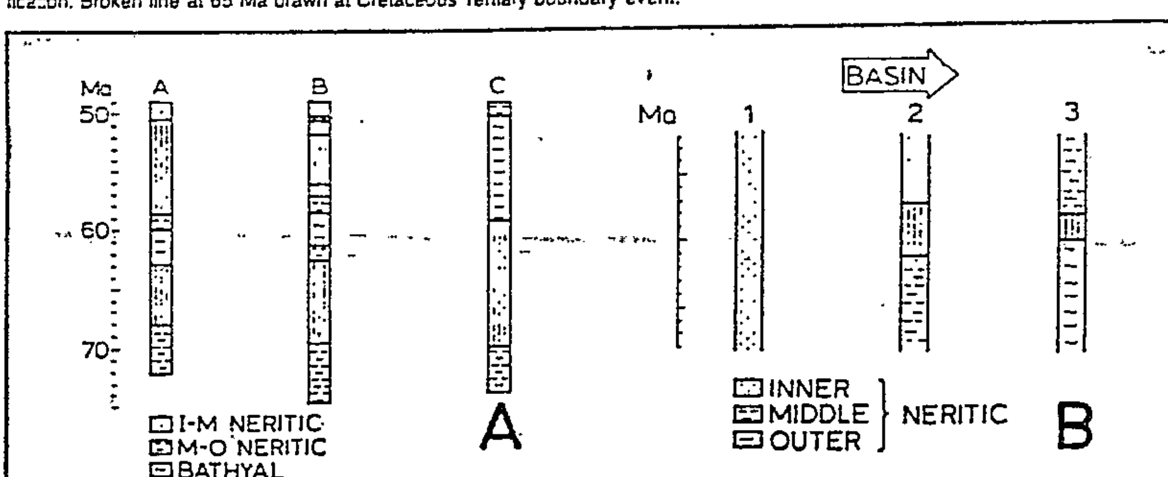

Fig A-27 – Columnar time sections of wells A, B, and C of Fig A-26 and of hypothetical wells 1, 2, and 3. Column shows depositional environments and presence or absence (vertical signature) of sedimentary record. Illustrates that analysis of unconformities is elementary in unraveling geologic history, and that comparison of real examples with cycle chart of Vail and Mitchum (1979) is most instructive. A — Upper conformity is regular effect of sea level drop, C is most basinward well. Lower unconformity suggests reversed basin position and or C is at paleo-high in larger regional setting. Knowledge of regional geology needed for further interpretation. B — Completeness of Well 1 indicates that unconformity has been overlooked in shallow-water section (probably quite common in literature), or implies strong differential movement between wells 1 and 2 during time of hiatus.

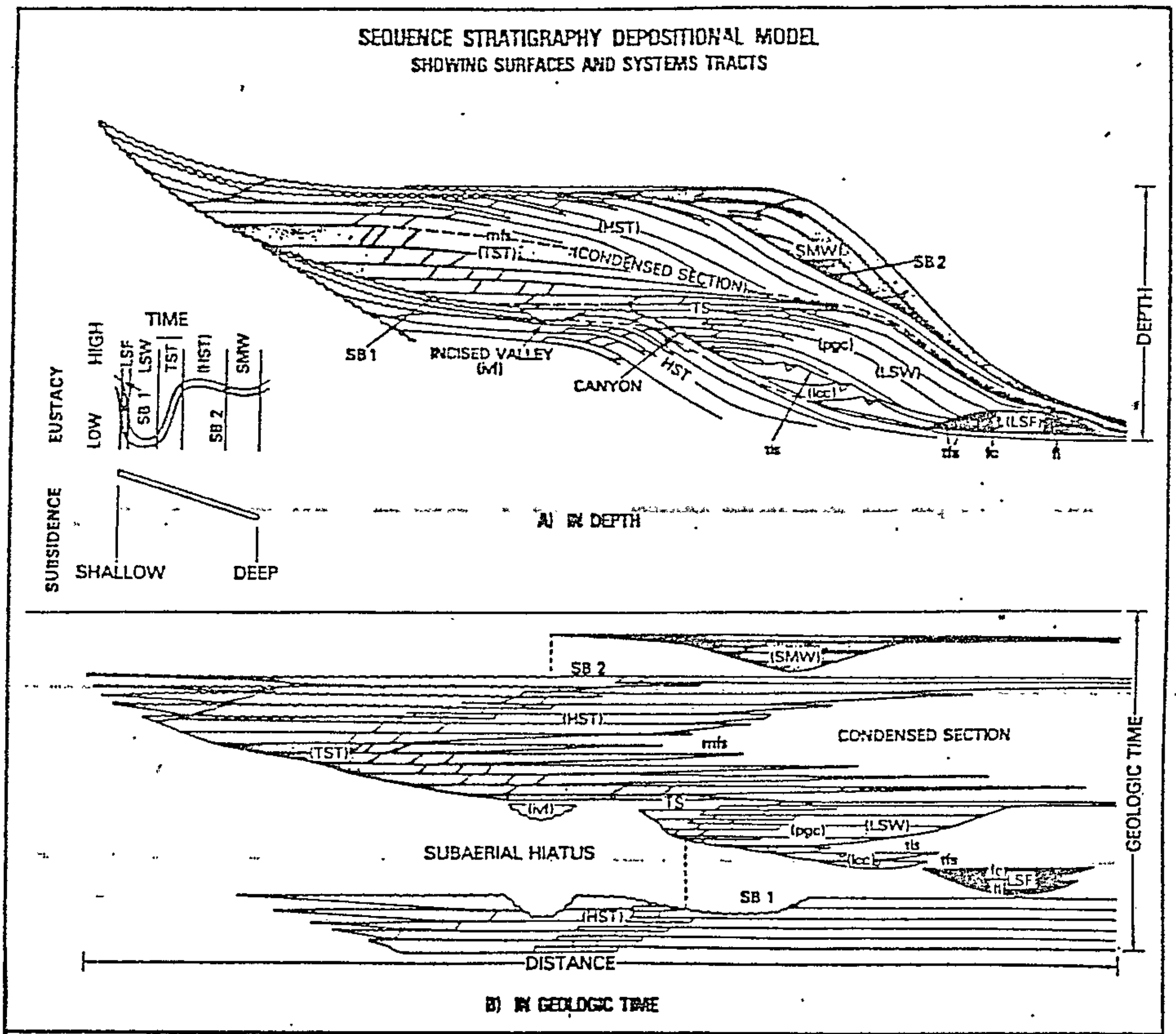

LEGEND

SURFACES

(SB) SEQUENCE BOUNDARIES
- (SB 1) = TYPE 1
- (SB 2) = TYPE 2

(DLS) DOWNLAP SURFACES
- (mfs) = maximum flooding surface
- (tfs) = top fan surface
- (tls) = top leveed channel surface

(TS) TRANSGRESSIVE SURFACE
- (First flooding surface above maximum regression)

SYSTEMS TRACTS

HST = HIGHSTAND SYSTEMS TRACT
TST = TRANSGRESSIVE SYSTEMS TRACT
LSW = LOWSTAND WEDGE SYSTEMS TRACT
- ivf = incised valley fill
- pgc = prograding complex
- lcc = leveed channel complex

LSF = LOWSTAND FAN SYSTEMS TRACT
- fc = fan channels
- fl = fan lobes

SMW = SHELF MARGIN WEDGE SYSTEMS TRACT

Figure A-28 Sequence-stratigraphic concepts.
(from Haq et al, 1987)

The magnitude of unconformities is better illustrated in a time-distance plot (Figure A-26), which uses time instead of depth as an ordinate. Again, you can add lithology, paleo-waterdepth or other geologic information, or an interpretation of the age of the event that caused the unconformity. Figure A-27 illustrates some applications of this approach.

A.3.3.2 Implications

Figure A-26 resembles figures published by Mitchum, Vail, and Thompson (1977, Figure 1b, p.54) and Haq et al (1987, Science in press, Fig. A-28) which illustrate the nature of the depositional sequences recognized in seismic sections. They consider that a seismic section to be an image of the time-stratigraphic depositional pattern. 'Primary seismic reflections are generated by physical surfaces in the rocks, consisting mainly of stratal (bedding) surfaces and unconformities with velocity-density contrasts.... the resulting seismic section is a record of the chronostratigraphic depositional and structural patterns and not a record of the time-transgressive lithostratigraphy.' (Vail and Mitchum, 1977, p.51).

In our cross-section of wells A, B and C we are looking at the same natural time-stratigraphic units. It just so happens that stratigraphic resolutions from modern seismic data and from fossils match and are sufficient to read the sedimentary record of the effects of sea-level changes. The improving chronologic resolution of the geologic time-scale has surpassed the frequency of eustatic changes and now allows for the distinction between individual eustatic events.

In most geologic settings, biochronostratigraphy may only separate the megasequences, and paleobathymetry and lithofacies interpretations are necessary to further identify individual sequences. The present technique may prove to be effective in handling such information and to achieve:

1. better regional age calibrations for sequences recognized on seismic sections
2. a correlation of regional seismostratigraphy to the Global Cycle Charts of Vail and Mitchum (1979) and Haq et al (1987, in press), their documentation and modification and their use for accurate time-stratigraphic prediction in undrilled areas and,
3. a better understanding of the eustacy that caused the sequential depositional pattern.

A better correlation of the seismic sequences with the relative time-scale (points 1 and 2) is needed. This is suggested by the fact that a number of the units given on the cycle charts do not match the conventional stages. Yet they should, for more than a hundred years ago d'Orbigny defined the stages in precisely the same terms, namely as 'unconformity bound units'. As a student of the catastrophist Cuvier, d'Orbigny (1850-1852) at that time related his stage boundaries (unconformities) to global sea level changes (floods). At the turn of the century, Suess (1908) introduced the term eustacy to name this cause for Stage boundaries. Whether improvement of numeric ages is most needed for the seismic sequences or for the old Stages is a question of moving the matching problem.

A.3.4 EUSTATIC SEA-LEVEL CHANGES

Observed relative changes of sea-level result from eustacy, sediment supply and vertical movement (Figure A-29a), a fact which complicates the determination of eustatic rates and magnitudes. Figure A-29c classifies possible contributions to vertical movement involving the crust or just the sediment column. For most single well data sediment supply can be calculated (pre compaction thickness), but it is impossible to separate, with any degree of certainty, the eustacy signal from the mixture of local vertical movements. The present cross-section technique, however, allows distinction of relatively high frequency-low amplitude eustacy from low frequency high amplitude regional vertical movements. Of course, this does not determine (Figure A-29b) whether we are dealing with glacial, tectonic, geoidal, thermal eustacy, the effect of an extra terrestrial body (large and hot) hitting the ocean from outer space, or the consequence of dessicating and refilling basins.

A.3.5 THE SYNTHETIC SEISMIC SECTION

A.3.5.1 Construction

The isochron cross-section of Figure A-25 is redrawn in Figure A-30 but with more natural, curved lines. We can apply seismostratigraphic terminology to the base and top of our units, including onlap, toplap, downlap, etc. This produces an image of the time stratigraphic depositional and structural pattern similar to a seismic section. In this manner our well- data assist geophysicists in dating sequences and correlating through bad data areas. Problems with a lack of control points to handle unconformities (Figure A-31) are unavoidable, however. Paleontologic data do not provide answers, and the interpreter must be guided by his ideas about local geology and the nature of the event causing the unconformity.

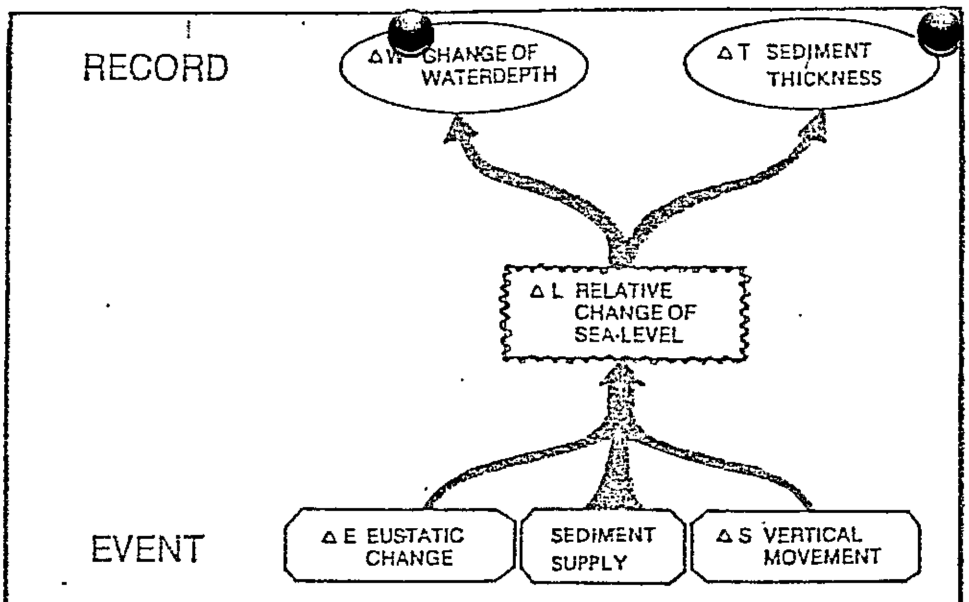

FIGURE A-29a

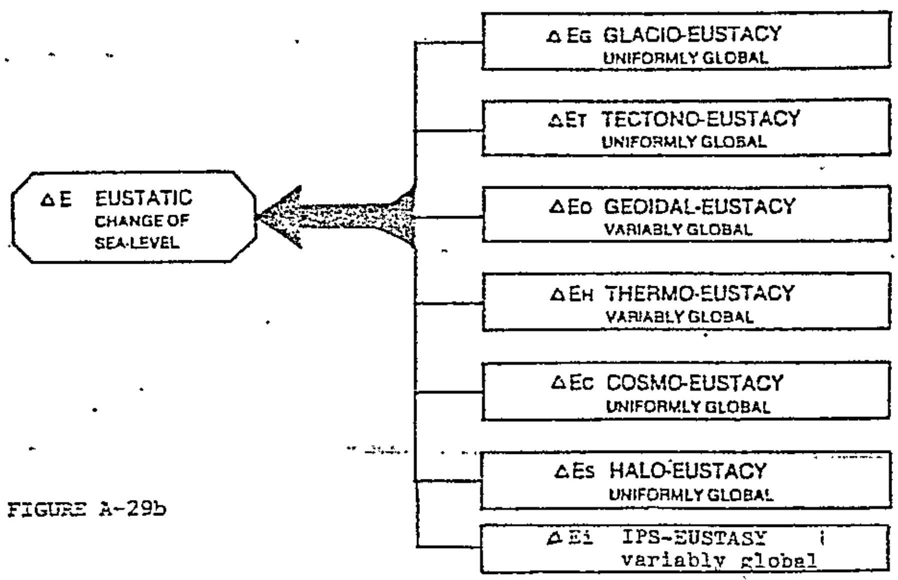

FIGURE A-29b

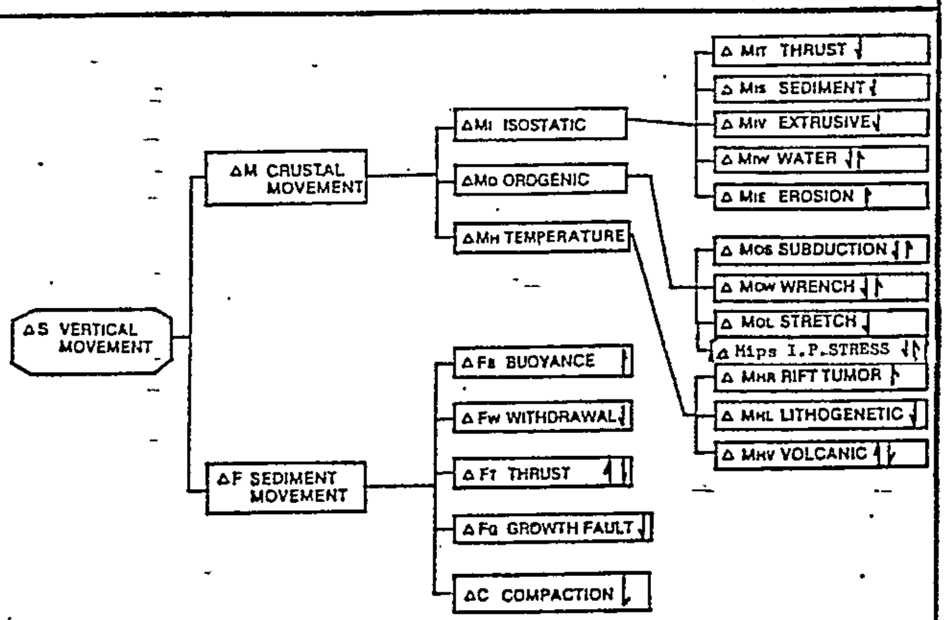

FIGURE A-29c

Eustasy can be caused by changing:

I. AMOUNT OF FREE SEA WATER
II. TOTAL VOLUME OF WATER
III. SIZE OF CONTAINER
IV. SHAPE OF SURFACE

Nature of deduced eustasy

a. LOW FREQUENCY
b. HIGH FREQUENCY

Possible mechanisms

Glacio-eustasy	ice-volume fluctuations	Ib
Limno-eustasy	fresh water volume fluctuations	Ia
Halo-eustasy	empty/fill salt basins	IIIb
IPS-eustasy	intraplate stress fluctuations	IIIb
Tectono-eustasy	average age ocean floor, a.o.	IIIa
Geoidal-eustasy	geoid fluctuations	IVa
Thermo-eustasy	average seawater temp. fluctuations	IIa
Cosmo-eustasy	catastrophic evaporation	Ib

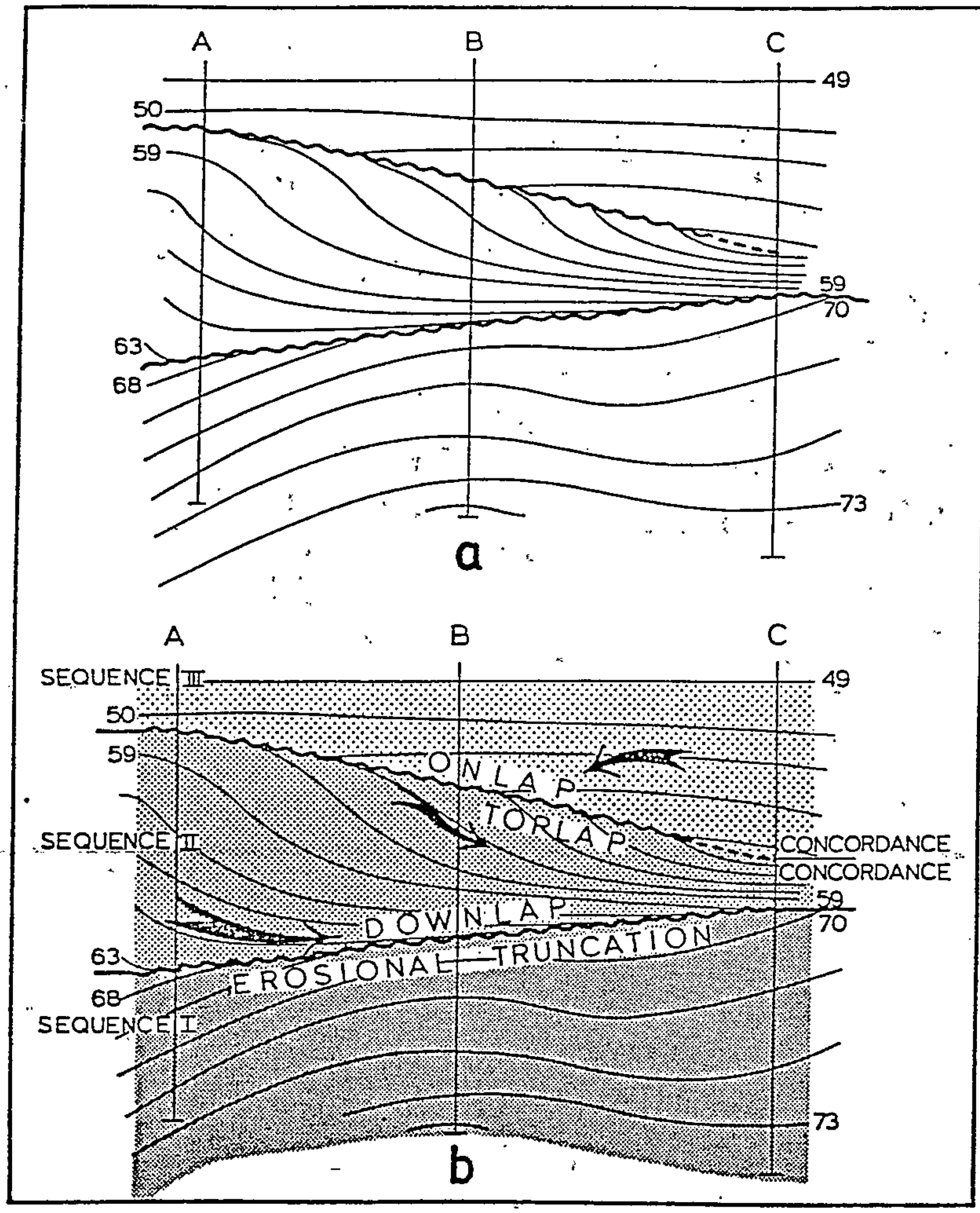

FigA-30 — Synthetic seismic section through wells A, B, and C of FigA-25 Naturally drawn isochrons (a) make applicability of seismostratigraphic terminology obvious (b). If A, B, and C were real wells, I through III would be supersequences rather than sequences.

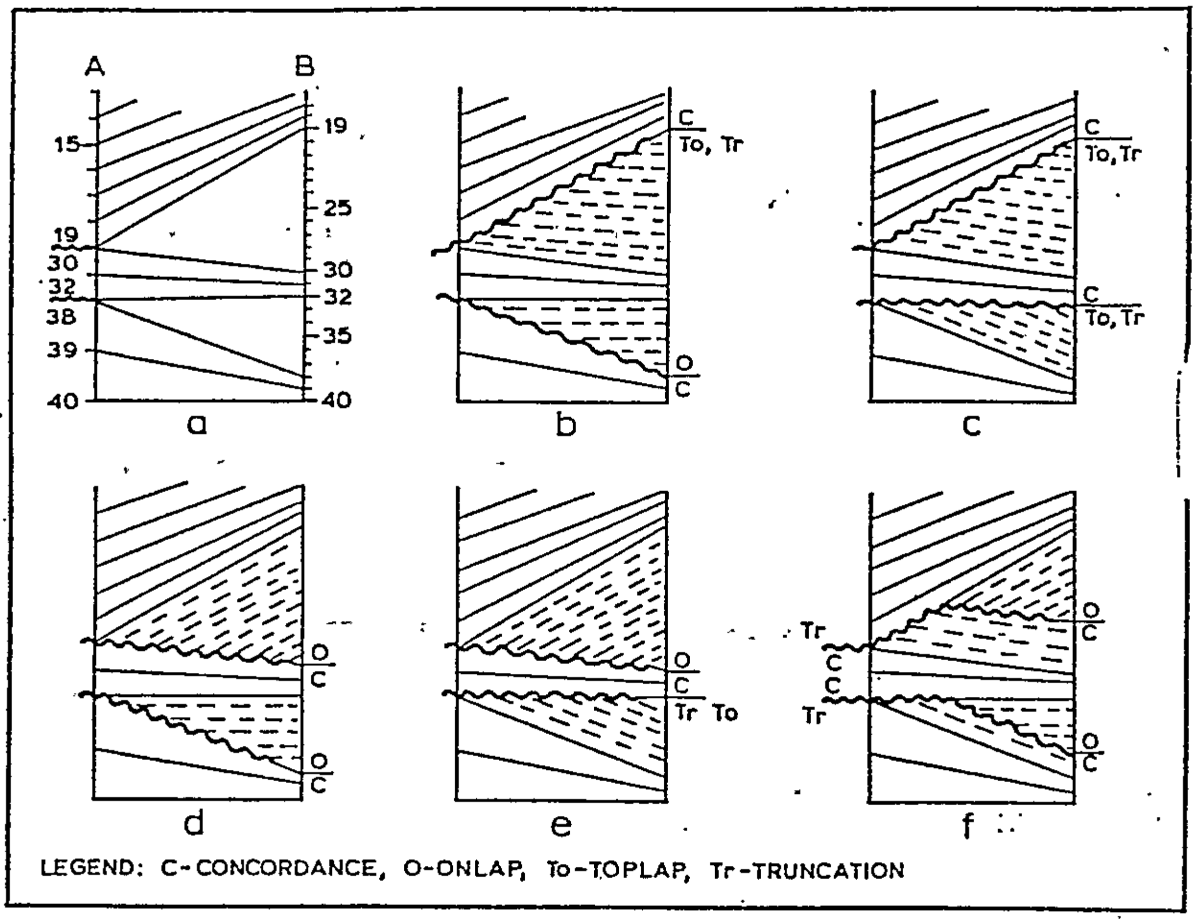

Fig A-31 – Pitfalls in construction of isochron cross section on depth-distance plot (compare with Fig A-25, Fig a shows full Ma levels found in sections A and B with straight line correlations of common ages giving isochrons at 1 Ma interval and leaving part of drawing unfinished. Stratigraphic section is complete at B. Figures b through f illustrate different ways to finish drawing, each completion having different geologic implications. Knowledge of regional geology and of depositional environment of sections, and use of Cycle Chart of Vail and Mitchum (1979), will assist in reaching an independent conclusion to be compared with seismic data.

A.3.5.2 Applications

Our approach may also solve conflicts similar to the one shown in Figure A-32. The seismic section and its interpretation are taken from Mitchum, Vail and Sangree (1977, Figure 3, p.120). The upper line drawing shows the seismic interpretation which suggests a substantial hiatus at the unconformity. Yet, the paleontologist who reports a 'complete section' can be right, as illustrated in the hypothetical 1 Ma isochron cross section of the lower line drawing. This synthetic seismic section is drawn on the same scale as the seismic section and shows lower resolution where sediment accumulation rates are high (20 cm/ka) but higher resolution where the rates are low (1.25 cm/ka). The bundle of 10 isochrons (left) corresponds to a complete section where a thick seismological pencil would draw a hiatus. This pseudo-problem arises in work on and near continental margins

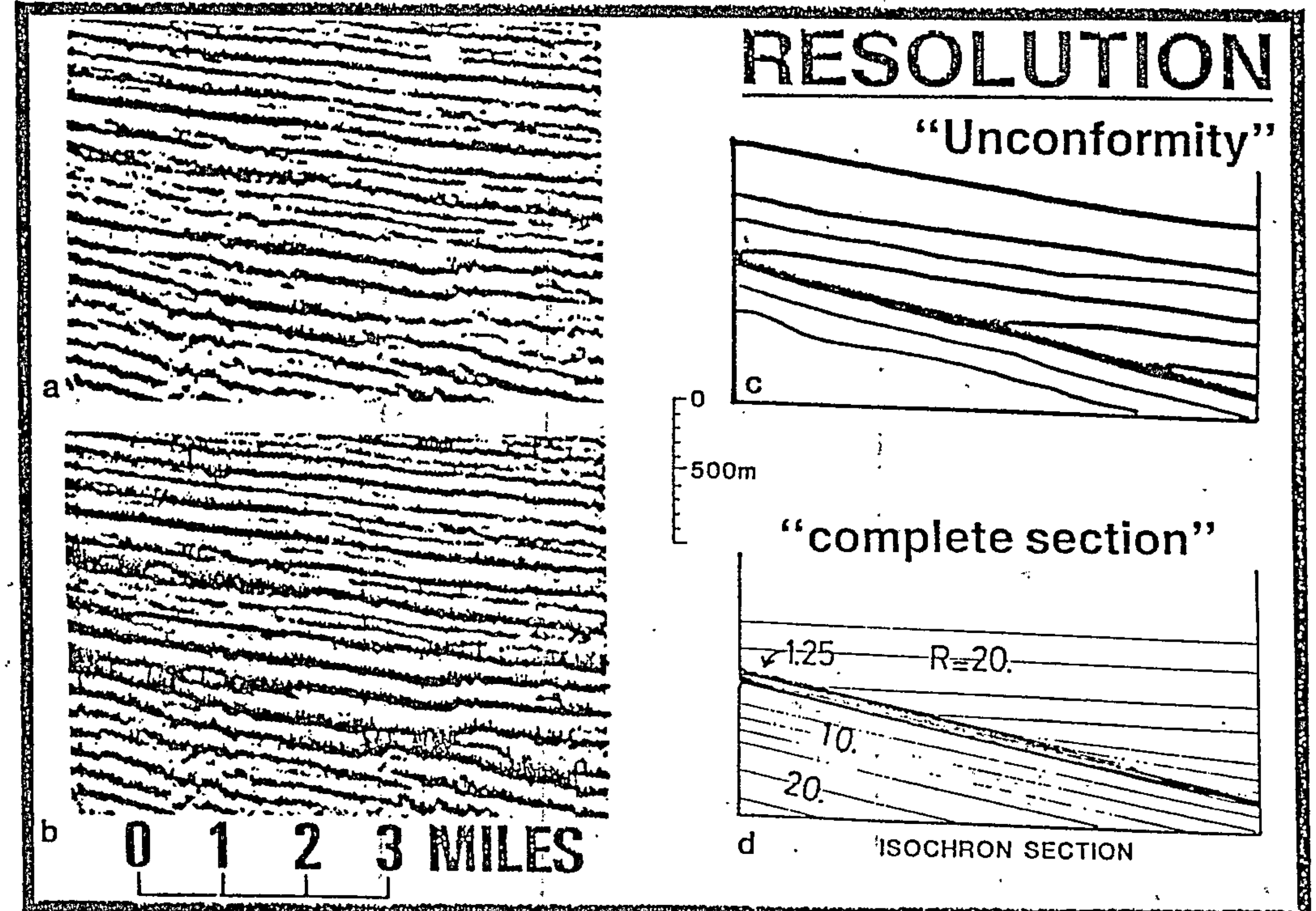

Fig: A-32— Illustration of scale problem hampering communication between different explorationists. Seismologists find unconformity with missing section, whereas paleontologists find no hiatus. Seismic section (a) and interpretation (b,c) after Mitchum, Vail and Sangree (1977, Figure 3). Synthetic seismic section (d), drawn to scale with isochron interval of 1 Ma. R = average rate of sediment accumulation; numbers are in cm ka. The isochron section is hypothetical and, in fact, quite unrealistic as one would rather expect such low accumulation rates in a downlap setting.

where low, pelagic sediment accumulation rates are not uncommon.

Synthetic seismic sections show chronostratigraphic depositional patterns similar to the seismic record. The geochronologic resolution of isochron cross sections is normally higher than that of seismic sections, so it can be used in the calibration and interpretation of the seismic record and in its extrapolation in 'bad data' areas. The depth-distance sections portray sediment accumulation rate patterns and form a useful base to plot parameters such as source and reservoir facies and geochemical and geophysical data. The numeric stratigraphic technique is particularly useful to continental margin explorationists where marine microfauna aid its application. With known vertical movements of a passive margin, the method detects sea level changes (that determined the sedimentary pattern) and local anomalies such as salt or shale movements.

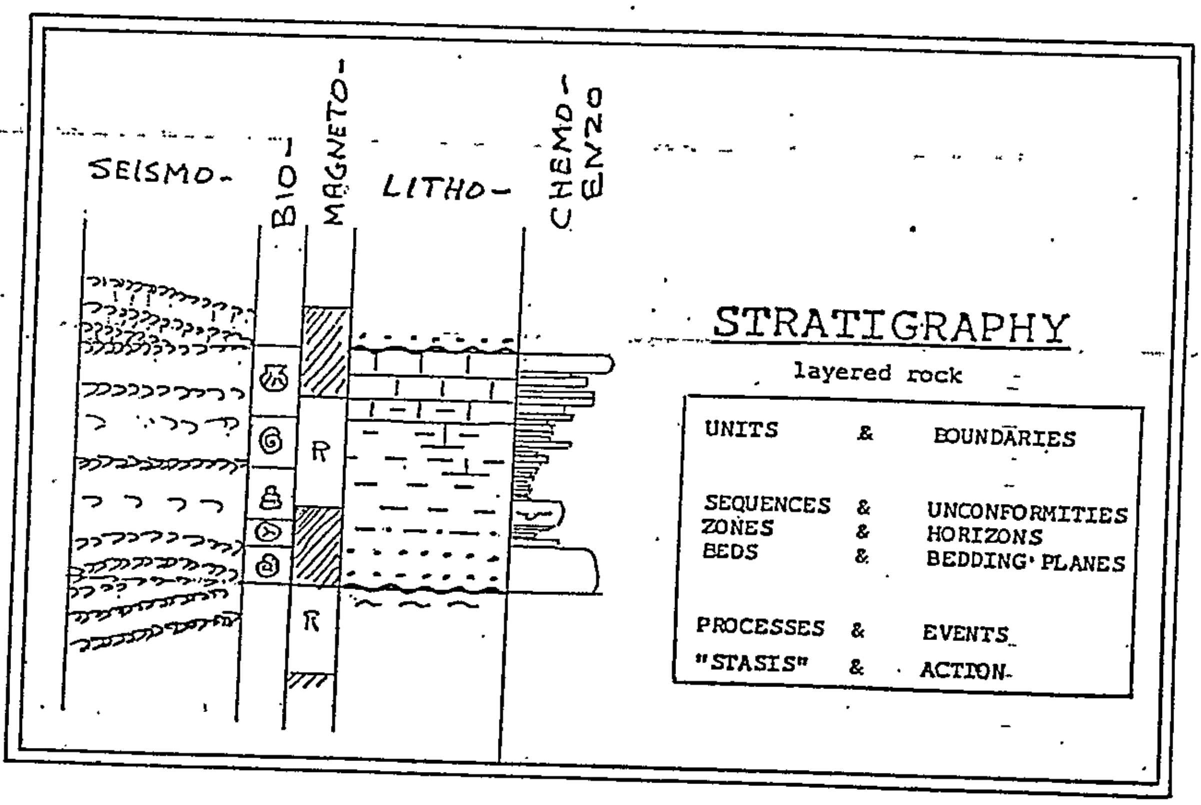

REFERENCES (includes references to thermal modeling)

ANDREWS-SPEED, C.P., et al, 1984 - Temperatures and Depth-Dependant Heat Flow in Western North Sea. AAPG Bull., v. 68, No 11, p.1764 - 1781

BALDWIN, B., & BUTLER, C.O., 1985 - Compaction Curves. AAPG Bull. 69, No 4, p 622-626

BANDY, O.L. & ARNAL, R.E., 1960 - Concepts of foraminiferal paleoecology. AAPG Bull., 44 : p. 1921-1932.

BARRELL, J., 1917 - Rhythms and the measurement of geologic time. Geol. Soc. America Bull., 28 : p. 745-904.

BERGER, W.H., 1974. - Deep-sea sedimentation, in C.A. Burk and C.L. Drake, eds., The Geology of Continental Margins. New York, Springer-Verlag, p. 213-241.

BERGGREN, W.A., 1972. - A Cenozoic time-scale -- some implications for regional geology and paleogeography. Lethaia, 5 : p. 195-215.

BERGGREN, W.A. & van COUVERING, J.A., 1974 - Biostratigraphy, geochronology and paleoclimatology of the last 15 million years in marine and continental sequences. Paleogeography, Paleoclimatology, Palaeocology, v.16, p.1-216.

BOND, G.C., 1978 - Speculations on real sealevel changes and vertical motions of continents at selected times in the Cretaceous and Tertiary Periods. Geology, 6 : p. 247 - 250.

BOND, G.C., 1979 - Evidence for some uplifts of large magnitude in continental platforms. Tectonophysics, 61 : p. 285-305.

BOTT, M.H., 1971 - Evolution of young continental margins and formation of shelf basins. Tectonophysics, 11 : p. 319-327.

BUROLLET, P.F., 1956 - Contribution a l'etude stratigraphique de la Tunesie Centrale. Tunesia Serv. Mines, Ann. Mines et Geologie, 18 : 345 p.

CARSLAW, H.S. & JAEGER, J.C., 1959 - Heat Conduction in Solids. 510 pp, Oxford University Press.

CERMAK, V., 1979 - Heat Flow Map of Europe. In Terrestrial Heat Flow in Europe, V.Cermak and L.Rybach eds., Springer Verlag. p3.

CHILINGARIAN, G.V. & WOLF, K.H., eds., 1975. Compaction of coarse-grained sediments, 1. Developments in Sedimentology, 18A : 522p.

COCHRAN, J.R., 1983 - Effects of finite rifting times on the development of sedimentary basins. Earth Plan. Sci. Lett., 66, p289-302.

DEIGHTON, I., FALVEY, D.A. & TAYLOR, D.J., 1976 - Depositional environments and geotectonic framework: Southern Australian Continental Margin. APEA Jnl., V16, pt 1, 25-36

DOW, W.G., 1977 - Kerogen studies and geological interpretations. Journal Geochemical Exploration, 7 : p. 79-99.

EICHER, D.L., 1968 - Geologic time. Englewood Cliffs, N.J., Prentice-Hall Inc., 149p.

FALVEY, D.A., 1974 - The development of continental margins in plate tectonic theory. APEA Jnl, 14 : p. 95-106.

FALVEY, D.A. & DEIGHTON, I., 1982 - Recent Advances in Burial and Thermal Geohistory Analysis. APEA Jnl., V.22,pt 1,65-81.

FALVEY, D.A. & Middleton, M.F., 1981 - Passive continental margins: evidence for a prebreakup deep crustal metamorphic subsidence mechanism. In: Colloquium on Geology of Continental Margins (C3), Oceanologica Acta, 4 (Supplement), : p.103-114.

FALVEY, D.A. & MUTTER, J.C., 1981 - Regional plate tectonics and the evolution of Australia's passive continental margins. BMR J. Aust. Geol., Geophys, 6 (1) : p. 1-29.

FRAKES, L.A., 1979 - Climates Throughout Geologic Time. Elsevier, 310 pp.

FRAKES, L.A. & KEMP, E.M., 1972 - Influence of continental positions on Early Tertiary climates. Nature, vol.240, No.5376, pp.97-100.

FRAZIER, D.E., 1974 - Depositional episodes: their relationship to the Quaternary stratigraphic framework in the northwestern portion of the Gulf Basin. Texas Univ. Bur. Econ. Geology Geol. Circ., 74 - 1 : 28p.

FULOP, J., 1971 - Les formations jurassique de la Hongrie, in Colloque du Jurassique Mediteraneen, Hungary, Magy. Allami Foldt. Intez., Evk., 54 (2) : p. 31-61.

GRETENER, P.E. & LABUTE, G.J., 1969 - Compaction - a discussion. Bull. Canadian Pet. Geol., 17 : p. 296-303.

GUIDISH,, T.M. et al., 1985 - Basin evaluation using burial geohistory calculations: an overview. AAPG Bull., v.69, No.1, pp92-105.

HAQ, B.U., HARDENBOL, J. & VAIL, P.R. 1987 - Chronology of fluctuating sea levels since the Triassic (250 million years ago to the present). Science. 235, 1156-1167.

HARDENBOL, J. & BERGGREN, W.A., 1978 - A new Paleogene numerical time scale: AAPG Studies in Geology, n.6, p.213-234.

HARDENBOL, J., VAIL, P.R. & FERRER, J., 1981 - Interpreting palaeoenvironments, subsidence history and sealevel changes of passive margins from seismic and biostratigraphy. In: Colloquium on Geology of Continental Margins (C3), Oceanologica Acta, 4 (supplement): p. 33-44.

HARLAND, W.B., et al., 1982 - A Geologic Time Scale. (Cambridge University Press).

HEROUX, Y., et al., 1979 - Compilation and Correlation of major thermal maturation indicators. AAPG Bull., 63, pp. 2128-2144.

HOOD, A., GUTJAHR, C.C.M. & HEACOCK, R.L., 1975 - Organic metamorphism and the generation of petroleum. AAPG Bull., 59 : p. 986-996.

HOROWITZ, D. H., 1976 - Mathemathical modelling of sediment accumulation in prograding deltaic systems. 9th Internat. Sedimentol. Cong. Proc., Pergamon Press.

JARVIS, G.T. & MCKENZIE, D.P., 1979 - Sedimentary basin formation with finite extension rates. Earth Planet Sci. Lett. 48, 42-52.

KEEN, M.J. & KEEN, C.E., 1973 - Subsidence and fracturing on the continental margin of eastern Canada. Canada Geol. Survey Paper, 71-23 : p. 23-42.

KUENEN, Ph., 1939. Quantitative estimations relating to eustatic movements. Geology en Mijnbouw, 18 : p. 194-201.

LEMOINE, P., 1911 - Geologie du bassin de Paris. Paris Librairie Sci. Hermann et fils.

LERCHE, I., et al., 1984 - Determination of paleo-heatflux from vitrinite reflectance data. AAPG Bull., 68, pp. 1704-1717.

LOPATIN, N.V., 1971. - Temperature and geological time as coalification factors (in Russian). Akad. Nauk. SSR Izv., Geolgy Series, 3 : p. 95-106.

McKENZIE, D., 1978 - Some Remarks on the development of sedimentary basins. Earth Planet. Sci. Lett., 40 : p. 25-32.

MITCHUM, R.M., VAIL, P.R. & SANGREE, J.B., 1974 - Regional stratigraphic framework from seismic sequences (abs). Geol. Soc. America Abs. with Programs, 6 : 873p.

MITCHUM, R.M., Jr., VAIL, P.R. & Thompson, S., III, 1977 - Seismic stratigraphy and global changes of sea level, part 2: the depositional sequence as a basis unit for stratigraphic analysis: AAPG Memoir, n.26, p. 53-62.

MITCHUM R.M., Jr., & SANGREE, J.B., 1977 - Seismic stratigraphy and global changes of sea level, part 6: Stratigraphic interpretation of seismic reflection patterns in depositional sequences: AAPG Memoir, n. 26, p. 117-133.

MURRAY, J.W., 1973 - Distribution and Ecology of Living Benthic Foraminiferids. Heinemann. 274pp.

OXBURGH, E.R. & ANDREWS-SPEED, C.P., 1981 - Temperature, thermal gradients and heat flow in the southwestern North Sea. in Petrolem Geology of the Continental Shelf of NW Europe, 62-75, (Heyden, London).

ORBIGNY, A. d'., 1850 - Cours elementaire de paleontologie et de geologie Stratigraphique: Paris, Masson, 2 volumes.

PERRIER, R. & QUIBLIER, J., 1974 - Thickness changes in sedimentary layers during compaction history : methods for quantitative evaluation. AAPG Bull., 58 : p. 507-520.

PFLUM, C.E., & FRERICHS, W.E., 1976 - Gulf of Mexico deep-water foraminiferas. Cush. Found. Spec. Publ., 14:125pp.

PHILIPP, W., 1961 - Struktur- und Lagerstattengeschichte des Erdolfeldes Eldingen. Deutsch. Geol. Gesell. Zeitschr., 112 : p. 414-482.

POSTUMA. J.A., 1971 - Manual of Planktonic Foraminifera, Elsevier, Amsterdam, 420pp.

ROBASZYNSKI, F. & CARON, M., 1979 - Atlas de Foraminiferes Plancton du Cretace Moyen (Mer Boreale et Tethys). Cahiers de Micropaleontologie, Pts 1 & 2.

ROBASZYNSKI, F., CARON, M., GONZALEZ DONOSO, J.M., WONDERS, A.A.H. & Eur. W.G., Plankt. Foram., 1984 - Atlas of Late Cretaceous Globotruncanids. Revue de Micropaleontologie, Vol 26, No 3-4, p.145-305

ROGERS, M.A. & van HINTE, J.E., in press. Organic geochemical evaluation of some Tertiary deep water sediments from the Atlantic North of 45 North. DSDP. Supp. Rept., North Atlantic.

ROLL, A., 1974 - Langfristige Reduction der Machtigkeit von Sedimentgesteinen und ihre Auswirkung - eine Ubersicht. Geol. Jahrb., series A, 14 : 76 p.

ROYDEN, L., SCLATER, J.G. & VON HERZEN, R.P., 1980 - Continental margin subsidence and heatflow : important parameters in formation of petroleum hydrocarbons. AAPG Bull., 64 (2) : p. 173-187.

RUFFMAN, A. & Van HINTE, J.E., 1973 - Orphan Knoll - a "chip" of the North American plate. Canada Geol. Survey Paper, 71 - 23, p. 407-449

RUTHERFORD, K.J. & QURESHI, M.K., 1981 - Geothermal Gradient Map of Southeast Asia. 2nd Edition. Southeast Asia Petroleum Exploration Society and Indonesian Petroleum Association joint publication.

RYAN, W.B.F., et al, 1974 - A paleomagnetic assignment of Neogene stage boundaries and the development of isochronous datum planes between the Mediterranean, the Pacific and Indian oceans in order to investigate the ressponse of the world ocean to the Mediterranean salinity crisis. Rivista Italiana Paleontologia e Stratigrafia, v. 80, n. 4 p. 631-688.

SAWYER, D. S., 1986 - Effects of basement topography on subsidence history analysis. Earth Plan. Sci. Lett. 78. pp.427-434.

SCLATER, J.G., ANDERSON, R.N. & BELL, M.L., 1971 - Elevation of ridges and evolution of the central eastern Pacific. Jour. Geophys. Research, 76 : p. 7888-7915.

SCLATER, J.G. & CHRISTIE, P.A.F., 1980 - Continental stretching : an explanation of the post-mid-Cretaceous subsidence of the central North Sea Basin. Journal of Geophysical Research, 85 : p. 3711-3739.

SEELY, D.R., VAIL, P.R. & WALTON, G.G., 1974 - Trench slope model, in C.A. Burk, et al., eds., The Geology of Continental Margins. New York, Springer-Verlag : p. 249-260.

SHIBAOKA, M. & BENNETT, A.J.R., 1977 - Patterns of diagenesis in some

Australian sedimentary basins. APEA Journal, 17 (1) : p. 58- 63.

SHINN, E.A. et al., 1977. - Limestone compaction: an enigma. Geology, 5 : p. 21-24.

SLEEP, N.H., 1971 - Thermal effects of the formation of Atlantic continental margins by continental break up. Royal Astron Soc. Geophys. Jour., 24 : p. 325-350.

SLEEP, N.J., 1976 - Platform subsidence mechanisms and 'eustatic' sealevel changes. Tectonophysics, 36 : p. 45-56.

SLITER, W.V. & BAKER, R.A., 1972 - Cretaceous Bathymetric Distribution of Benthic Foraminifers. J. of Foram. Res. V2. No 4 p167-183.

SMITH, A.G. & HALLAM, A., 1970 - The Fit Of The Southern Continents. Nature. Vol. 225. p139-144.

STAINFORTH, R.M., et al, 1975 - Cenozoic planktonic foraminiferal zonation and characteristics of index forms: University of Kansas Paleontological Contribution, article 62, p. 1-425.

SUESS, E., 1909 - Das Antlitz der Erde. Prag. Tempsky, v.3, part 2, 789 p.

TISSOT, B. & WELTE, D.H., 1983 - Petroleum Formation and its occurence. Springer Verlag, New York.

UMBGROVE, J.H.F., 1939 - On rhythms in the history of the earth. Geol. Mag., 76 :p. 116-129.

VAIL, P.R., & MITCHUM , R.M., Jr., 1977 - Seismic stratigraphy and global changes of sea level, part 1: Overview. AAPG Memoir, n. 26. p.51-52.

VAIL, P.R., & MITCHUM, R.M., Jr., 1979 - Global cycles of relative changes of sea level from seismic stratigraphy: AAPG Memoir, n.29, p.469-472.

VAIL, P.R., MITCHUM, R.M., Jr. & THOMPSON, S., 1974 - Eustatic cycles based on sequences with coastal onlap (abs). Geol. Soc. America Abs. with Programs, 6 : p. 993.

VAIL, P.R., MITCHUM, R.M. Jr., & THOMPSON, S., III, 1977 - Seismic stratigraphy and global changes of sea-level, part 4: global cycles of relative changes of sea level. AAPG Memoir, n. 26, p. 83-97.

VAN COUVERING, J.A. & BERGGREN, W.A., 1977 - Biostratigraphical Basis of the Neogene Time Scale. Concepts and Methods of Biostratigraphy. Edited by E.G. Kauffman & J.E. Hazel. Dowden, Hutchison & Ross Inc. Stroudsberg, Pennsylvania.

van HINTE, J.E., 1976a - A Jurassic time scale. AAPG Bull., 60. p.489-497.

Van HINTE, J.E., 1976b - A Cretaceous time scale. AAPG Bull.,60. p.498-516.

Van HINTE, J.E., 1978 - Geohistory analysis - application of micropalaeontology in exploration geology. AAPG Bull., 62 : p. 201-222.

Van HINTE, J.E., 1982 - Synthetic Seismic Sections from Biostratigraphy, AAPG Mem.

Van HINTE, J.E., COLIN, J.P. & LEHMAN, R., 1980 - Micropaleontologic record of the Messinian event at Esso Libya Inc. Well B1-NC35A on the Pelagian Platform , in Proceedings, Second Symposium on the Geology of Libya: London, Academic Press, v.. I.p. 205-244.

VEEVERS, J.J. & COTTERILL, D., 1978 - Western margin of Australia ; evolution of a rifted arch system. Geological Society of America, Bull., 89 : p. 337-355.

VOGT, P.R., 1970 - Magnetized basement outcrops on the south-east Greenland continental shelf. Nature, 226 : p. 743-744.

VOGT, P.R. & OSTENSO, N.A., 1967 - Steady state crustal spreading. Nature, 215 : p. 810-817.

WAPLES, D.W., 1980 - Time and temperature in petroleum formation : application of Lopatin's method to petroleum exploration. AAPG Bull., 64 : p. 916-926.

WATTS, A.B. 1981 - AAPG Course notes #19. Atlantic City, New Jersey.

WATTS, A.B. & STECKLER, M.S., 1979 - Subsidence and eustasy at the continental margin of eastern North America. In : Talwani, M., Hay, W. and Ryan, W. (Eds.). Deep Drilling Results in the Atlantic Ocean : Continental Margins and Palaeoenvironments. American Geophysical Union, Maurice Ewing Series, 3 : p. 218-234.

WATTS, A.B., KARNER, G.D. & STECKLER, M.S., 1982 - Lithospheric flexure and the evolution of sedimentary basins. Phil. Trans. R. Soc. Lond. A 305, pp. 249-281.

WHEELER, H.A., 1958 - Time stratigraphy. AAPG Bull., 42 : p. 1047-1063.

WISE, D.U., 1972 - Freeboard of continents through time, in Studies in earth and space sciences. Geol. Soc. America Mem., 132

ZIEGLER, P.A., 1981 - Evolution of sedimentary basins in North-West Europe in Petrolem Geology of the Continental Shelf of NW Europe, 3-42, (Heyden, London).

ZIEGLER, P.A., 1982 - Faulting and graben formation in Central and Western Europe. Phil. Trans. R. Soc. Lond. A., 305, pp. 113-143.

PROBLEM 2

We drilled well A and got the following information from paleo:

depth	top	environment
x m	Middle Eocene limestone	Inner-Middle Neritic
1300 m	Lower Eocene limestone	
1550 m	Upper Paleocene marl (Thanetian)	Outer Neritic-Upper Bathyal
2050 m	Lower Paleocene marl (Danian)	Upper Bathyal
2700 m	Upper Cretaceous limestone and shales	Outer Neritic
	2700 m Maastrichtian	
	3050 m Campanian	

From the paleo-log we further read: the top of a shallow water equivalent of the M. aragonensis Zone at 1450 m, a marker for the top of the M. angulata Zone at 1700 m and for the S. trinidadensis Zone at 2500 m; the top of Bolivinoides miliaris is given at 2800 m and the base of G. calcarata at 3250 m. No other markers have been recorded till TD at 3430 m. E-log pattern changes occur at 1550 and 2700 m.

a. Complete the attached figure by drawing Stage boundaries and unconformities.
b. Mark in the Ma column all numerical ages you know and calculate an estimate for the ages at the unconformities.
c. Calculate the depth for all other whole number numeric ages between 49 and 72 Ma.

Use Paleogene and Cretaceous reference schemes.

Problem 2.

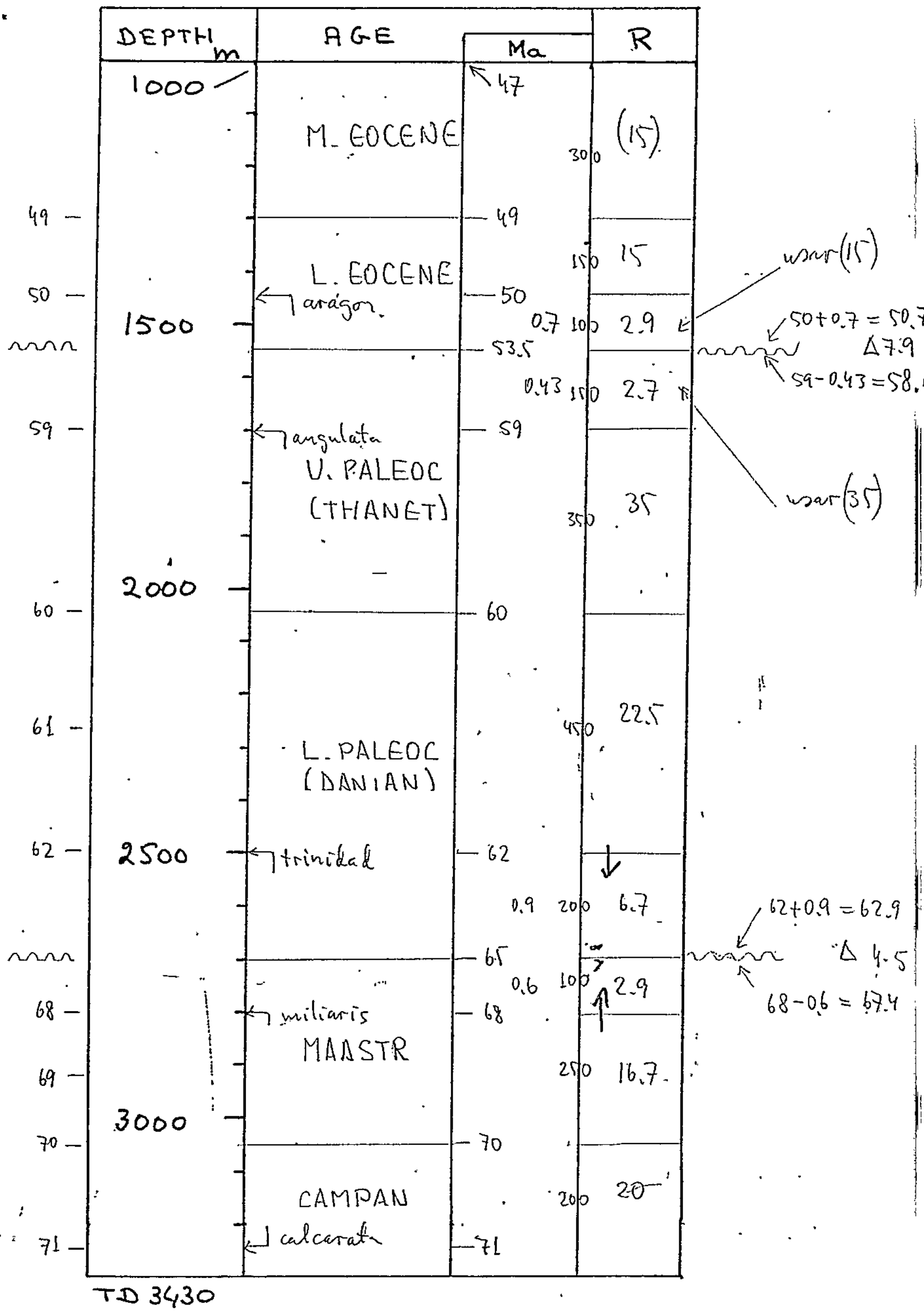
DEPTH m
AGE
Ma
R
1000
47
M. EOCENE
300
(15)
49
49
L. EOCENE
150
15
50
50
arágon.
1500
0.7 100
2.9
wsar(15)
53.5
50+0.7 = 50.7
Δ 7.9
59-0.43 = 58.
0.43 150
2.7
59
angulata
59
U. PALEOC
(THANET)
350
35
wsar(35)
2000
60
60
61
450
22.5
L. PALEOC
(DANIAN)
62
2500
trinidad
62
0.9
200
6.7
62+0.9 = 62.9
Δ 4.5
68-0.6 = 67.4
65
0.6
100
2.9
68
miliaris
68
MAASTR
69
250
16.7
3000
70
70
CAMPAN
200
20
71
calcarata
71
TD 3430

Problem 2. Solution.

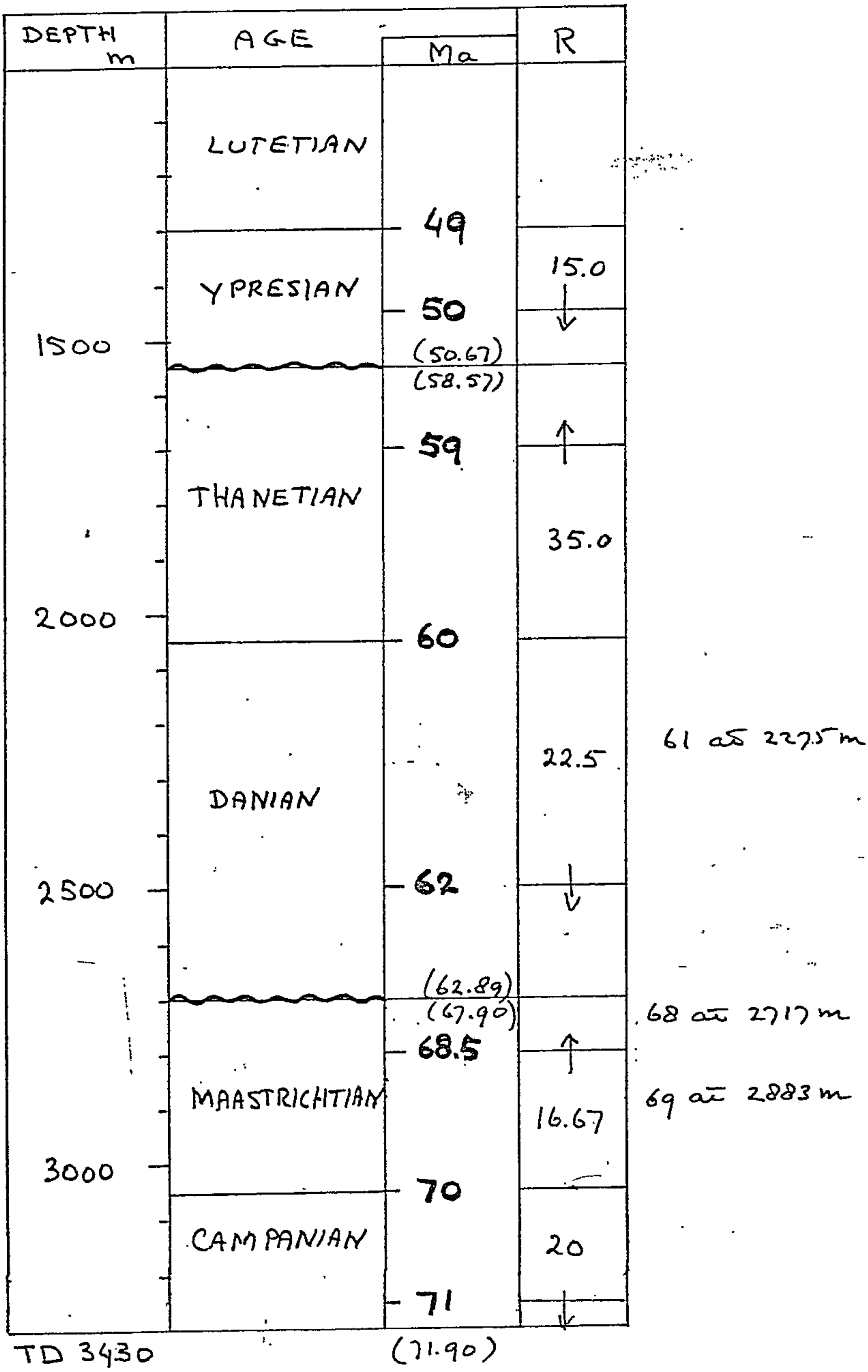

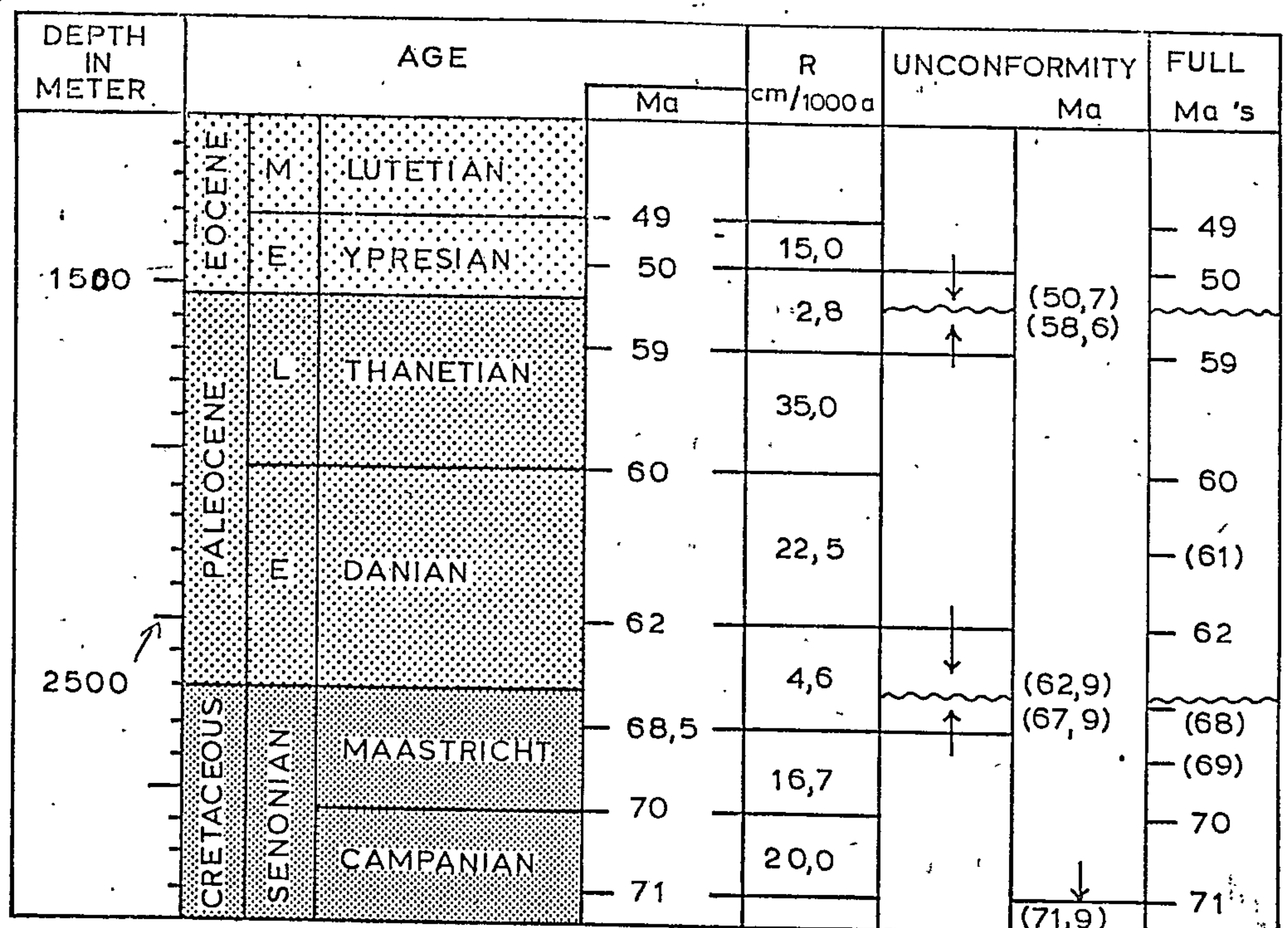

Problem 2. Solution.

PROBLEM 3

In addition to well A of problem 2, wells B and C were drilled. The attached cross-section is a conventional correlation between the three wells. Like we did for well A of problem 2, a friend extracted the following whole number numeric age depths and the ages at the unconformities from the paleo-reports on wells B and C.

Well B Age Ma	depth m	Well C Age Ma	depth m
49	1300	49	1300
50	1500	50	1525
51	1650	51	1700
51.9	1800	52	1900
56.0	1800	53	2100
57	2000	54	2200
58	2200	55	2240
59	2300	56	2280
60	2400	57	2320
61	2460	58	2360
62	2500	59.0	2400
62.4	2520	69.7	2400
69.5	2520	70	2500
70	2650	71	2800
71	2850	72	3200
72	3100	73	3500
73	3300	TD 73.7	3700
74	3450		
TD 74.5	3500		

a. How would you draw a cross-section correlating the three wells?
b. Draw a cross-section with isochrons at 1 Ma interval and depth as a vertical linear scale. Use attached frame.
c. Apply seismostratigraphic terminology on your section (onlap etc.).
d. Draw the cross-section with linear time as vertical scale. Use attached frame.
e. Compare your results with the conventional cross-section.

Problem 3.

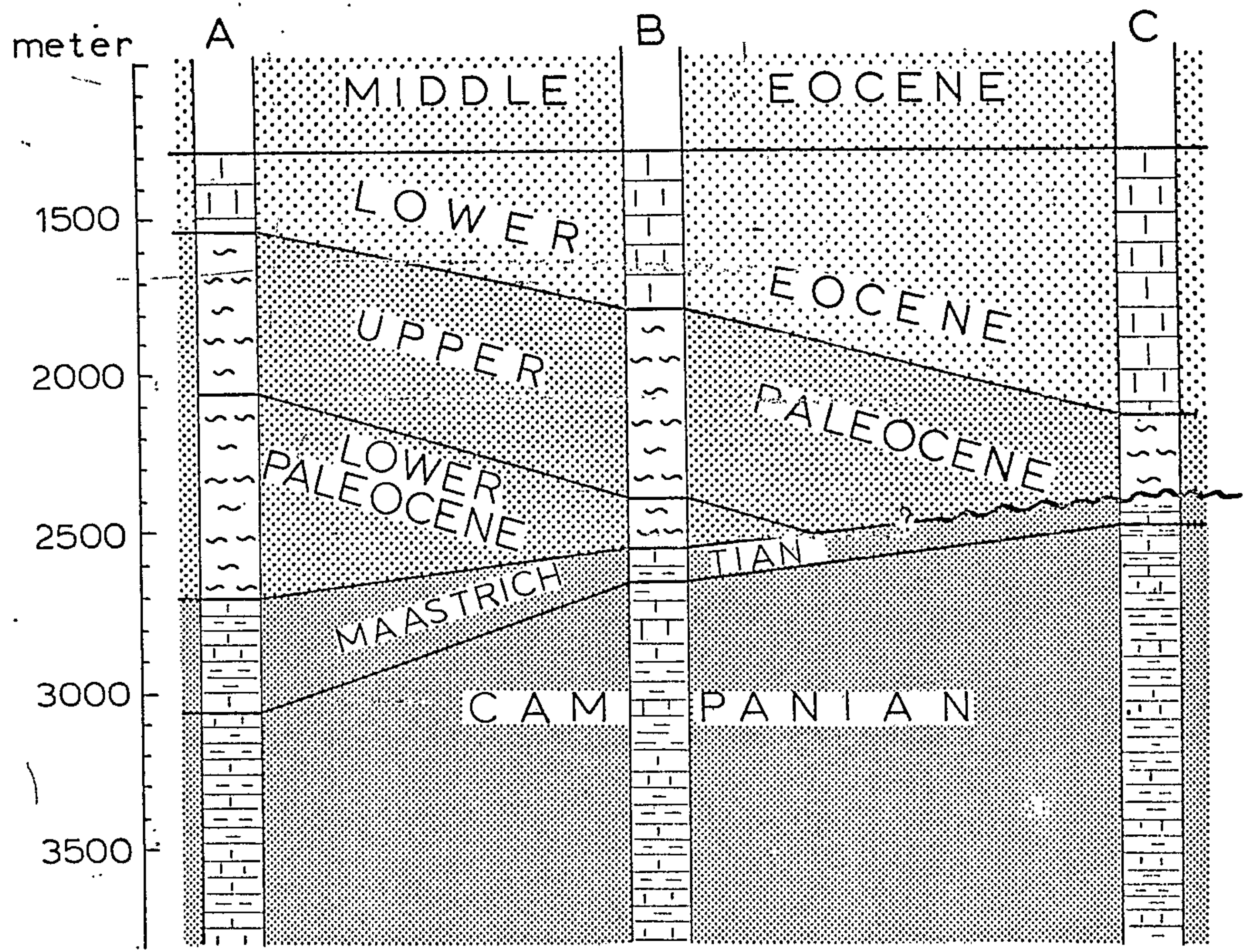

CONVENTIONAL CORRELATION

PROBLEM 3b,c.

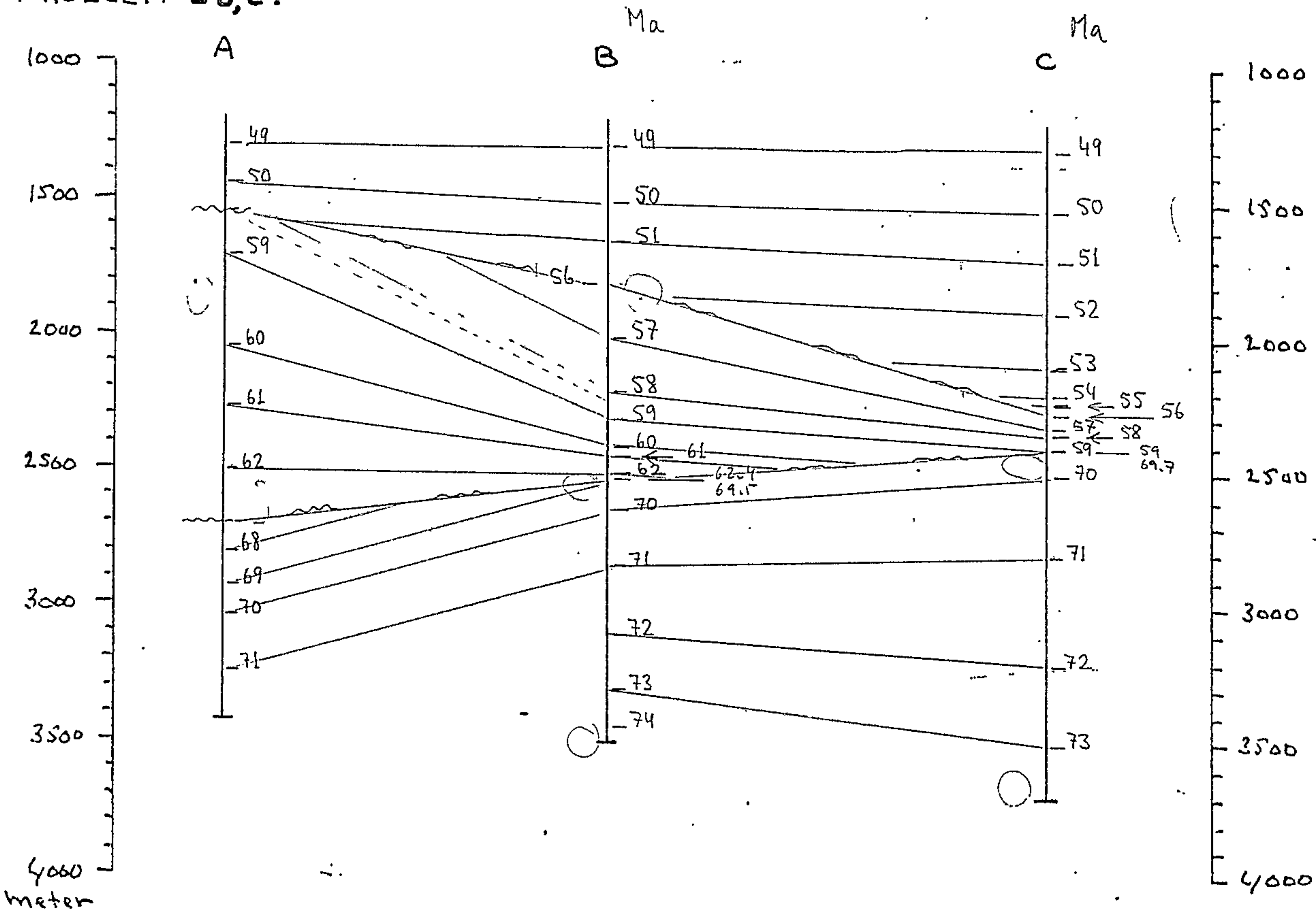

A
B
C
Ma
Ma
1000
1500
2000
2500
3000
3500
4000
meter
49
50
51
52
53
54
55
56
57
58
59
60
61
62
68
69
70
71
72
73
74
62.4
69.5
59
69.7

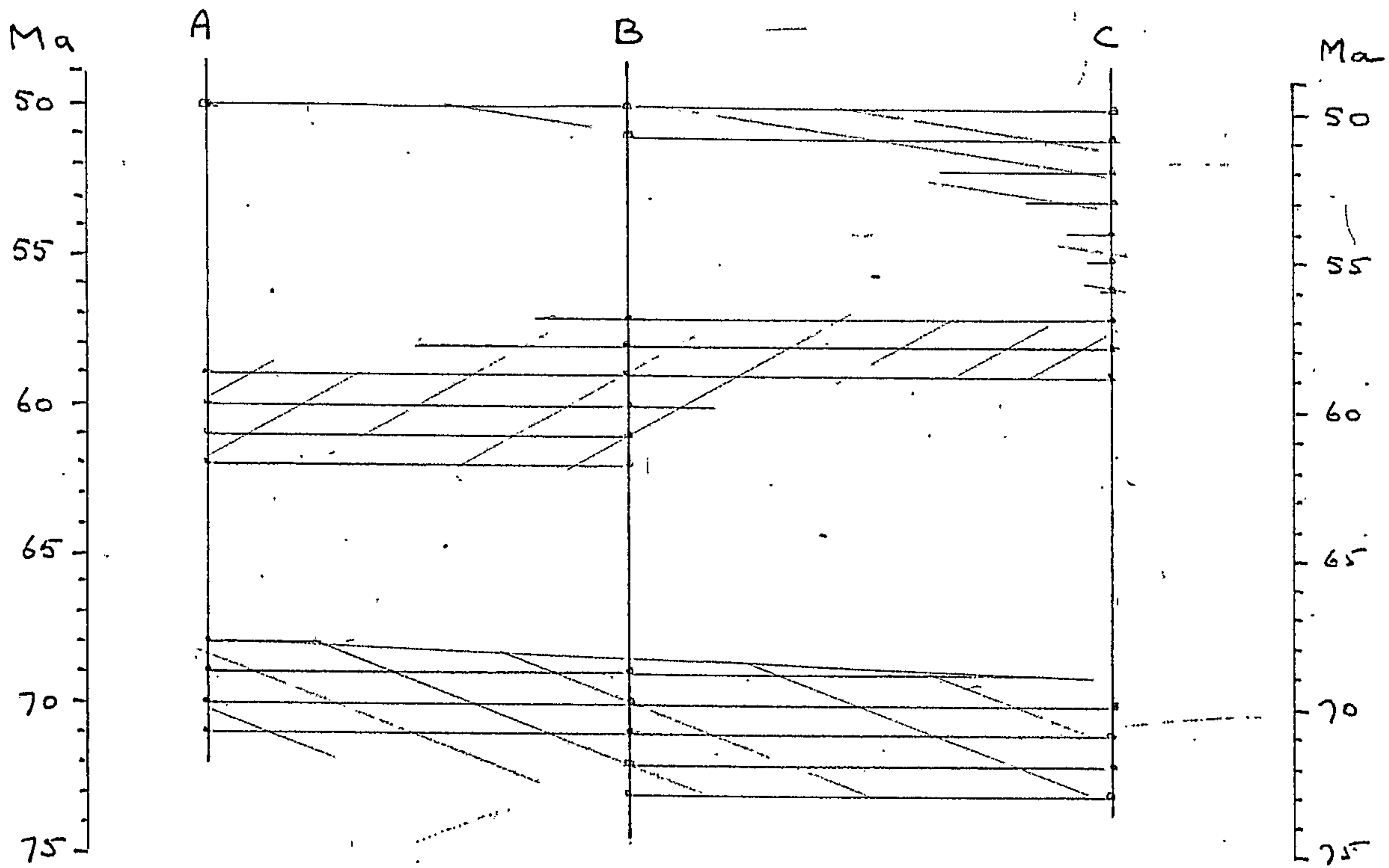

Problem 3d.

Problem 3.
Solution 3c.

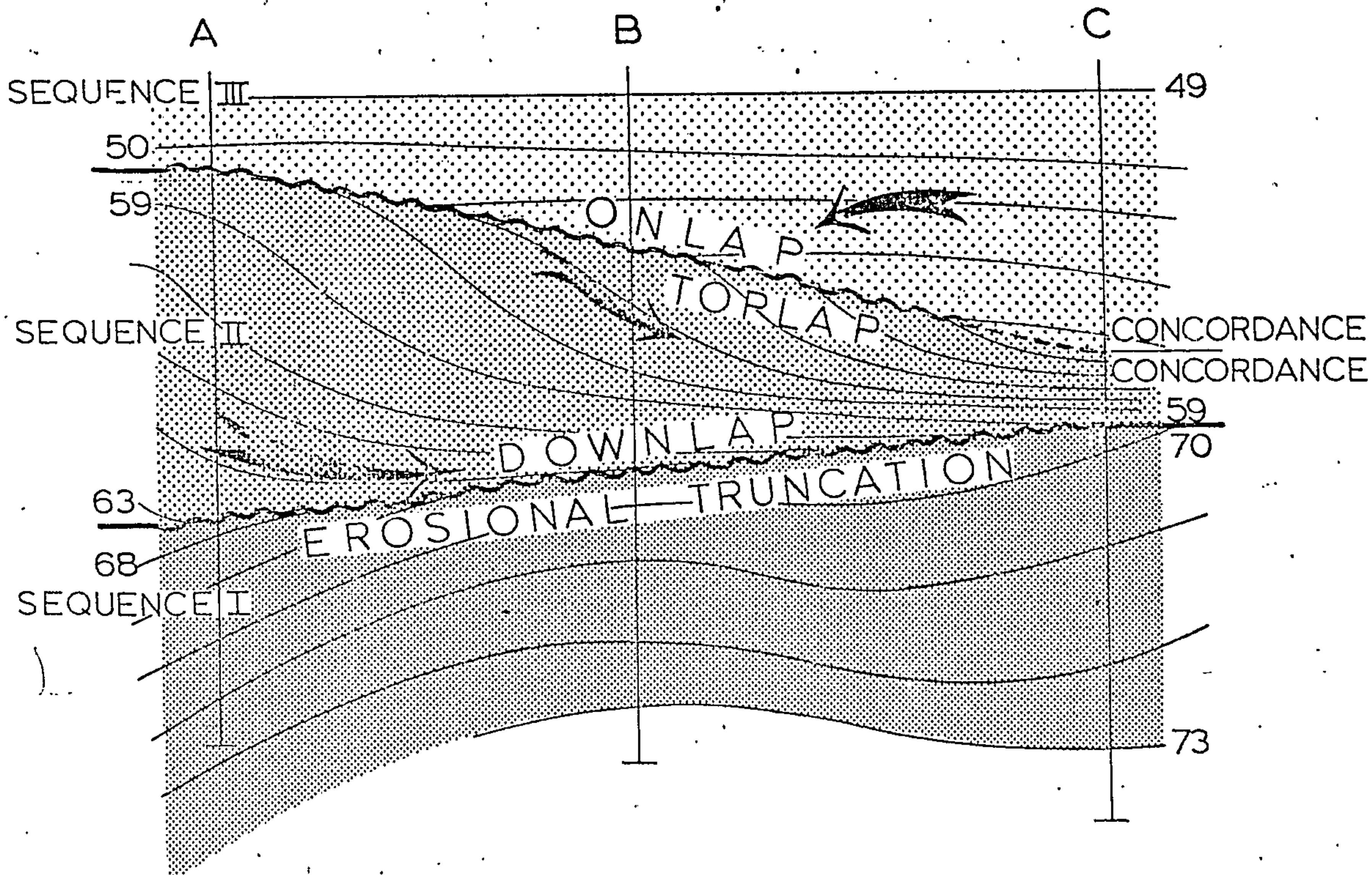

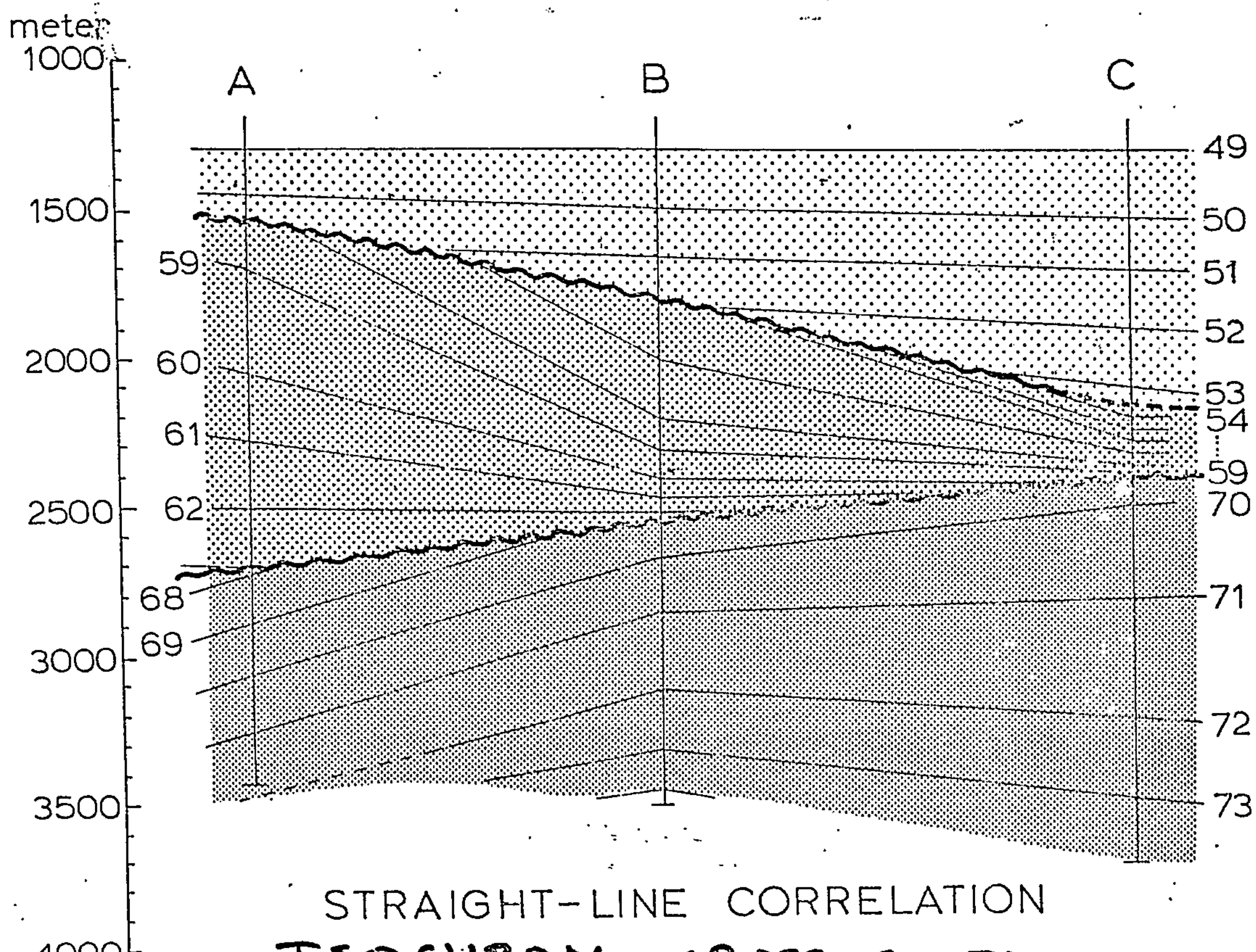

Problem 3.
Solution 3b.

STRAIGHT-LINE CORRELATION

ISOCHRON CROSS-SECTION

Problem 3.
Solution 3b.

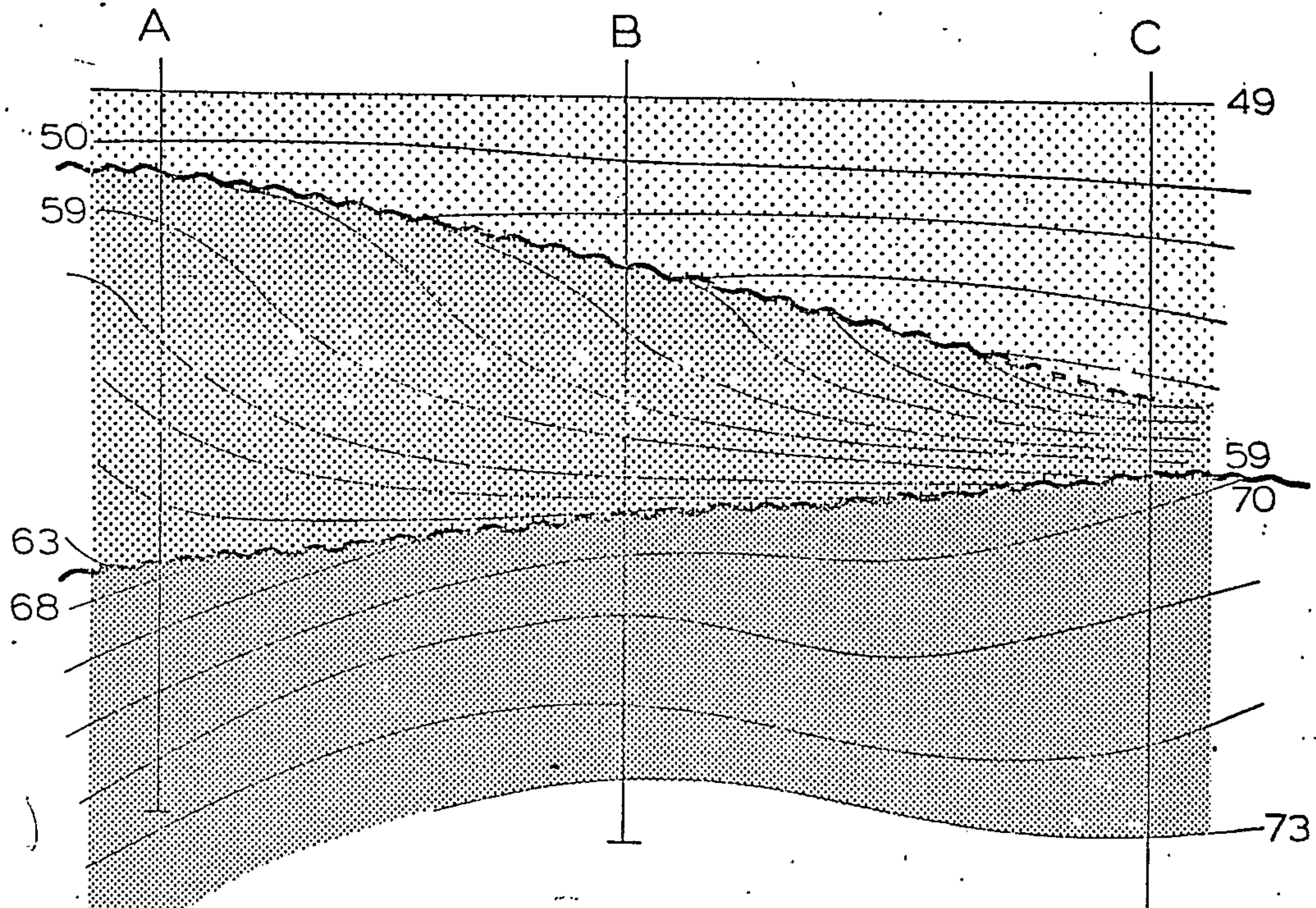

CORRELATION + GEOL. INTERPRETATION

Problem 3.
Solution 3d.

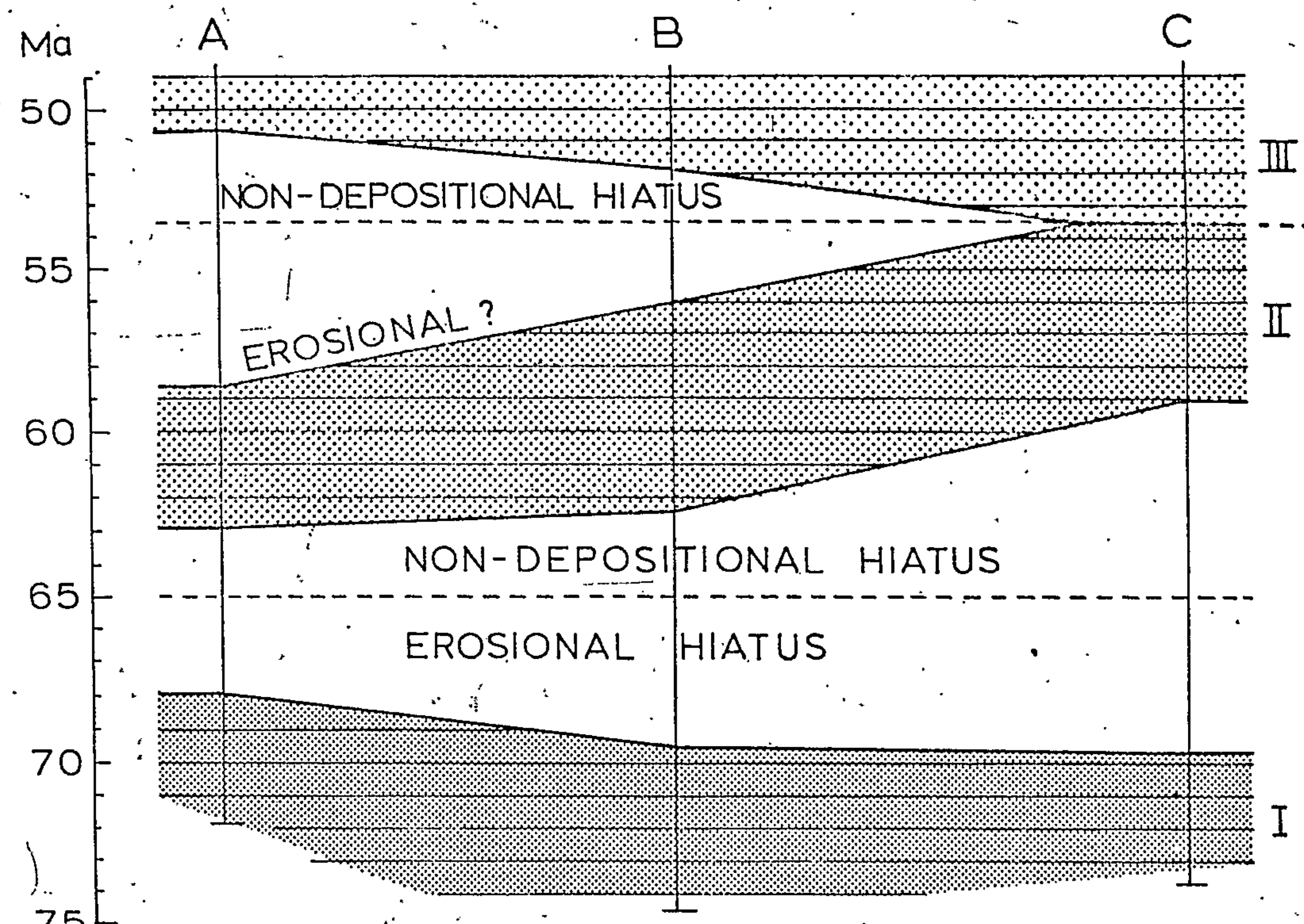

TIME - DISTANCE PLOT

Análisis Geohistórico 10/Nov/89

Time units Wickman, 1968

Paleobath. est by forams, ostracs, microfacie

neritic good resolution { 0 – 200

bathyal ± resolution { 200 – 2.000

abyssal + hadal poor resolution { 2000 – 6000

— . — . —

numerical technique
allows to: calculate: rate of fill & rate of subsidence
portray: geologic events & processes

— . — . —

Problem 1. cálculos

Armando Fasola

Geohistory Analysis Workshop

CARACAS, November 10 - 12, 1989

Friday November 10.

09:00 Introduction

09:30 Basic principles and techniques of Geohistory Analysis

10:00 Exercise No. 1
Computer solution

12:00 Lunch

13:00 Exploration paleontology: a data base of biosignals

13:30 Paleobathymetry

14:00 Time-scales

14:30 tea/coffee

15:00 HC exploration applications
Compaction correction
Stripped basement vs sediment movement
Temperature history
Computerized applications

17:00 End of day 1.

Saturday November 11.

09:00 Stratigraphic record of sea level change

10:00 Exercise No. 2

12:00 Lunch

13:00 Unifying stratigraphic concepts

14:00 Exercise No. 3
Construction of synthetic seismic section
Computer solution

16:00 Conditions for Geohistory Analysis

16:30 Wrap-up and general discussion

17:00 End of day 2.

Sunday November 12.

09:00 - 17:00. Discuss delegate's case histories either in class or individually.

Jan E. van Hinte
Amsterdam 6/9/89

EARLY TERTIARY — TIME-STRATIGRAPHIC REFERENCE SCHEME — AREA: — AUTHOR: DATE:

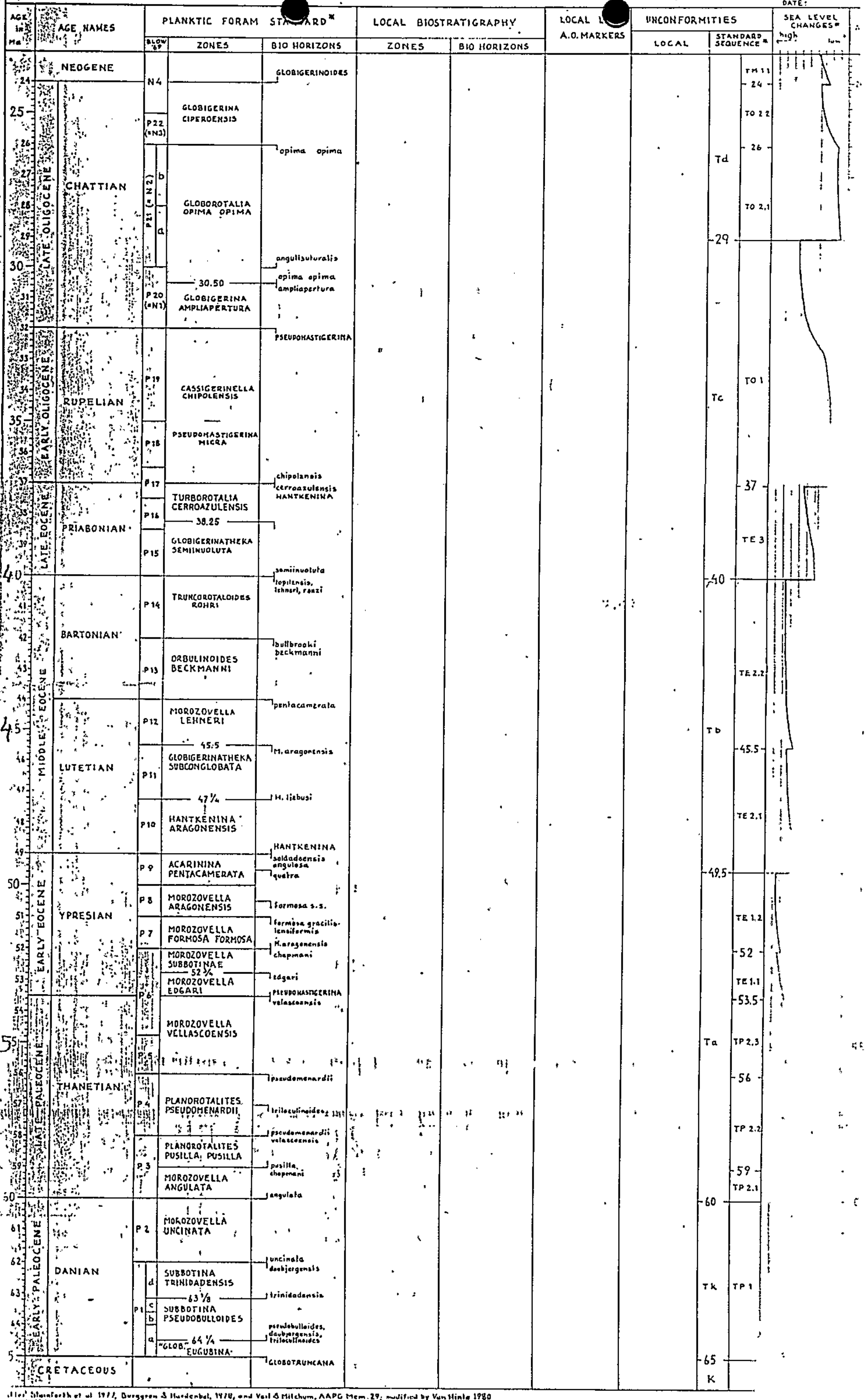

after Stainforth et al. 1977, Berggren & Hardenbol, 1978, and Vail & Mitchum, AAPG Mem. 29; modified by Van Hinte 1980

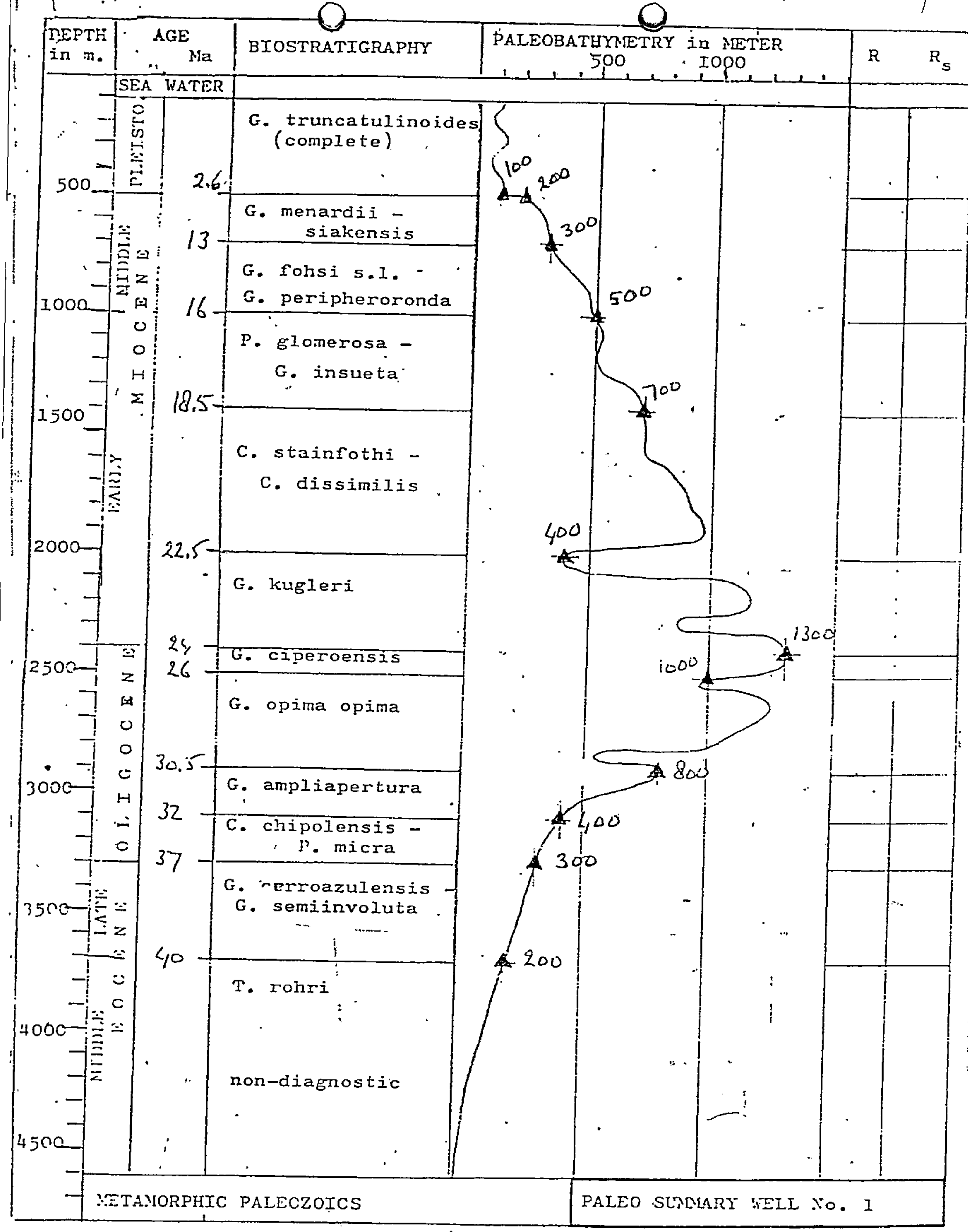

Problem 1, Steps 1 and 2.

DEPTH	T	AGE	A	R	WD	ΔW	RS
100	400	0			100		
500	200	2.6/(11)	2.6 (8.4) (2)	15.4 (0) (10)	100/200	0 100 100	15.4 (1.2) (5) –1.2
700	300	13	3	10	300	200	3.3
1000	400	16	2.5	16	500	200	8
1400	600	18.5	4	15	700	-300	22.5
2000	400	22.5	1,5	27	400	900	-33
2400	100	24	2	5	1300	-300	20
2500	400	26	4.5	8.8	1000	-200	13.2
2900	200	30.5	1.5	13.3	800	-400	40
3100	200	32	5	4	400	-100	6
3300	400	37	3	13.3	300	-100	16.6
3700	900	40	(6.8)	(13.3)	200	-200	16.2
4600		(46.8)			0		

Problem 1. Step 3.

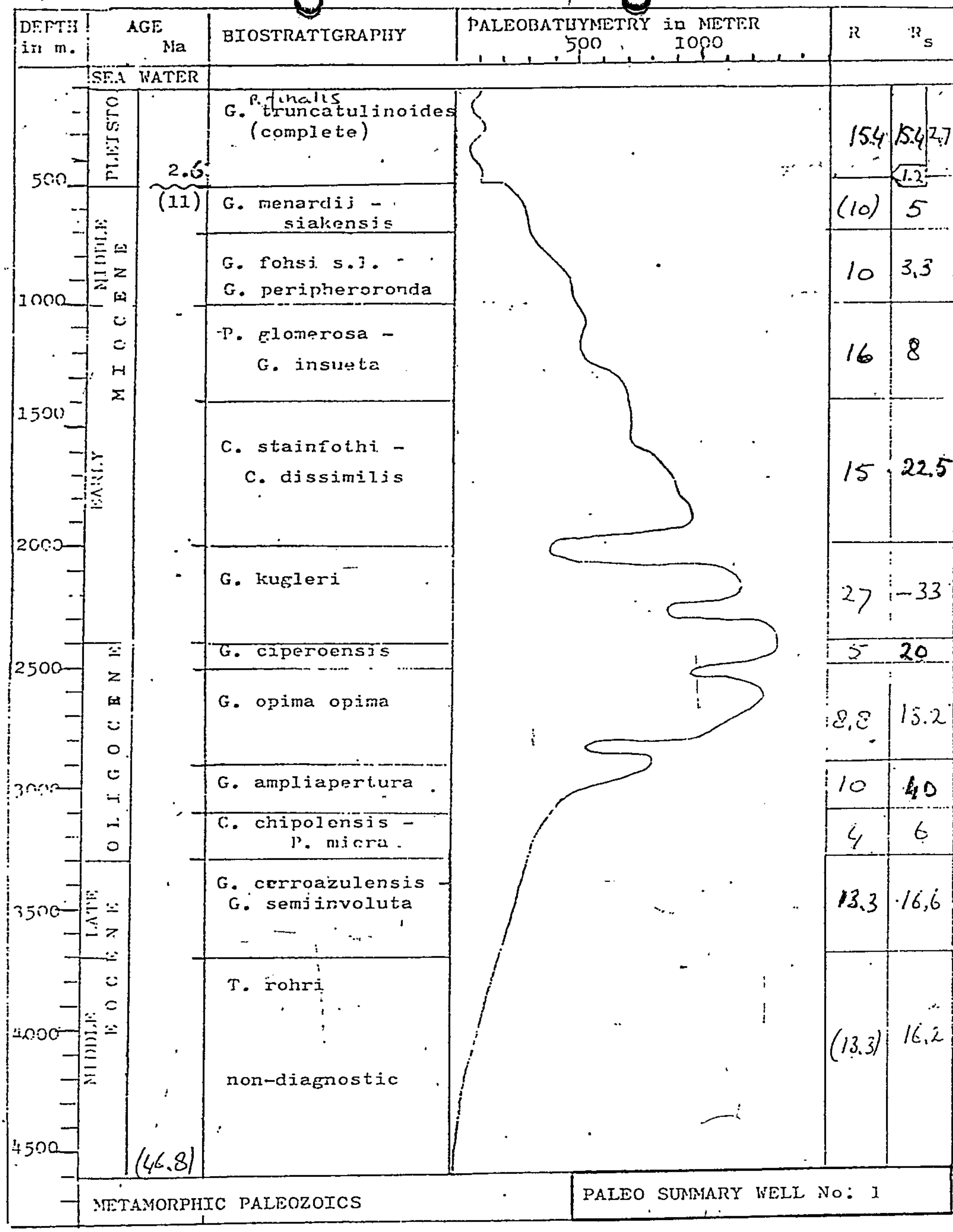

Problem 1.

Steps 4, 5 and 6.

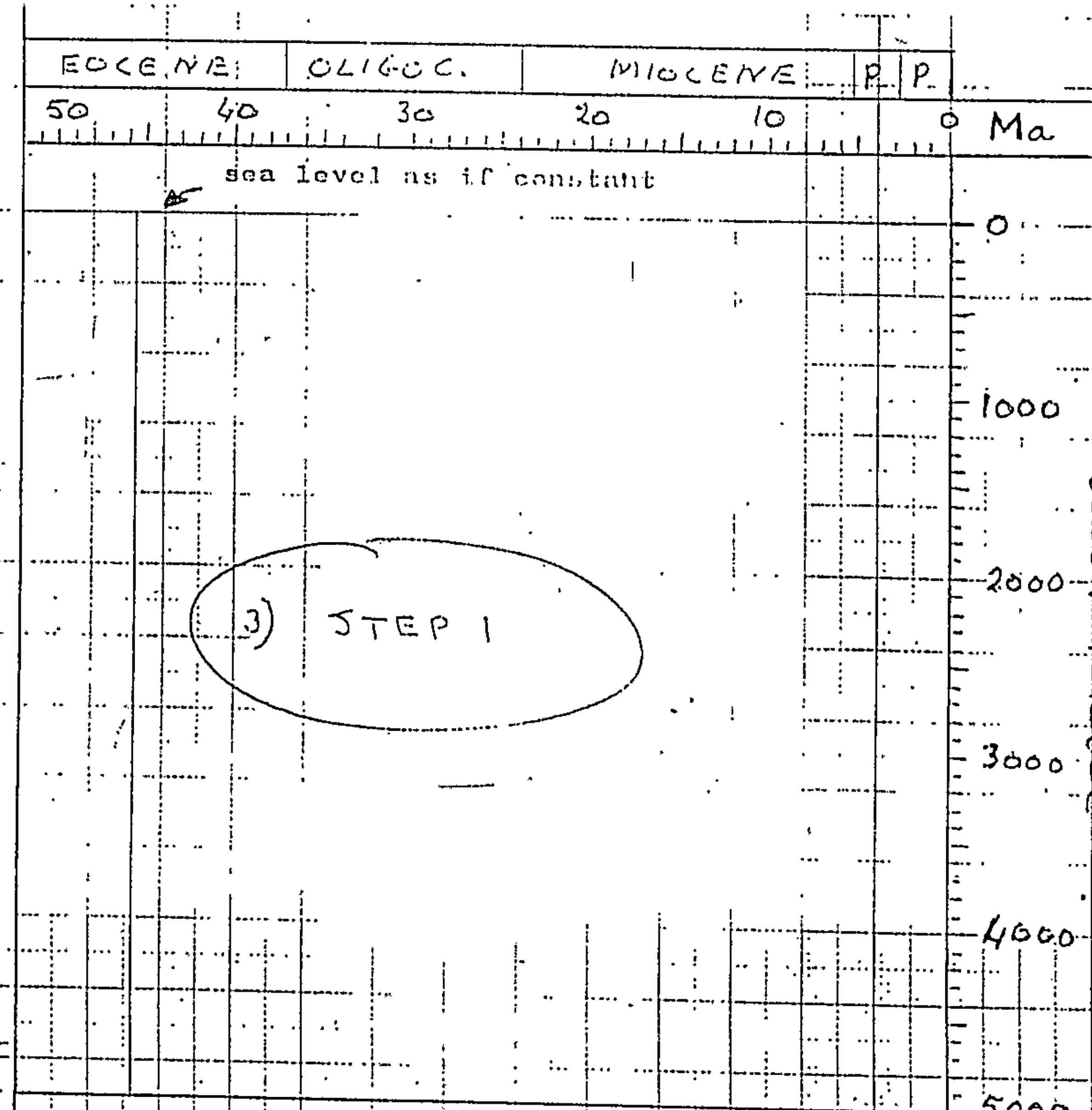
EOCENE
OLIGOC.
MIOCENE
P.
P.
50
40
30
20
10
0
Ma
sea level as if constant
0
1000
2000
3000
4000
5000
DEPTH in METER
3) STEP 1

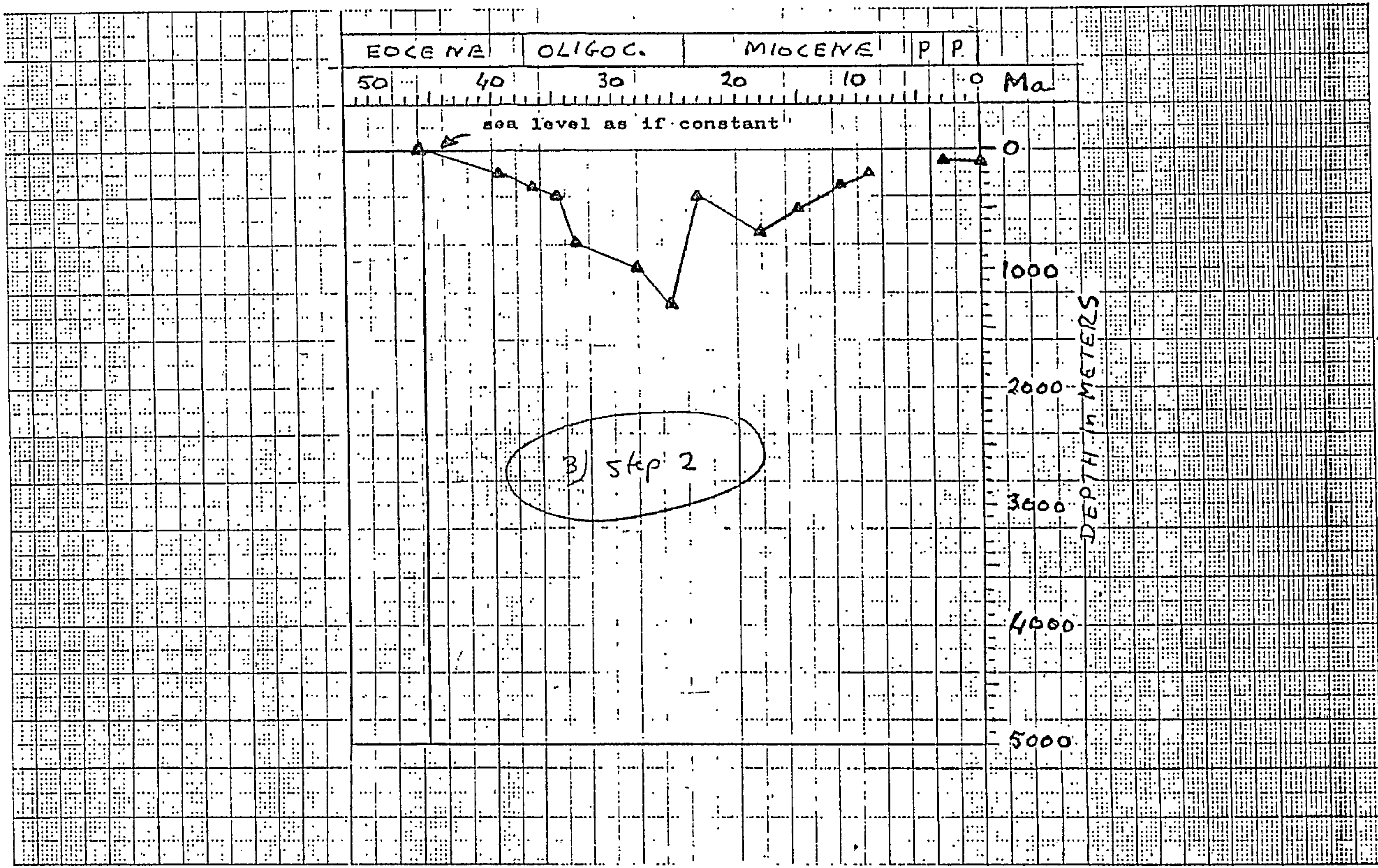

EOCENE
OLIGOC.
MIOCENE
P
P
50
40
30
20
10
0
Ma
sea level as if constant
0
1000
2000
3000
4000
5000
DEPTH in METERS
3) step 2

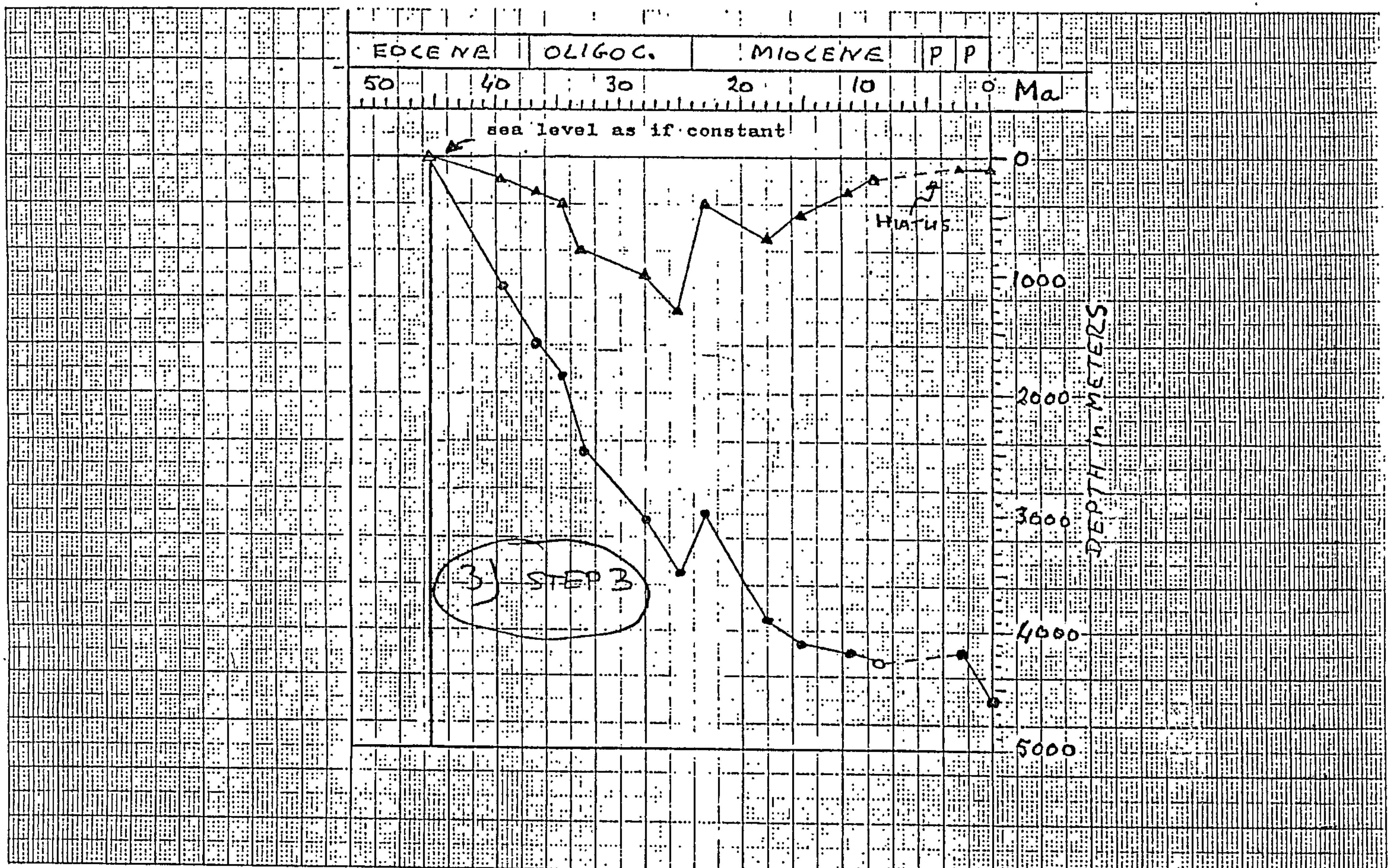
EOCENE
OLIGOC.
MIOCENE
P
P
50
40
30
20
10
0
Ma
sea level as if constant
HIATUS
0
1000
2000
3000
4000
5000
DEPTH in METERS
3) STEP 3

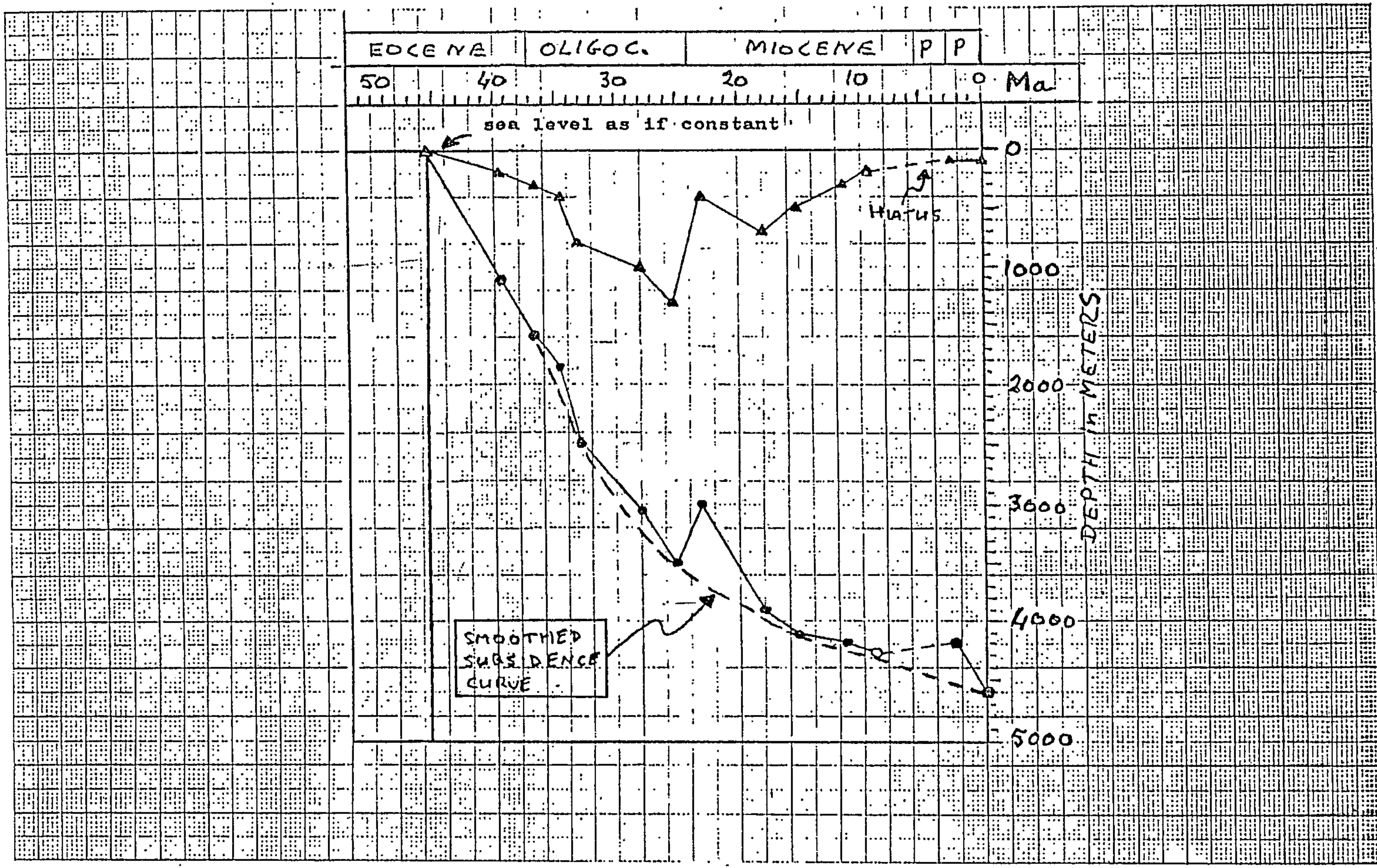

EOCENE
OLIGOC.
MIOCENE
P
P
50
40
30
20
10
0
Ma
sea level as if constant
0
1000
2000
3000
4000
5000
DEPTH in METERS
HIATUS
SMOOTHED SUBSIDENCE CURVE

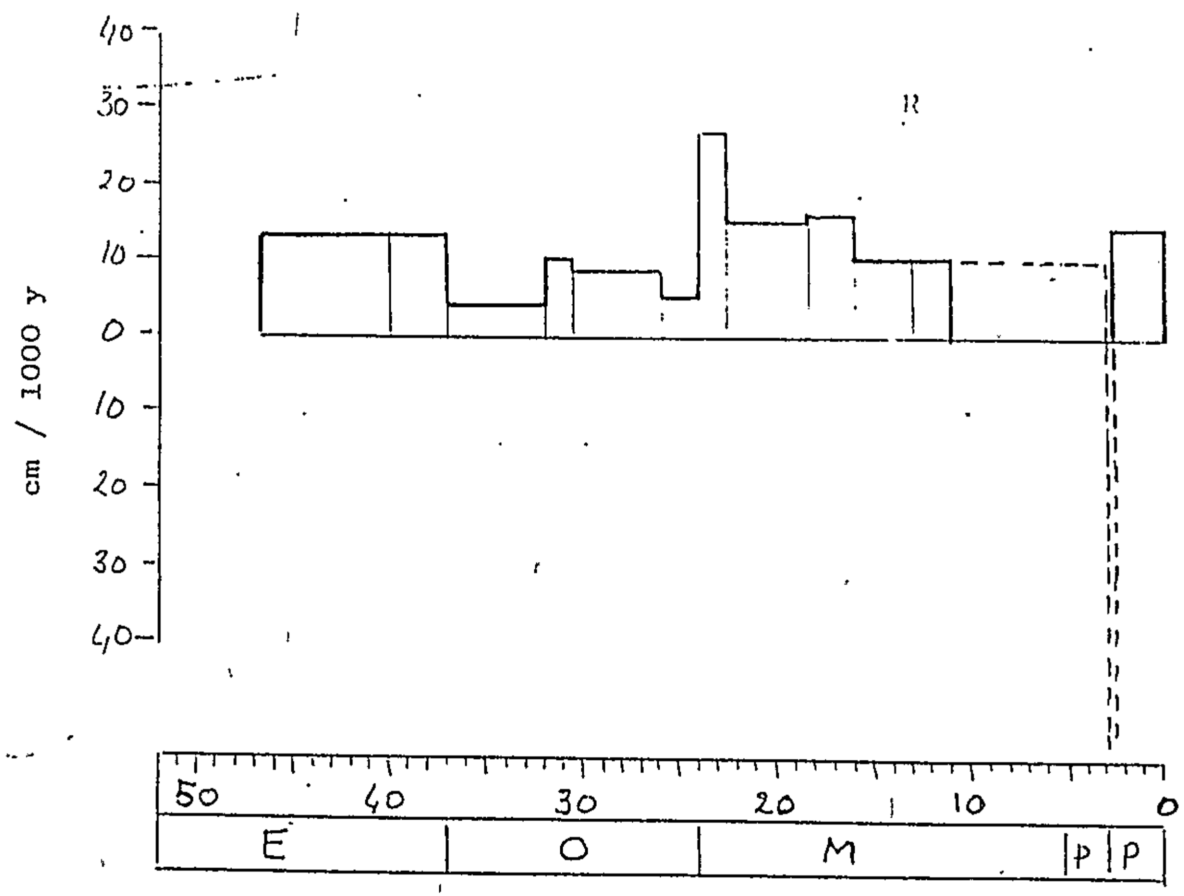

40
30
20
10
0
10
20
30
40
cm / 1000 y
50
40
30
20
10
0
E
O
M
P
P

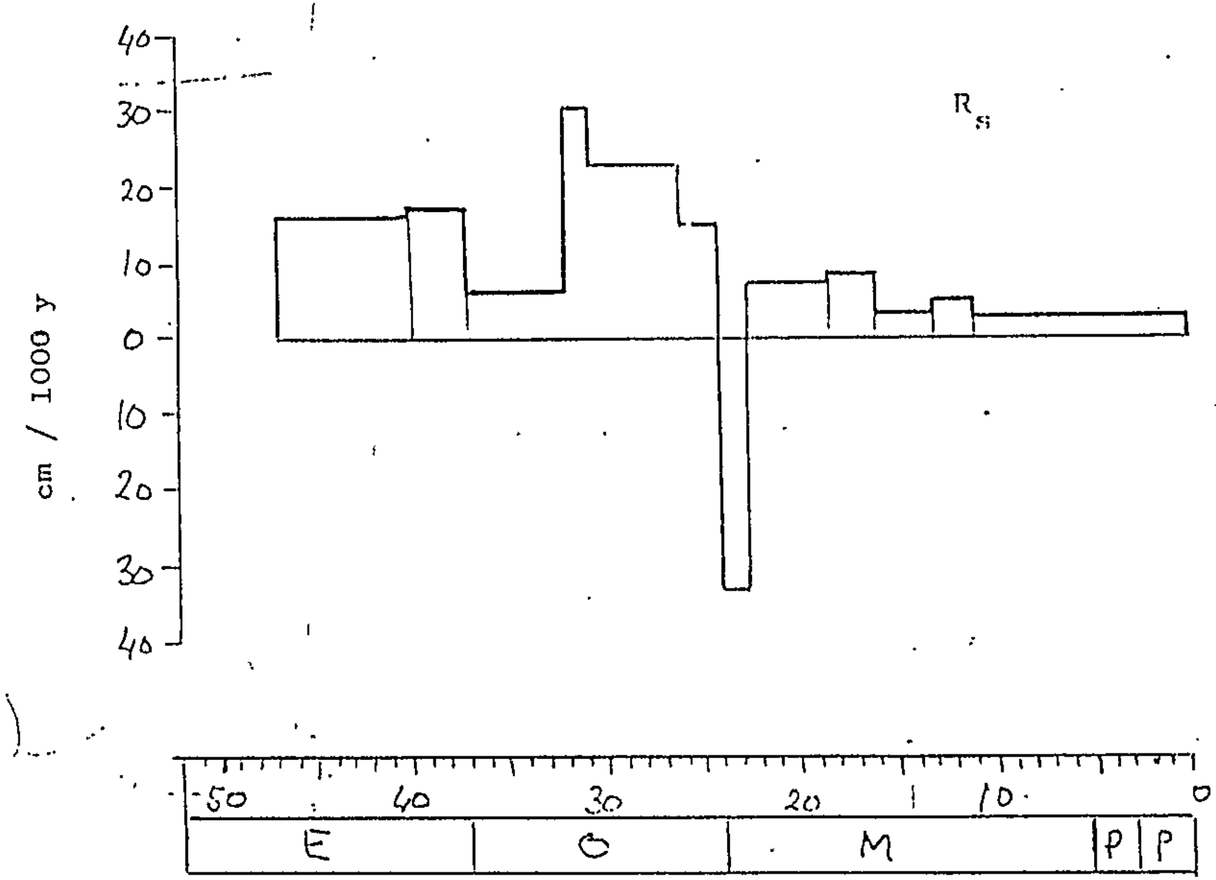

R_s
cm / 1000 y
40
30
20
10
0
10
20
30
40
-50
40
30
20
10
0
E
O
M
P
P

P R O B L E M   1

Given: Paleo summary well No. 1.

Asked: 1) the average rate of sediment accumulation for each unit of well No. 1. R_o.

2) the average rate of subsidence during deposition of each unit of well No. 1. R_s. No correction for compaction, isostacy or eustacy.

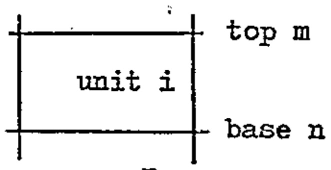

$$R_i = \frac{T_i}{10\,A_i} \text{ cm/ka} \qquad T_i = R_i \cdot 10A_i \qquad A_i = \frac{T_i}{10\,R_i}$$

$$Rs_n = \frac{T_i - dW_i}{10A_i} = R_i - \frac{dW_i}{10A_i} \text{ cm/ka}$$

T - thickness in meter

A - duration in millions of years

dW - change in waterdepth in meter

R and Rs in cm/1000 y, or cm/ka

3) construct a "Geohistory Diagram" for well No. 1.

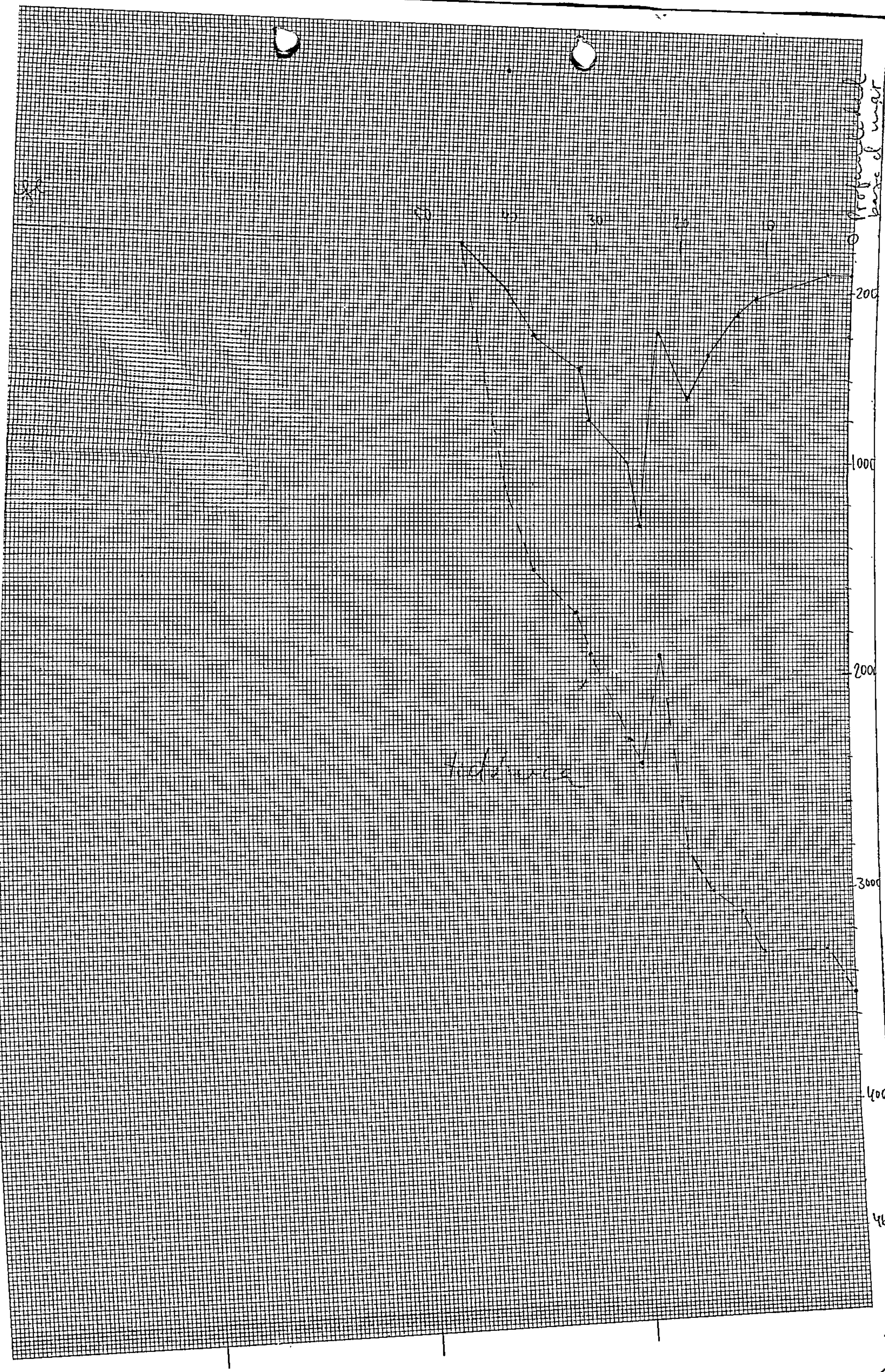

50
40
30
20
10
0
200
1000
2000
3000

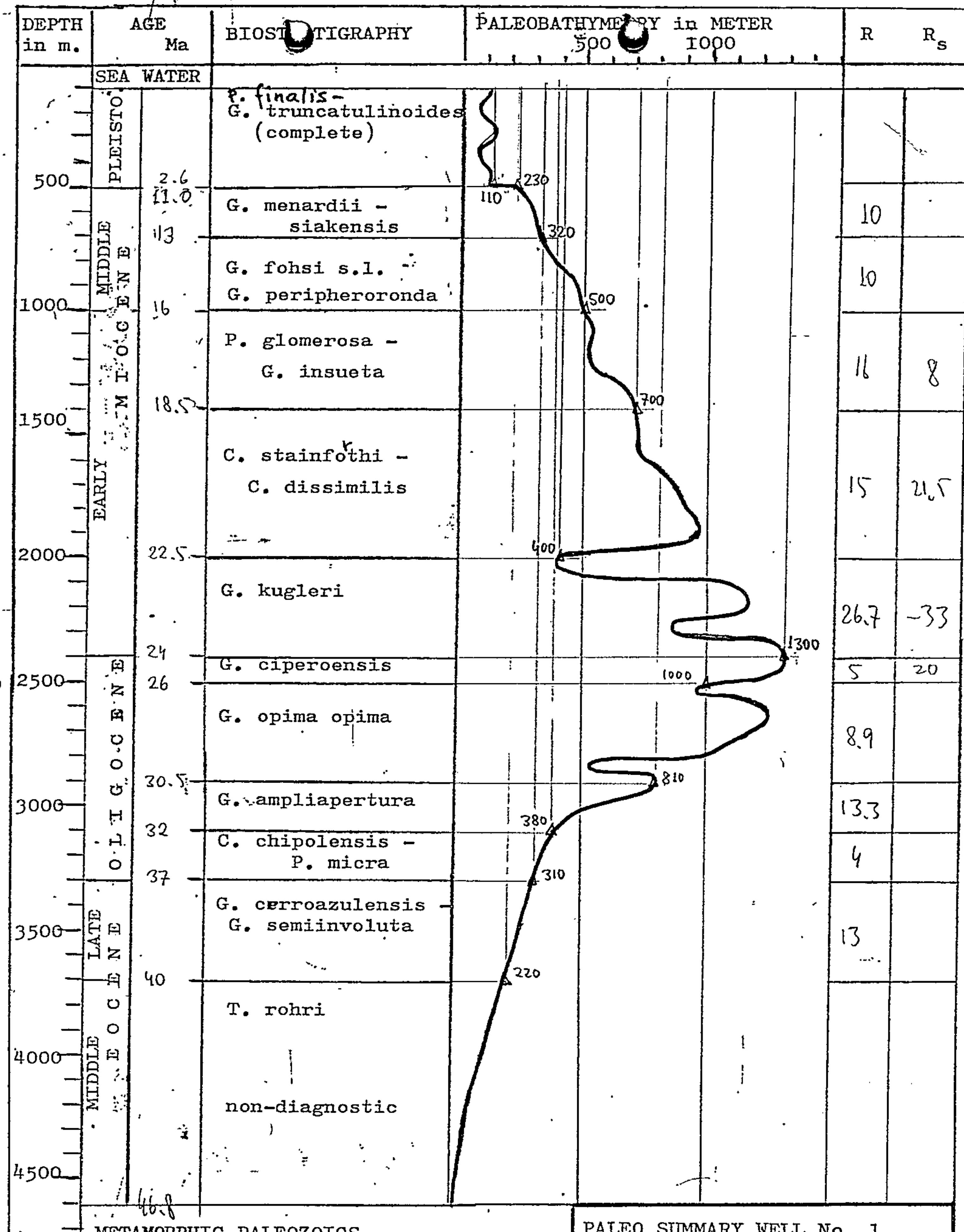

Well No. 1 Problem 1.

9

<u>PROBLEM 1</u>

Questions 1) and 2).

Step 1. Determine WD at marker levels, mark with solid triangle.
Step 2. Mark numeric ages from standard reference.
Step 3. Tabulate data.
Step 4. Calculate R.
Step 5. Calculate ages at unconformities and/or TD.
Step 6. Calculate Rs.

Question 3).

Step 1. Draw convenient scale.
Step 2. Plot WD at marker levels.
Step 3. Add accumulated sediment thickness.
Step 4. Interpretation.

$R_i = \frac{400\ m}{10 \times A_i} = 1.538$

depth	Δ thickn	age	Δage	ΔW	
100	0				
500	500	2.6	2.6	0	
500	0	11	7.2	120	
700	200	12.0	2.2	90	
1000	300	16	4	180	
1400	400	18.5	2.5	200	
2000	600	22.5	4	-300	
2400	400	24	1.5	900	
2500	100				
2900	400				
3100	200				
3300	200				
3700	400				

LATE TERTIARY TIME-STRATIGRAPHIC REFERENCE SCHEME

AREA:

AUTHOR: A. Tasovac

DATE:

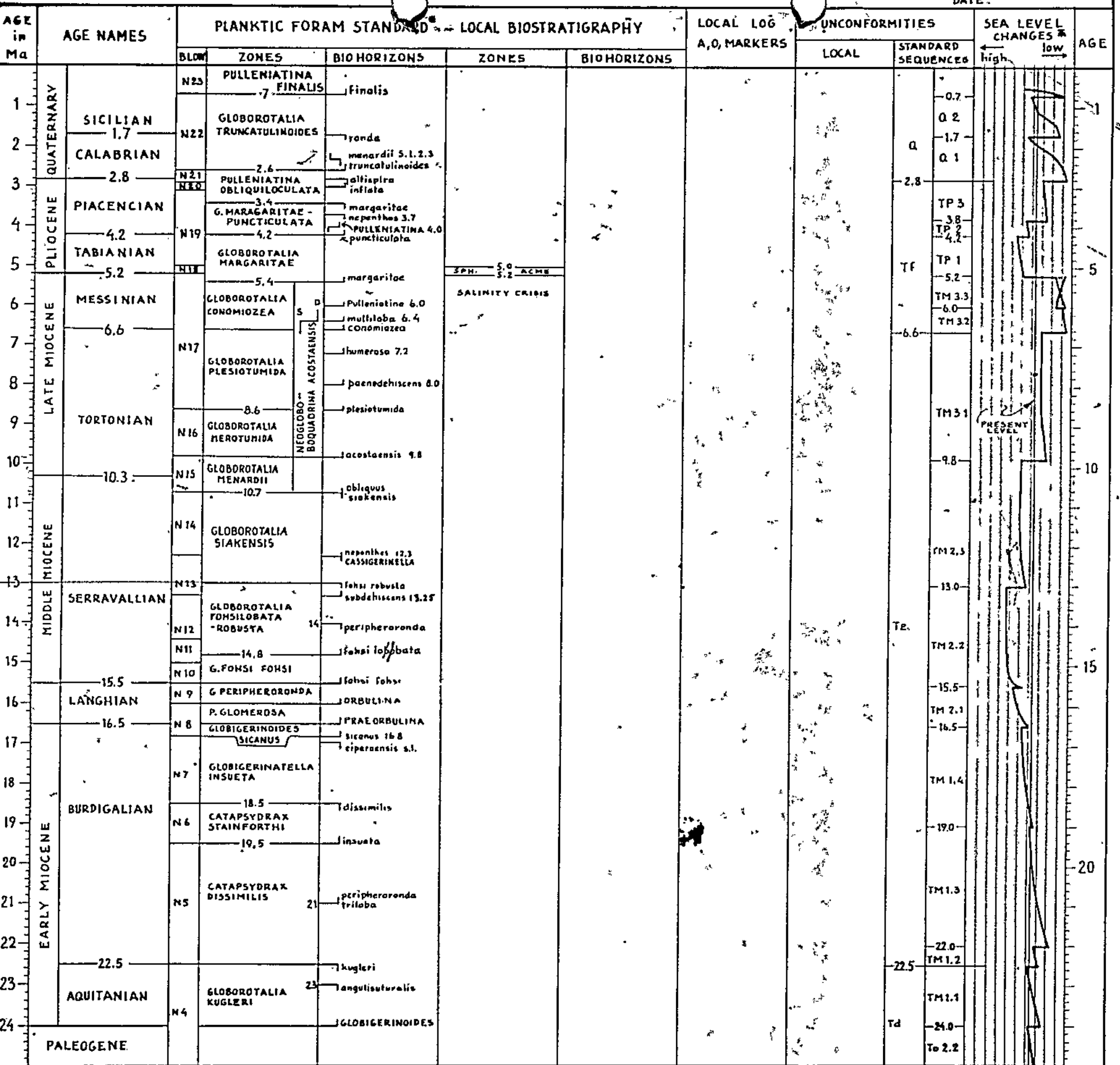

* AFTER: STAINFORTH ET. AL. 1975; VAIL & MITCHUM, 1979; VAN HINTE ETAL, 1980.